ALMA MATER STUDIORUM
UNIVERSITÀ DI BOLOGNA

DEPARTMENT OF CIVIL, CHEMICAL, ENVIRONMENTAL AND MATERIALS ENGINEERING (DICAM)

SECOND-CYCLE DEGREE / ENVIRONMENTAL ENGINEERING – CURRICULUM EARTH RESOURCES ENGINEERING

INTEGRATED NUMERICAL MODELING WITH LEDAFLOW, PIPESIM AND ECLIPSE SOFTWARE FOR EFFICIENT CO2 INJECTION AND STORAGE

Supervisor

Prof. Villiam Bortolotti

Defended by

Vasilii Anisimov

---

21 / July/ 2025

Academic Year 2023/2024

Abstract

The master's thesis presents relevant topic about integrated numerical modeling of CO_2 injection into saline aquifers. At the outset the Smeaheia (Norwegian Continental Shelf) model was constructed in the Ledaflow and Pipesim simulators (specific for surface infrastructure and wellbore) to understand the physical processes during CO_2 injection. These models were compared and Ledaflow's model was chosen for further work and coupling with the reservoir simulator. Eclipse E100 and E300 simulators for black oil and thermal compositional cases were employed for reservoir modeling. The models was developed to examine the flow of CO_2 plume, change in pressure and temperature in transient flow. A "loose-coupling" simulation approach was proposed and used to understand and address the issues of geological storage of CO_2 in saline aquifers. This approach connected Ledaflow with Eclipse. It enable to handle changes in pressure, temperature and phase distribution in transient mode. It showed that at the injection initialization the gas distribution could reach high values – around 93%, it underscores the importance of gas-impermeable infrastructure. Then, Eclipse advanced modules (CO2SOL, WSEGDIMS) was employed to see how application of outflow control devices might affect the CO_2 plume distribution in the reservoir. Comparing the simulation results showed differences in how phase behavior and storage capacity are predicted by the three reservoir simulators (E100, E300CO2STORE, E300CO2SOL). Afterall, the implementation of outflow control devices assessed. The results were 8% improvement in outflow for the low-permeable layers.

Acknowledgements

I would like to express my deepest gratitude to Professor Villiam Bortolotti, who always supported and helped me in every aspect of my studies, including during my exchange period.

I am also very grateful to Professor Milan Stanko (Norwegian University of Science and Technology) and postdoctoral researcher Ahmed Hasan for giving me the opportunity to collaborate with them. Their regular weekly meetings provided an excellent environment to present my results and enhance my skills in scientific discussion and presentation. Their ideas, insights, and constructive feedback were instrumental in successfully completing this research under their supervision. I am truly thankful for their generous support and guidance.

I would also like to acknowledge the University of Bologna for giving me the opportunity to pursue my studies there, for its outstanding libraries and high-quality courses, and for the solid foundation of knowledge I acquired during the first year of the programme.

I wish to thank the Norwegian University of Technology and Science for the convenient and beautiful exchange period in Trondheim. I am especially grateful for the excellent facilities, such as well-equipped laboratories and access to software, which supported my research and practical training. The University provided comprehensive courses that strengthened my academic foundation, including Norwegian language classes.

Finally, I would like to thank my family and friends for their love, support and patience during my period of education abroad. Their great support has been my source of motivation and strength.

Table of Contents

Nomenclature

CCS – Carbon Capture and Sequestration

CDR – Carbon Dioxide Removal methods

OCD – Outflow Control Device

MMP – Minimum-Miscible Pressure

EGR – Enhanced Gas Recovery

Mt – Million tonnes

EOR – Enhanced Oil Recovery

ECBM – Enhanced coal-bed-methane

PVT – Pressure-Volume-Temperature properties

PR – Peng-Robinson equation of state

EOS – Equation of State

TOC – Total Organic Content

DFM – Drift-Flux Model

ICD – Inflow Control Device

WAG – Water-Alternating-Gas injection

VFZ – Vette Fault Zone

ØFC – Øygarden Fault Complex

SRK – Soave-Redlich-Kwong equation of state

ID – Internal Diameter

BHP – Bottom-hole Pressure

PS – Pipeline Start

MFR – Mass-flow Rate

PID – Proportional-Integral-Derivative

THP – Tubing Hanger Pressure

BHT – Bottom-hole Temperature

GVF – Gas Volume Fraction

MAPE – Mean Average Percentage Error

MD – Measured Depth

Chapter 1. Introduction

1.1 Background and Motivation for CO_2 Geological Storage

The growing concentration of greenhouse gases such as CO_2, CH_4 and water vapor warns our society increasingly. It represents one of the severest problems of our time. The atmospheric concentration of those gases has grown at a fast rate to reach high level since pre-industrial time. The main reason for that change is human activity. The Intergovernmental Panel on Climate Change (IPCC, 2023) has recently reported that the concentration of CO_2 has reached around 415 parts per million. The Earth has not seen such high levels of greenhouse gases for the last two million years according to paleoclimate studies (IPCC, 2023).

As mentioned before, the main reason for this drammatical change in the concentration of CO_2 is antropogenic factor. Carbon emissions has increased mostly because of the fossil fuels burning and industrial operations (IPCC, 2023). The Global Carbon Budget has presented ecological report that shows that human activity produce almost 37,8 billion tones of CO_2 during the last years (Global Carbon Budget, 2023). The figure 1.1 presents annual world CO_2 levels since 1850s. There can be seen the rapid CO_2 emissions growth from the period after second world war when the massive oil and gas flieds development as well as industrialization occurred.

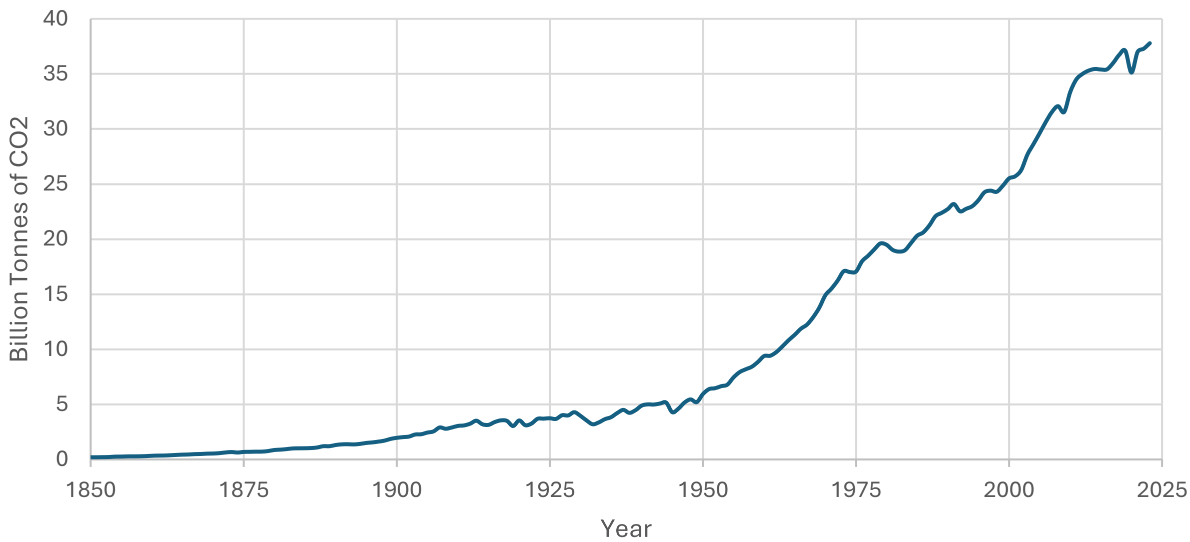

Figure 1.1 – Annual world CO_2 emissions (Global Carbon Budget, 2023).

According to the Global Carbon Budget report, the worldwide emission pattern continue to present steady increasing path despite of the regional difference. For example, the United States and European Union has decreased the emissions by around 29,2% and 42,6% respectively. On the other hand, China and India increased theirs by 281% and 200% respectively since 1990 (Global Carbon Budget, 2023). Scientists warns society that it will lead to severe catastrophic events since this difference cannot meet the steep emissions reductions that is required for achievement of international climate targets.

International cooperation emerged as a result of climate change and subsequent events. One of the last international treatments in this field was the Paris Agreement (UNFCCC, 2015). It was an international treaty to fight climate change. One of the main objectives of the treaty was to maintain global average temperature at level below 1,5°C pre-industrial levels (UNFCCC, 2015). The average annual temperature increase correspond to pre-industrial levels presented in figure 1.2.

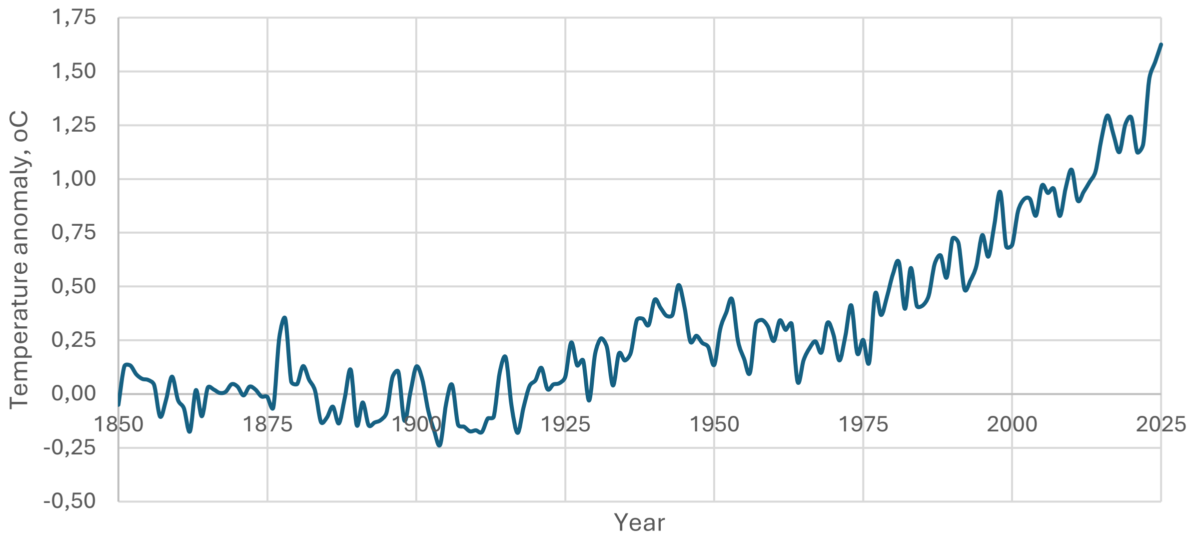

Figure 1.2 – Average annual temperature anomaly related to the pre-industrial period (Our Would in Data).

However, the Paris agreements were only advisory in nature, meaning that they were not binding. Each signatory country proposed an action plan (Nationally Determined Contributions) to reduce emissions, but there were no obligations to implement them. The worldwide transition from the traditional sources of energy (oil, gas and charcoal) to renewable sources and new industrial processes alongside the implementation of CO_2 removal technologies will require a lot of efforts and time. One of the promising solutions is carbon capture and storage (CCS) technologies that includes capture, transportation and sequestration carbon dioxide on special underground structures, geological storage. Figure 1.3 illustrates the trend of implementing these perspective technologies in future.

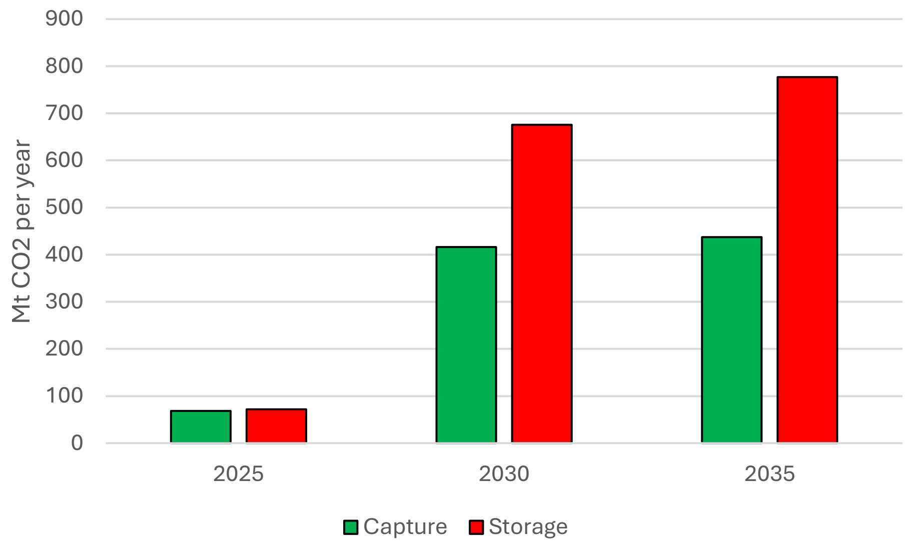

Figure 1.3 – Operational and planned capacity for CCS in 2025,2030 and 2035 (CCUS Projects Explorer, 2025).

Increasing CO_2 concentrations cause increased sea levels because of thermal expansion of sea water and glacier melting (IPCC, 2023). According to the IPCC reports, sea levels has increased by approximately 0,2 meters during the period from 1901 to 2018 (IPCC, 2023). The current rate is still dramatic, since it stands at 3,7 mm per year. The 21st century meet the glacier melting in Greenland and Antarctica. The ice loss in Greenland has increased dramatically fast during 2010-2019 compared to the levels during 1990-2000.

Increasing temperatures could also affect the hydrologic cycle. Air's moisture capacity increases by 7% as a response to the increased average temperature by 1°C (Trentberth, 2011). Since the increased temperature, oceans, seas and rivers starts evaporating more vapor in the atmosphere, which results in intensified rainfall during storms in wet areas. On the other hand, increased evaporation of those regions leads to drying soil, so it creates more severe droughts. These patterns results in increased moisture in wet areas and decreased moisture in dry areas (Trenberth, 2011).

The development of fossil fuels and industrial activities made CCS an essential component for mitigation strategies. According to IPCC, CCS is a separation of CO_2 from industrial factories and energy-related sources, followed by transportation and sequestration (IPCC, 2005). Nowadays climate change policies heavily rely on this promising technology. The cement industry and chemical manufacturing sector along with power generation facilities have identified CCS as their main emission reduction option (IPCC, 2005).

There can be various options for geological storing of CO_2 – saline aquifers, depleted oil and gas fields, coal seams and clastic or basaltic formations (Muhammad, 2023). The most studied of these are saline aquifers – generally, geologically porous media that contains highly saline water. This water cannot be used for domestic, industrial or agricultural purposes because of high salinity, so it can be sustainable solution to use it as storage for CO_2. This method offers different advantages among others since it allows CO_2 to exist in a supercritical state while covering vast underground areas. It should be noted that this method also employ different trapping mechanisms that will be described in the following chapters.

Among CCS there can also be employed carbon dioxide removal (CDR) methods to struggle against climate change caused by CO_2. These methods describe human-imposed methods which extract carbon dioxide from the atmosphere, some of them are reforestation, ocean fertilization and soil carbon sequestration.

The dangerously increasing CO_2 concentration together with the resulting events has led humanity to apply new methods for reduction of emissions. CCS technology has proven to be a promising solution for the future.

1.2 Problem Statement and Challenges

CCS presents some challenges nowadays related to fluid dynamics, geological heterogeneity and thermal effects. While CO_2 injection underground is becoming a perspective method for long-term CO_2 storage, the process usually involves two-phase flow regions particularly under varying pressure and temperature conditions.

One of the fundamental challenges today is how to accurately predict two-phase flow behavior during CO_2 injection. As CO_2 is injected into subsurface it faces different ranges of thermobaric properties from the atmosphere (1 bar, 10°C) to underground structure (100-200 bar, 30-100°C). Also, there might be pressure and thermal drop because of gas expansion in a wellhead choke. So, in these ranges CO_2 could exist in three different phases: gas, liquid and supercritical fluid. Therefore, the challenge is to define the proportions of these phases during the injection and migration. This challenge became more complex since there is modeling of pressure profiles, mobility ratios, displacement efficiency and gravitational segregation. If this miscalculated, it can lead to inaccurate predictions of injectivity and storage capacity as well as it can lead to risk of leakage.

Sharp cooling also make it harder since it is still complex challenge to predict fluid behavior passing through a choke. The main reason for sharp cooling is Joule-Thompson. This cooling effect leads to quick vaporization that introduces some risks of leakages. Nonetheless, sharp cooling might change density and viscosity that can alter both flow regimes and phase stability of the CO_2 plume in the subsurface reservoirs. Understanding and accurate predictions of these processes – are essential for integrity.

Reservoir heterogeneity adds another level of complexity, since reservoir properties are continuous variables. Variations in permeability and porosity across the area affects flow paths. It could cause early breakthroughs, inefficiencies in swept and uneven CO_2 distribution. Traditional well completion that is used in the injection well are not sufficient for mitigating these effects. Therefore, implementation of special devices – outflow control devices (OCD) are needed. These devices and their effect should be accurately predicted and assessed.

Finally, coupling surface infrastructures with reservoir to analyze phase distribution, pressure and temperature profile is not trivial. Lots of traditional simulators presents only surface infrastructure and well or reservoir simulations, ignoring critical interactions between them. It should be noted that there are not so many simulations that can predict transient pressure and temperature effects from the inlet of pipeline into the reservoir.

1.3 Research Objectives and Questions

The master's thesis aims to develop a numerical model which will combine CO_2 injection simulations in saline aquifers to study two-phase flow behavior. These models (surface and reservoir) will be coupled to analyze the process.

Specific research objectives:

- The thesis aims to assemble a hydrodynamic model that simulates CO_2 flow behavior under different pressure and temperature conditions. It will be done by using SLB's software – Eclipse E100 and E300 (CO2STORE and CO2SOL).
- The study will develop surface model that include horizontal surface pipeline (riser), wellhead choke and well. This model will be used to analyze pressure and temperature profiles in steady-state and transient mode. It will be done by using proven industrial simulators, such as Pipesim (SLB) and Ledaflow (KONGSBERG).
- The research will then couple these models to see the distribution patterns with attention to CO_2 phase behavior change alongside the scheme in transient and steady-state mode.
- The thesis will evaluate an application of OCD to prevent flow segregation while maintaining sufficient bottom hole pressure.

1.4 Significance of Study

The master's thesis examine the relationship between surface equipment requirements and subsurface storage to fill knowledge gaps. This research will develop an advanced predictive model to simulate CO_2 flow in those systems to enhance CCS performance results.

The outcomes will achieve the following objectives:

- The thesis will improve predictive accuracy of CO_2 injection simulations that operate under real-world fields and conditions.
- The outcomes will help CCS to be more efficient, resilient and secure in sense of risks
- The research will provide a complex guidance to couple infrastructure and reservoir to analyze processes
- The study provides scientific evidence for future direction works in the field of multiphase flow behavior and reservoir management in CCS practices.

The aim of the study is to establish a practical link between theory and practice through scalable solutions aimed at addressing one of the major environmental challenges of our time.

1.5 Thesis Structure

This thesis consists of five major chapters that evolve from one to the next providing encompassing knowledge about both CO_2 injection and modeling practices with their analyses.

The content of each chapter are the following:

- Chapter 1: This chapter will present a short introduction to the main topic with climate problems, their reason and consequences. It provides some basic information about CCS and CO_2 injections in saline aquifers.
- Chapter 2: This chapter will present current review about CCS study in literature with particular emphasis on two-phase flow cases, thermal and pressure profiles and outflow control applications. At the end of the chapter will be presented existing scientific gaps that this thesis is aiming to cover.
- Chapter 3: This chapter will explore the field (Smeaheia) and simulation tools that were chosen for this study. It covers the assembling of models and proposal strategy for coupling the simulators. It will also present ideas about modeling OCD in those simulators.
- Chapter 4: This chapter shows the simulation results and their analyses, including analysis of pressure and temperature profiles, phase distribution and thermal effects from the start of the pipeline to the reservoir. It will also present comparison between different industrial software – Pipesim and Ledaflow, Eclipse E100 and Eclipse E300. Advanced scenario, such as OCDs are also evaluated.
- Chapter 5: The conclusion of the thesis and outlining limitations and proposals for future directions of study.

Chapter 2. Theory and Literature Review

This chapter will present theoretical part of the master's thesis with literature review. At the end of the chapter the existing knowledge gaps in existing studies will be presented.

2.1 CO_2 Geological Storage Mechanisms

2.1.1 Reservoir Types for CO_2 Geological Storage

The existence, far-reaching availability and capacity potential have made deep saline aquifers be on the spotlight as perspective side of CO_2 storage. The saline aquifers are going to be introduced in this subchapter and compared to the other types of reservoirs and various other aspects of the CO_2 storage in the saline aquifers will be examined.

The saline aquifers can be referred to as porous and permeable geological reservoirs which has a high salted fluid in the pores (Bentham, 2005). In most cases they are formed at depths which are below the layers of drinkable water and hence they are located at 800-3000 m depths (Bentham, 2005). These enormous underground deposits of rock are filled with, which is estimated to be about 10 times saltier than seawater, and that has been sealed in a rock by an impenetrable layer of caprock in the form of a roof of rock or even years previously (Muhammad, 2023). It is also interesting fact that large regional atlases, such as UK CO2Stored, US NATCARB or China onshore assessments has consistently allocated more than 90% of storage resource to saline aquifers.

Among all opportunities for storing CO_2, one has some options: it could be depleted oil and gas fields, saline aquifers, coal seams or clastic/basaltic formations (Muhammad, 2023). The study by Muhammad presented the main advantages and disadvantages for each of these geological formation for storing CO_2.

Former hydrocarbon reservoirs already possess sufficient and useful traps for not only oil and gas, but also for CO_2. Operators can often re-open the exploitation wells, pipelines and platforms for carbon dioxide injections. This step could lower development costs and shorten permitting schedules (IEAGHG, 2024). This structures are also proven to have structural integrity, since they have saved hydrocarbons retained millions of years. Huge fields has extensive datasets (such as seismic and well logs data) to create detailed subsurface reservoirs.

In this field two types of displacement mechanisms exist – miscible and immiscible pathways. Miscible pathway exists when the pressure exceeds the minimum-miscible pressure (MMP), so in other words, the oil and carbon dioxide becomes single phase after multiple contacts (Zhao et al, 2024). Consequently, the immiscible mechanism occurs when the reservoir pressure is lower than MMP. CO_2 stays a separate phase but still interacts with oil/gas.

In practice, miscible mechanism occurs individually for each case. One case study presents e.g. 30–45 MPa at 120 °C for light oils (Zhao et al, 2024). The main consequence is that MMP increases with the water cut, reservoir temperature and presence of C_{7+} components. This makes miscible mechanism more preferable in comparison to immiscible, since it provide very high storage efficiency: production data from Permian & Sarir pilots show ≥ 90 % of net-injected CO_2 retained after 5 years shut-in, thanks to residual, solubility and capillary trapping once pressure falls under MMP (Rajandran et al, 2024).

On the other hand, immiscible mechanism have been usually chosen for heavy oils and enhanced gas recovery (EGR) cases (Al-Jeboore, 2023). Study by Al-Jeboore (2023) presents that oil by interacting with CO_2 swell by 10–20 %, so it led to cut viscosity by 30–50 %. Then CO_2 front pushes the oil and the brine ahead.

Large scale pilot projects shows that the concept of hydrocarbon fields reuse for CO_2 storage perfectly works. At Weyburn-Midale, Saskatchewan (Canada) more than 7 million tonnes (Mt) of CO_2 have been injected since 2000 during the enhanced oil recovery (EOR) operation (IEAGHG, 2024). This project reveals that around more than 26 Mt of CO_2 can be permanently stored over the life of the field. In Europe, Croatian project with name Ivanić-Žutica is injecting around 0,65 million tonnes of CO_2 per year into mature oil fields, while UK's Acorn project plan to store more than 5 million tonnes in the depleted Goldeneye gas field. So, these storage in depleted oil and gas fields gain more and more attention nowadays.

Depleted-field CCS hubs in Europe surged after 2021: Porthos, Bifrost, Greensand, Acorn and K6 each targeting start-up before 2030. Projects under construction rose from four in 2021 to nine in 2024 (Havercroft, 2024).

The key advantages of this concept includes:

- Well-characterized geology and property of the well.
- Existing reusable wells that lower and cut capital expenditures. Some studies shows that business can save up to 40% of initial investments because of existing infrastructure (Kirchin, 2019).
- Potential revenue from late-life EOR offsets some costs.

However, these projects has some disadvantages:

- Lots of these wells need to be tested for integrity, since most of them have a risk of leakage pathways after years of exploration. It is usual practice to use acid and alkaline treatments of the bottomhole wellbore zone. These aggressive fluids could reduce the impermeability of concrete that can lead to potential leakages.
- Re-pressurizing depleted reservoirs can trigger undesirable seismicity events such as earthquake or blow-outs if integrity is poor.

In deep, useless coal seams, CO_2 can be stored mainly by the adsorption process onto the microporous coal matrix, displacing methane and enable concept of enhanced coal-bed-methane (ECBM) recovery. This concept leads to the fact that coal seems to be able to hold roughly twice as much CO_2 as CH_4 per unit volume.

One of the examples of this technique is from Allison Unit pilot (San Juan Basin, USA), where 4 advanced injectors and 16 producers demonstrated methane production and efficient CO_2 storage between 1995-2001 (Shi, 2005). Unfortunately, no commercial-scale coal seam storage is operating nowadays. Since, the most of the projects struggle against some technical hurdles – injectivity decline, faulted seam leakage risk and economic limits, so it keep most proposals at pilot stage.

The main advantages of them include (Shi, 2005):

- Dual revenue stream – storage fees incorporated with methane sales, it can significantly improve the project viability.

— Strong adsorption and potential for up-dip stratigraphic trapping provide variative retention mechanisms.

The cons are:

— Coal matrix swells when CO_2 absorbs, often decreasing the permeability of the coal seams. Some studies (Shi, 2005) present that it can decrease the injectivity by up to 40% in early years.

— Storage capacity is modest on a per-site basis.

Another possible solution for storing CO_2 can be basaltic formations. Reactive mafic rocks such as flood basalts provide different storage pathways. The reason is that injected CO_2 dissolved in water and react with rich-mineral ions, such as Ca^{2+}, Mg^{2+}, Fe^{2+}, Fe^{3+} (Pogge von Strandmann et al, 2019).

One of the example is CarbFix project in Iceland. There were 175 tonnes of dissolved CO_2 in 2012. Isotopic mass-balance shows that more than 70% mineralized within two years, while it can me increased for more than 90% in case of later injections – demonstrating that it can be speed at temperatures 20-50°C (Pogge von Strandmann et al, 2019).

Advantages of these rare types of storage include:

— Mineral trapping converts CO_2 to solid carbonates – arguably the most secure form of storing.

— Very large areal extents can offer huge opportunities for capacity in regions lacking of sedimentary basins.

Disadvantages are:

— Permeability is typically low.

— Still there is not so many examples as well as data of these storages.

— Reactive fluids may mobilize other metals, implementation of monitoring systems for groundwater chemistry is vital.

Therefore, one of the most popular solutions, as presented above, is saline aquifers. They offer the largest theoretical global capacity both on- and offshore. CO_2 in this case is stored as a separate supercritical state, then progressively immobilized by residual, solubility and mineral trapping.

There are huge number of successful examples of them. One of the largest is Sleipner project in the Norwegian North Sea. This project has injected more than 23 Mt since 1996 into highly permeable Utsira formation. Another example is Snøhvit in the Barents Sea that has is sequestrating around 0,7 Mt per year since 2008.

The main advantages of them are:

— Vast capacity – order of magnitude larger than annual emissions and worldwide distribution.

— Vast majority of trapping mechanisms that increase the buried amount of CO_2.

Unfortunately, there are some cons:

- Higher site-characterisation cost and uncertainty compared with depleted oil and gas fields. The predicted injectivity and rates can vary widely
- Pressure management is crucial, since it has been proved by Snøhvit case, where hydrodynamic models still cannot be matched with the real field.
- Brine displacement and pressurization may lead to undesired events. It requires careful monitoring.

Each geological option has demonstrated great capacity to store CO_2, but their suitability varies from site to site. Saline aquifers and depleted fields are now ready to injection for million tonnes of CO_2. On the other hand, coal seams offer niche opportunities coupled with methane production, and basaltic structures hold transformational promises for permanent mineral storage.

2.1.2 Experimental Determination of Thermophysical Properties of Carbon Dioxide

All trapping mechanisms, that will be presented, need information on Pressure-Volume-Temperature (PVT) properties of Carbon Dioxide in order to understand it. A PVT is a scientific investigation that depicts the nature of fluids used when pressure, volume and temperature react against one another. The principle of thermodynamics and fluid mechanics demands the awareness of PVT properties to study the behavior of gas and liquids in various environmental conditions.

These properties can be measured by means of the following approaches:

- PVT properties of CO_2 are generally measured in special PVT cells. The cells ensure high accuracy of pressure and temperature control and monitor the volume variation to deliver an accurate evaluation of CO_2 behaviors under different conditions.
- Viscosity measurements entail specific high-pressure viscometers to work. The measurement of the instruments is flow resistance of within the CO_2 at various temperature and pressures which are critical data on the modeling of both wellbore and reservoir systems.
- High-pressure densitometers can be used as an instrument to measure the density of CO_2 in its various phases. The correct measurements of density will filter Equation of State (EOS) models and correctly predict flows.

PVT properties define the physical properties of CO_2 along with its reaction to the changes in pressure, temperature and change in volume. The properties act as fundamental functions of modeling and explains the behavior of CO_2 in various environments including underground reservoir, within a pipeline and the carbon capture and storage systems.

CO_2 exists in four different forms – solid, gas, liquid and supercritical phase. In sense of carbon storage, the supercritical phase is most preferable. Above critical point, this supercritical fluid minimizes the pore volume required for storage while still saving low viscosity that facilitate injection and migration in the reservoir. By contrast, gaseous CO_2 has around 300 times lower density, demanding much larger reservoir for storing it. Recent studies in PVT modeling presents that CO_2 can be in supercritical state that has density even larger than formation brine (>1030 kg/m^3) (Parisio et al, 2020). The supercritical reservoirs must have pressure more than 21,8 MPa and temperature more than 374°C. This state is best condition for CCS implication, since it bury completely CO_2 – it cannot leak under the brine.

Phase diagram of carbon dioxide is provided in figure 2.1.

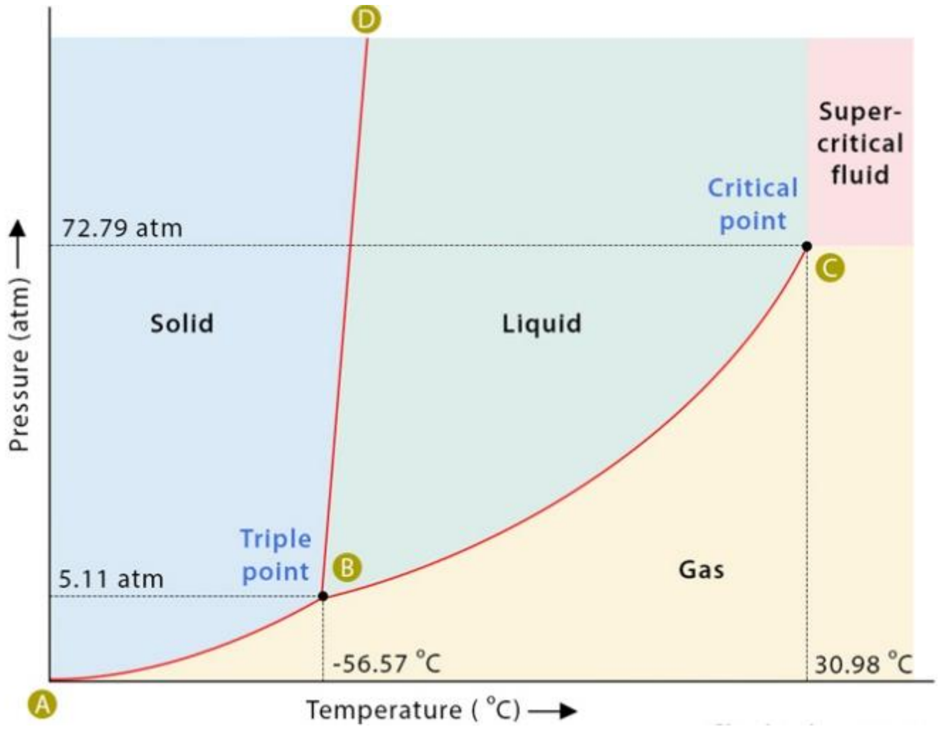

Figure 2.1 – Phase Diagram of Carbon Dioxide (Gupta, 2023).

The critical point of CO_2 is the temperature and pressure at which the difference between liquid and gas phase has disappeared.

Critical point for CO_2 has the following pressure (P_{cr}) and temperature (T_{cr}):

$$P_{cr} = 73{,}773\ bar$$

$$T_{cr} = 304{,}128\ K\ (273{,}15°\mathrm{C})$$

Above these presented conditions, CO_2 enters a supercritical state, where it exhibits properties of both gaseous and liquid state. So, this condition is characterized as high density and low viscosity. It makes this state ideal for applications in enhanced oil recovery and carbon storage in salien aquifers. In the supercritical state, CO_2 can diffuse through solids like a gas but dissolve materials like a liquid.

A huge number of scientists studied CO_2 EOS from 1969 with different range of Pressure and Temperature (Span and Wagner, 1996).

One of the most popular and common EOS was presented by Peng and Robinson (PR):

$$P = \frac{R \cdot T}{v - b} - \frac{a(T)}{v(v+b) + b(v-b)}$$

$$b = 0{,}778 \cdot \frac{R \cdot T_c}{P_c}$$

$$a(T) = 0{,}45724 \cdot \frac{R^2 \cdot T_c^2}{P_c} \cdot \left(1 + n\left(1 - \sqrt{\frac{T}{T_c}}\right)\right)^2$$

$$n = 0{,}37464 + 1{,}54266 \cdot \omega - 0{,}26993 \cdot \omega^2$$

Where P – pressure (Pa), T – absolute temperature (K), v – molar volume (m^3/mol), R – universal gas constant (J/ mol·K), b – special co-volume parameter for PR EOS (m^3/mol), $a(T)$ – temperature-dependent parameter (Pa·m^6/mol^2), T_c – critical temperature (K), P_c – critical pressure (Pa), n – empirical temperature-correction parameter in PR EOS (-), ω – acentric factor (-).

The most detailed and accurate, but the most needed sources EOS was presented by Span and Wagner in 1996 (Span and Wagner, 1996):

$$\varphi(p_r, T_r) = \varphi^0(p_r, T_r) + \varphi^1(p_r, T_r)$$

Where φ – reduced (dimensionless) Helmholtz free energy (-), φ^0 – Ideal-gas Helmholtz free energy (-), φ^1 – residual Helmholtz free energy (-), T_c – critical temperature (K), P_c – critical pressure (Pa).

All quantities reported above are non-dimensional; namely:

$$\varphi = \frac{A}{RT};\ P_r = \frac{P}{P_c};\ T_r = \frac{T}{T_c}$$

Where φ – reduced (dimensionless) Helmholtz free energy (-), A – molar Helmholtz free energy (J/mol), R – universal gas constant (J/mol·K), T – absolute temperature (K), T_c – critical temperature (K), P – pressure (Pa), P_c – critical pressure (Pa).

Here A represents the dimensional Helmholtz free energy. The equation represents its division into two terms; the first represents the contribution due to ideal quantities and is defined analytically, while the second represents the real gas contribution and is determined by the fit of experimental data.

Ideal Helmholtz energy is defined as follows:

$$A^0 = h^0(T) - RT - TS^0(P, T)$$

Where A^0 – Ideal-gas molar Helmholtz free energy (J/mol), $h^0(T)$ – Ideal-gas molar enthalpy as a function of temperature (J/mol), R – Universal gas constant (J/mol·K), T – absolute temperature (K), $S^0(P, T)$ – Ideal-gas molar entropy as a function of pressure and temperature (J/mol·K), P – pressure (Pa).

So, the task of finding PVT properties of pure CO_2 is already lighten by some manual books in which represents tons of data about properties in different pressure and temperature (Anwar & Caroll, 2016).

To know the exact PVT properties of CO_2 is one of the most important task today, since it has huge impact on the whole process. The proper choice of the developing model is nevertheless presents

2.1.3 Trapping Mechanisms

As presented above, saline aquifers represents the most encouraging solution for CO_2 storing, since it has many potential places around the world.

It is important to understand what makes saline aquifers to be one of the best solution as storage for carbon dioxide – their multivariate mechanisms for CO_2 trapping. Classification of CO_2 trapping mechanisms in saline aquifers presented in figure 2.2.

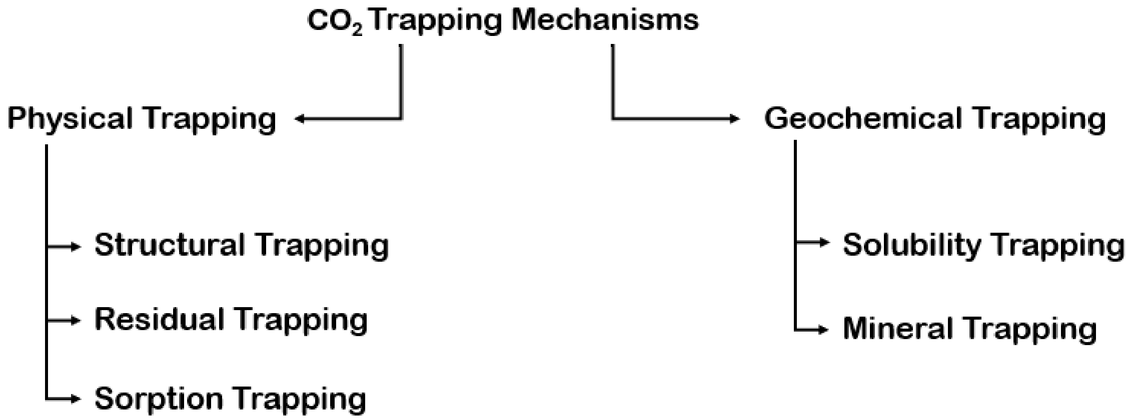

Figure 2.2 – Different CO_2 trapping mechanisms in saline aquifers.

Geologic sequestration of carbon dioxide relies on the trapping mechanisms in nature, which means, in order to store the carbon dioxide that has been injected, it must be trapped by the mechanisms by which the injected carbon dioxide must not find its way back to the surface. This way can be done through legacy wells, artificial fractures or natural faults.

Trapping processes involve storage operations whose timescales of operation translate to instant and long-term protection of injected CO_2. Physical trapping alongside geochemical trapping characterize the major processes in carbon dioxide storage in dividing custody of separate phase storage of CO_2 and changes in chemistry of CO_2. The storing controls through physical trapping techniques hold CO_2 storage only during the initial hundred years of operation time but geochemical processes are necessary to store over a long period of several decades to millennia. Ajayi (2019) noted that the 3 main physical trapping processes working in the initial parts of the storage are structural (or hydrostratigraphic), residual (capillary) and sorption trap. All these storage mechanisms work together to provide an increase in the overall CO_2 capacity and safety when carbon sequestration is being conducted.

Physical trapping involves storing CO_2 in the natural subsurface retention without the utilization of the chemicals. At this stage there is a buoyant phase of injected CO_2 that is either in the supercritical or gaseous phase and it is constrained by geologic barriers (caprock) and capillary forces so it will not flow to the surface through the permeable porous media. The first physical trapping process of containment begins right after the end of injection and extends through the first century as stated by Ajayi (2019).

Structural trapping of CO_2 is an initial mechanism to lock it in the geologic storage (also referred to as a stratigraphic trap or hydrostratigraphic trap) (Ajayi, 2019). Figure 2.3 illustrates this example. The vital requirements covering the effective use of this mechanism are the use of an impermeable barrier (caprock or seal) and a decent geologic framework that will physically trap the buoyant CO_2 under it. In the deep injection process, carbon dioxide becomes less dense than formation brine thus once the injection ceases, it has the natural tendency to rise because of buoyancy.

CO_2 flows up where it accumulates under laterally extensive caprock (low-permeability rocks) that acts in the same way as oil and gas entrapment in a subsurface reservoir. CO_2 storage must be placed in anticlinal folds with seal rock or stratigraphic trap where a closed space to store the CO_2 plume has to be created using depository pinch-outs or sealed faults as explained by Ajayi (2019) and presented in figure 2.3.

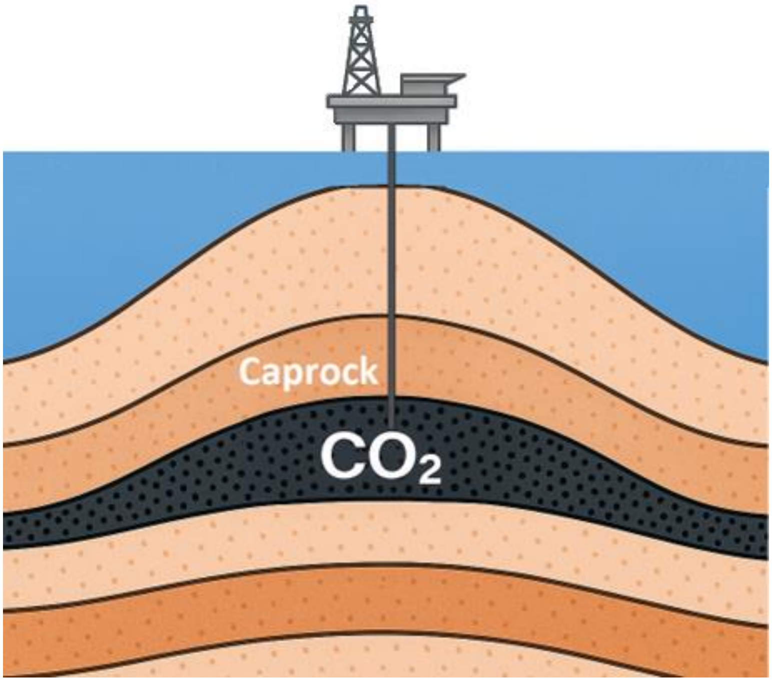

Figure 2.3 – Example of structural trapping for CO_2.

In case of depleted oil and gas fields as CO_2 storage, petroleum geology possesses structural and stratigraphic elements that preserves hydrocarbons under surface for millions of years, and this as well fulfills the qualification of carbon storage. To ascertain how structural trapping acts as the primary arm against upwards movement of CO_2 (Hepple and Benson, 2005) explain that impermeable seals act as barriers of flow. The North Sea structure of the Sleipner gas field proves structural trapping because the injected CO_2 is trapped under a thick shale caprock that acts as a natural gas trap (IPCC, 2023). Structural trapping is contingent on the quality as well as composancy of the seal substance since the caprock must possess very low permeability along with ensuing capillary entrance pressure to bar the CO_2 column (Org, 2008).

Ai Hameli (2022) reports that the main proportion of trapped CO_2 after the injection is conducted by the structural trapping mechanism. Two major risks affecting the long-term structural trapping security is the possibility of fractures in the caprock that will be beyond the detection limitations and legacy wells that cut the seal particularly could facilitate leakage of the CO_2 through these means. The other trapping mechanisms should be combined with structural containment techniques with the aim of realizing maximum safety as the resultant effect of the two will realize improved security. Scenarios of structural trapping found on natural reservoir architecture combined with seal constructions trap upraised CO_2 flumes temporarily or in the course of short-to-intermediate periods, making use of the subsurface CO_2 trapping mechanism.

Residual trapping (also called capillary trapping) is another process used in the trapping of CO_2 in rock pore spaces in the form of small, separated droplets due to their inability to move due to capillary forces (Ajayi, 2019). Figure 2.4 illustrates this example of residual trapping. The injection of CO_2 in the reservoir rock causes it to be trapped during and after injection as it makes its way through the pore network of the reservoir rock. In cases when the flowing rate of CO_2 reduces or the brine re-enters the plume, isolated CO_2 droplets form in the pore spaces under capillary hysteresis after the displacement of brine (Ajayi, 2019).

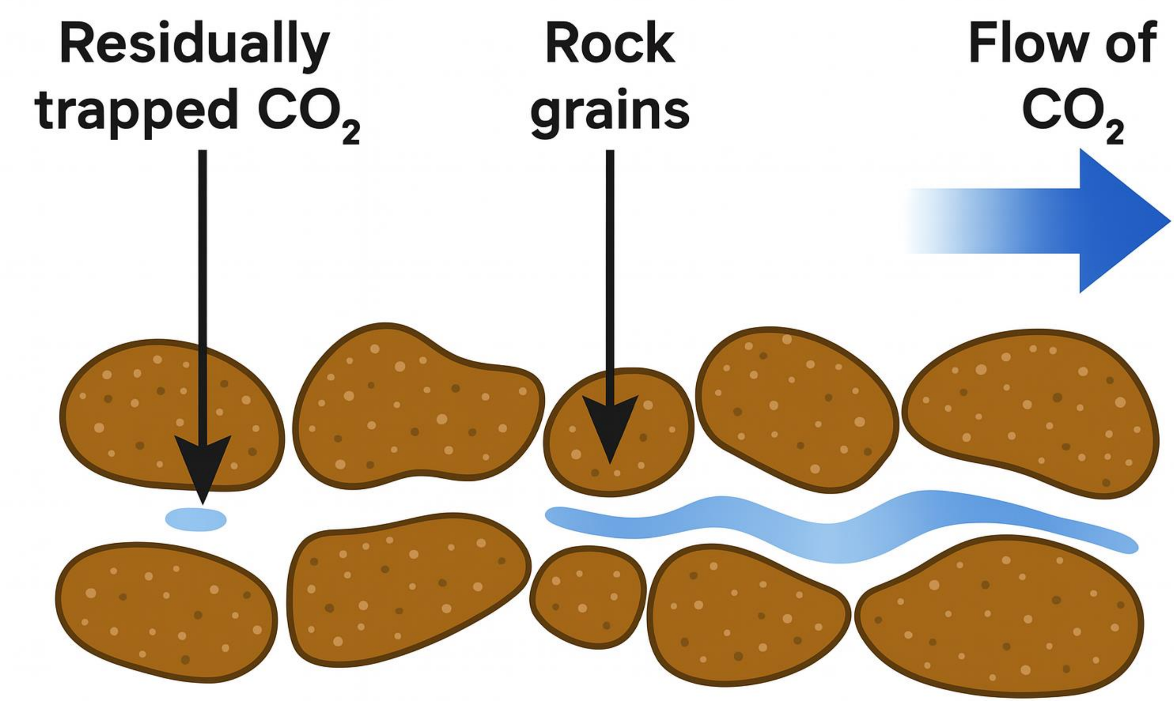

Figure 2.4 – Example of residual trapping for CO_2.

Squeezing of pores leads to the trapping of CO_2 blobs that are present in the corners of the pores and crevices being trapped by the imbibition of brine. The repulsion between brine and CO_2 builds pressure that does not allow the movement of the CO_2 blobs. In other words, the carbon dioxide is squeezed off and remains as a fixed immobile gas at the pore scale to the residual level of the gas saturation point. The CO_2 is trapped in this manner since it could not flow or move due to the presence of the capillary forces. The process is associated with benefits of the rocks having complex pore systems coupled with narrow pore channels to ensure that the phase of the CO_2 is further separated into individual droplets.

Residual trapping acts as a quick efficient mechanism that improve the levels of storage integrity immediately after injection. The studies revealed that much of the injected CO_2 will remain in a residually trapped state during a period of first few years of the injection operation hence decelerating the advancement of the plume (Alcalde, 2018). In an experimental measurement under reservoir conditions, it has been indicated that major fractions of CO_2 can be held immobile due to residual trapping at exactly the time that the plume is passing through the rock. The experiments of core floods and field tests indicated residual CO_2 saturations range between 10-30% of pore volumes that signify 10-30% of pore spaces is occupied with immobile phase of residual CO_2 after percolation of the plume (Ajayi, 2019).

It can be proved by figure 2.5. The CO_2 plume does not move because of the residual entrapment by dipping aquifers without structural barriers as this forms a physical barrier to indefinitely up-dip migration (Szulczewski, 2013). Figure 2.5 illustrates the explanation of residual trapping mechanisms, since some amount of CO_2 in pores (10% in the graph) is immobilized and trapped.

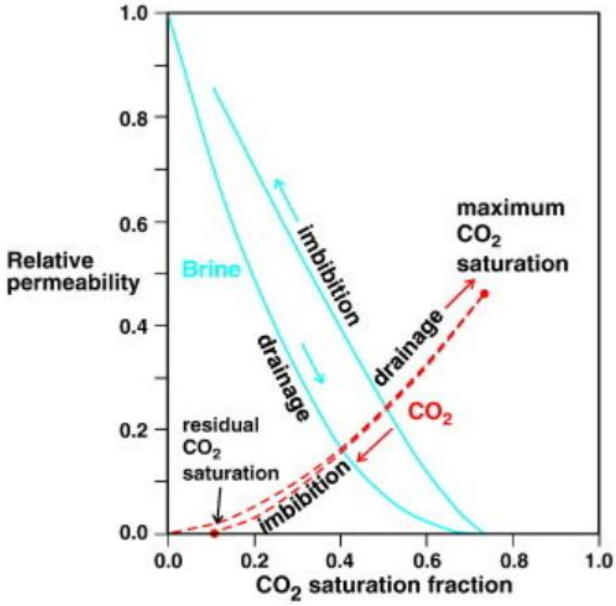

Figure 2.5 – Relative permeabilities for CO_2-brine system (Kampman et al, 2014).

The storage method of residual trapping offers a better storage, as opposed to the use of a single structural trap. Large number of small constituent bubbles of CO_2 of micro-order prevents any large leak. The CO_2 entrapped in the capillary will remain trapped in the same position since it is not needed to have the seal on the capillary to remain fixed even after the structural trap collapses (Ajayi, 2019). When CO_2 is trapped in using this technique then chances of leakage is reduced since the entire pool of CO_2 in an area covered by a caprock does not become one single phase, a gas which upon losing the caprock may leak. CO_2 is held in trap under stable conditions due to the fact that major perturbation of reservoir parameters is required to free the CO_2 (e.g. pressure drawdown may mobilize some CO_2 but remaining saturations usually persist). The Reliance of residual capillary trap as a storage security mechanism to the CO_2 storage on a decadal level is attributed to its stable character.

Sorption trapping is the process through which CO_2 molecules adsorb on solid reservoir surfaces through physical adsorption in organic-rich reservoirs including coal seams and organic shales. CO_2 molecules tend to adsorb or attach themselves on porous matrix surfaces (adsorption) and penetrate microporous space (absorption in amorphous matrices) of such rock units which enables them to adsorb on solid matter and abandon the fluid phase.

Storage by sorption trapping is highly important in ECBM cases as well as shale units because such rocks contain widespread microporosity and organic matter which enables them to possess high gas sorption capacity (Ai Hameli, 2022). Coal internal surface areas naturally contain methane (CH_4) adsorption which converts to CO_2 adsorption through CO_2 injection leading to the recovery of ECBM (Qu, 2012). Coal's surface strongly adsorbs CO_2 molecules and organic matter in shale, thus enabling coal to be able to store huge immobile amounts of CO_2. White et al. (2005) proved that coal's microporous nature creates expansive surface space for gas adsorption which makes adsorption the primary storage mechanism in coal seams (Qu, 2012). A high percentage of gas in coal is stored in the form of adsorbed molecules because studies indicate 95-98% of coal seam gas capacity is by adsorption.

Organic-rich shale reservoirs are subjected to the same process as the other storage mechanisms. Shale reservoirs contain free gas that occupies pore volume and organic matter, and clay surfaces contain adsorbed deposits of gas. Adsorption capacity in the shale deposits depends primarily on total organic carbon content (TOC) and also on the distribution of clay fraction.

Research indicates that the amount of adsorbed gas in shales may be 20% greater up to 85% greater than free gas depending on TOC and mineral content. Injecting CO_2 into depleted shale gas storage reservoirs triggers absorption of CO_2 molecules by organic-rich matrix and clay reducing mobile-free CO_2 saturation. Adsorption in shales and coals occurs instantaneously because pressure/temperature equilibrium is achieved within hours to days which leads CO_2 to bond to the rock surface the moment it comes into contact. The mechanism performs effectively under injection operation.

Sorption trapping supports operation by freeing hydrocarbons because CO_2 has greater adsorption properties for coal than CH_4 so the injected CO_2 pushes out adsorbed methane in order to release the methane to be produced and occupy its place on the coal surface. Various pilot tests as well as research (Qu, 2012) have proven that the sorption trapping not only traps CO_2 but also increases methane production. Coal's strong affinity for CO_2 allows its storage by what effectively amounts to chemical sequestration although the mechanism is based on physical adsorption rather than chemical bonding.

Geochemical trapping of CO_2 in the long-term scale accentuates the role of the process in the permanent storage of this greenhouse gas. The process of geochemical trapping begins when CO_2 behavior is as a second phase which converts to dissolved fluids or solid mineral phase after reacting with other chemical components. The processes exclude CO_2 in moving phases to incorporate it into liquid or solid reservoir stages that reduces strongly the chances of leakage over several centuries to millenniums.

The security of long-term storage by geochemical trapping becomes complete since mineralized or dissolved CO_2 becomes non-buoyant form and hence it will not leak out. The most important process in regard to geochemical trapping is solubility trapping which occurs when CO_2 penetrates formation brine which is then converted to ions via ionic speciation and convective mixing processes. The mineral trapping occurs due to the carbonate mineral ($CaCO_3$ and $MgCO_3$) formation as a result of the dissolved CO_2 with minerals of the rocks. These processes take a longer time than physical trapping and hence the storage security is enhanced over time since they are able to trap higher amounts of CO_2.

In solubility trapping, the CO_2 dissolves diluting the native brine that is found in the reservoir. This is the same process that happens when sugar dissolves in tea since supercritical or gaseous CO_2 dissolves in water at levels when the solution is already saturated. When CO_2 erupts into the brine, it becomes a non-buoyant form of CO_2 that rules upward buoyancy forces on a given portion of CO_2. The fluid that results is CO_2-enriched brine that is present in one homogeneous phase with dissolved CO_2 molecules. The released CO_2 is dissolved in the water, changing into the weak carbonic acid (H_2CO_3). This weak acid decomposed into a bicarbonate (HCO_3^-) and carbonate (CO_3^{2-}) ions. The reaction hosts how bicarbonate and a proton are created when there is a reaction between CO_2 and water as $CO_2 + H_2O \rightleftharpoons H^+ + HCO_3^-$. The ionic particles created by way of dissolution are competent to engage with the cations in the solution (Ca^{2+}, Mg^{2+}, Na^+) to create neutral or ionic partners ($CaHCO_3^+$) in the solution.

There are two key dissolution processes that the brine incorporates in the absorption of the CO_2. They are the diffusive mixing as well as convective mixing. At the initial stage of being introduced into the brine, CO_2 plumes create a certain boundary. Diffusion in concert with the CO_2 plume-brine interface acts as the initiation point to the CO_2 dissolution due to the concentration gradients in the adjoining CO_2 plume and brine. Molecular diffusion of CO_2 into still water is comparatively slow and would result only in a slow intake of CO_2 over the course of time.

Molecular diffusion of CO_2 into still water is comparatively slow and would result only in a slow intake of CO_2 over the course of time. Fortunately though, there exists a phenomena that slows down the process by a large margin, this is the fact that when CO_2 dissolves, the brine becomes a little bit denser (CO_2-saturated brine will end up being about 1 to 3% denser than the CO_2-free brine depending on the pressure-temperature-salinity conditions present).

Figure 2.6 illustrates trapping mechanism. Convective dissolution is an important process due to the ability to produce a rapid dissolution of abundant amounts of CO_2. Realistic storage structures exhibit convective stirring which starts within a few years to tens of decades after injection occurs. After the convection is established, the rate of reaction of CO_2 dissolving in the brine escalates dramatically since fresh water keeps on encountering CO_2. The solubility trapping accounts the high volumes of the additional CO_2 injected into the solution of the brine water during the long periods of time that may course thousands to hundreds of years. Illustration based on time-lapse seismic data that has been used to document a well-known saline storage project (the Sleipner project) indicates that the CO_2 dissolves into formation water over time and potential modeling estimates that a big percentage of the CO_2 (up to 30-40%) may dissolve over time as the convective mixing process proceeds on over various centuries (Lindeberg et al, 2002).

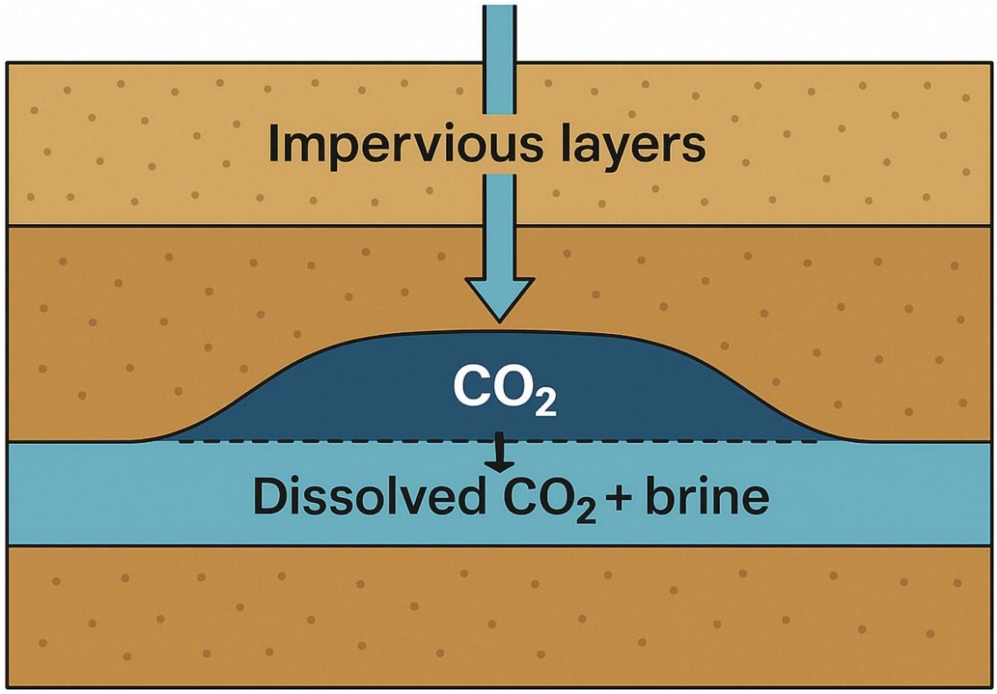

Figure 2.6 – CO_2 solubility trapping.

When solubility trapping is completed, the formation brine maintains dissolved CO_2 in a homogeneous concentration. When CO_2 is in this form it is virtually impossible for leakage since the gas no longer occurs as a buoyant distinct phase capable of moving through the system. Movement of dissolved CO_2 is by the mechanism of hydrodynamic dispersion along with the slow regional groundwater flow that moves at less than a meter per year. Ionization of dissolved CO_2 as bicarbonate results in aqueous solute that geochemical reactions such as ion exchange or slightly acidified water interacting with minerals are capable of trapping quite effectively. The geochemical solubility trapping mechanism converts free-phase CO_2 to dissolved phases in reservoir brine by using convective mixing to speed the process of dissolution with time. It inhibits CO_2 escape by buoyancy and is the foundation of the permanent trapping mechanism by mineral precipitation.

The safest and most resilient mode of CO_2 sequestration is by mineral trapping that transforms dissolved CO_2 into stable solid mineral carbonates through chemical reactions with host rock. The

CO_2 (as bicarbonate and carbonate ions in solution) reacts with present metal cations (calcium, magnesium, iron, sodium, or potassium) present in the formation water and forms carbonate minerals such as calcite ($CaCO_3$), magnesite ($MgCO_3$), siderite ($FeCO_3$) or dolomite ($CaMg(CO_3)_2$).

Mineral trapping geochemical process transforms carbon into stable crystalline solids that will stay for thousands to millions of years in geological reservoirs. Figure 2.7 illustrates the process. Mineral trapping is safest in the view of most because entrapment into rock does not allow migration or leakage of carbon. The process takes naturally longer time compared to the others since geochemical reactions take decades or more to make significant progress under natural reservoir conditions. The brine solution with dissolved CO_2 must first experience solubility trapping before mineral reactions can occur. The large-scale mineral sequestration process becomes critical in the time scale of hundreds to thousands of years in average sedimentary reservoirs. The slow mineral trapping process is still useful in the long-term storage because the process allows the entrapment of large CO_2 amounts into solid form over long periods. Mineral trapping is the most stable and permanent process for CO_2 storage because carbon becomes part of rock matrix components.

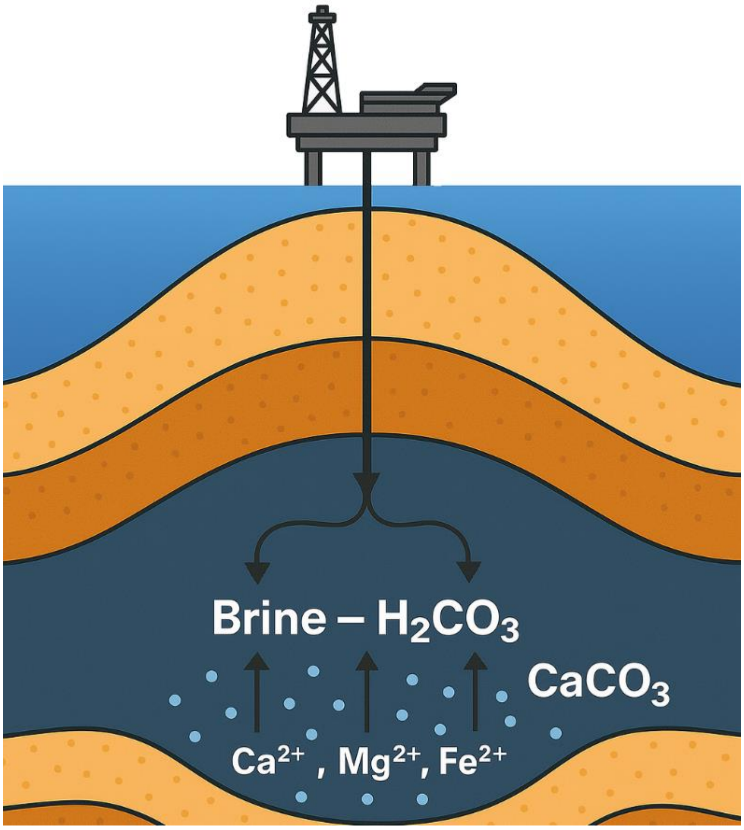

Figure 2.7 – Mineral Trapping of CO_2 in saline aquifers.

These reactions were tested in labs to show proof of their efficacy but the rate of progression within situ is sluggish. Long period of time consuming to trap minerals is the major disadvantage of this process as argued to goodman et al. (2002). According to the modeling studies, it is reflected that a significant part of the CO_2 will not convert to mineral until the first 200 years but the conversion rate will be very high in the next 1000 years. The report by IPCC (2005) shows that mineral trapping would emerge as the most dominant form of CO_2 trapping in diverse reservoirs even after 1000 years whereas the mineralization rate would be low after 100 years. Xing (2022) reports that the CarbFix project in Iceland achieved impressive conversion of injected CO_2 into sturdy carbonates of 95% within only two years. Basalt precipitated mineral of calcite and other carbonates with high calcium and magnesium content and the injection of aqueous phase of CO_2 to reduce kinetic barriers (Matter et al., 2016). The outstanding account of this research study shows that mineralizing the CO_2 is dependent on the system-specific phenomena as the ultramafic and basaltic rocks cause the various rates at which the CO_2 gets trapped compared to taking place in decades in the sedimentary reservoirs (Xing, 2022).

Safe retention of CO_2 underground is highly reliant on physical and geochemical trapping systems that will keep the CO_2 incorporated in geological CO_2 storage. Physical entrapment regulates CO_2 storage at a young age of years to decades through three processes; structural traps and impermeable caprock layers hold buoyant CO_2, capillary forces entrap CO_2 in the pore space and surface sorption expels CO_2, free phase. The quick procedure simulates the natural storage of hydrocarbons since these operations mimic procedure which have kept hydrocarbons secure after a thousand years in reservoirs.

2.2 Two-Phase Flow Dynamics in Pipes, Wellbores and Subsurface Systems

Pipeline distribution of CO_2 is a crucial part of the operation of many industrial procedures, such as CCS projects, EOR schemes, and chemical manufactures. Understanding the dynamics of how CO_2 flows in pipelines is also critical in optimizing efficiency in transporting CO_2, reducing risks and in safely and effectively operating CO_2 transport systems under various conditions.

The transportation of CO_2 differs with that of oil and natural gas. CO_2 and CH_4 are under normal conditions. Nevertheless, the difference between these two is that the C atom in CO_2 is already oxidized: it already is a positively charged ion (+4), and thus CO_2 cannot be burned, whereas C atom in CH_4 is negatively charged (-4). Therefore, the given feature can be utilized in compressor station where it is possible to split flow within a pipe in 2 directions - small quantity into gas turbine engine and rest into a compressor.

On the other hand, oil in normal condition is in liquid form and basically transported using pumping stations. Cavitation is one of the most important problems of oil transportation. The oil cavitation is a phenomenon which happens in the oil-based system, it is presented by the generation and collapse of vapor or gas blisters in the liquid on the basis of the change of the pressure. It is widely noted in hydraulic system, pumps, bearings, hydraulic cylinders and other mechanisms that make use of oil as a working medium. Control of this process is important as cavitation could destroy pumps.

Generally, the transportation of CO_2 is being carried out in dense-liquid state. As it is stated above, CO_2 has both critical and triple points, which complicate the process. The next challenge could be that post CCS stage, in most cases, CO_2 is not necessarily pure, it will always have some particles of impurities. Such impurities will affect the thermodynamic properties.

Other alternative ways of CO_2 transportation were showed in figure 2.8. It should be noted that the pressure drop of supercritical transport is higher than the pressure drop of liquid transport and dense-phase transport and the pressure drop of the liquid transport is higher than the pressure drop of dense-phase transport. Pressure drop of the pipeline is influenced by the ambient temperature to a higher level. The more the ambient temperature, the higher the drop in pressure is. Furthermore, on an equal operating condition, the CO_2 pipeline will experience a lower pressure drop than the natural gas pipeline, however, the temperature drop will be larger and CO_2 is more prone to forming hydrates than natural gas.

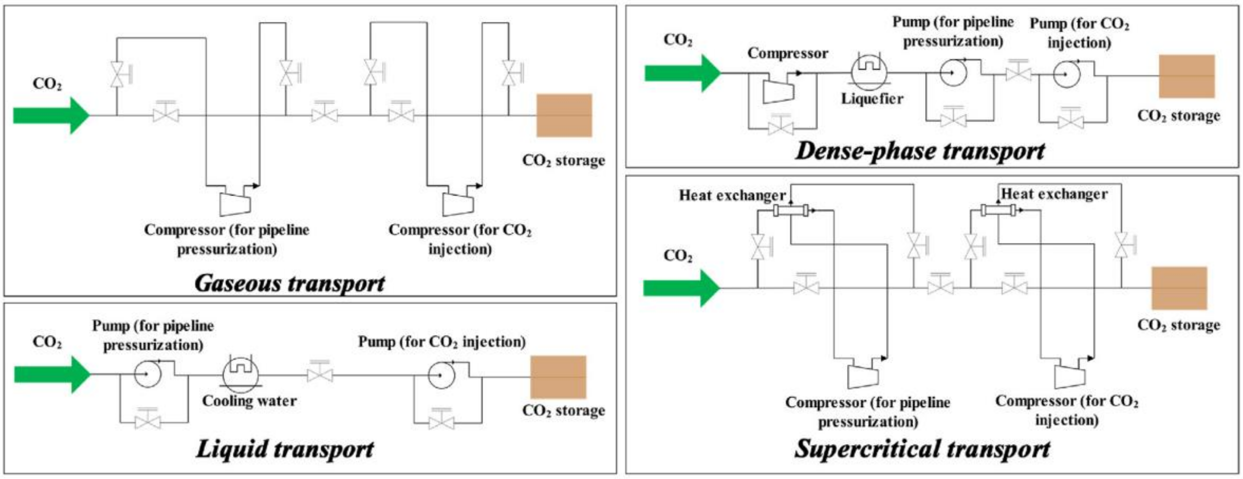

Figure 2.8 – Four process flow diagrams suitable for large-scale CO_2 pipeline transport (Lu et al, 2020).

Hence, the gaseous transport of CO_2 demands temperature and pressure control to a great extent. In the case dense-phase transportation is chosen, the influence of the pipeline inlet temperature on the change in pressure of the media is insignificant, whereas its impact on temperature is drastic (Lu et al, 2020).

When supercritical transportation is employed the effect of pipeline inlet temperature on the pressure is minimal. But, on the way of transportation, the temperature is falling swiftly, therefore, the phase transition would take place within a reduced highway length. The ambient temperature influences the pressure drop of the pipeline less but the temperature of one more (Lu et al, 2020).

Typically, the process can be outlined in figure 2.9. The ways through which CO_2 can be captured are – post-combustion, pre-combustion and oxy-fuel combustion capture. Capturing of CO_2 takes place after it is in the form of gas. Then it will go to the compressor where the gaseous matter will get converted to the liquid form and move to pump.

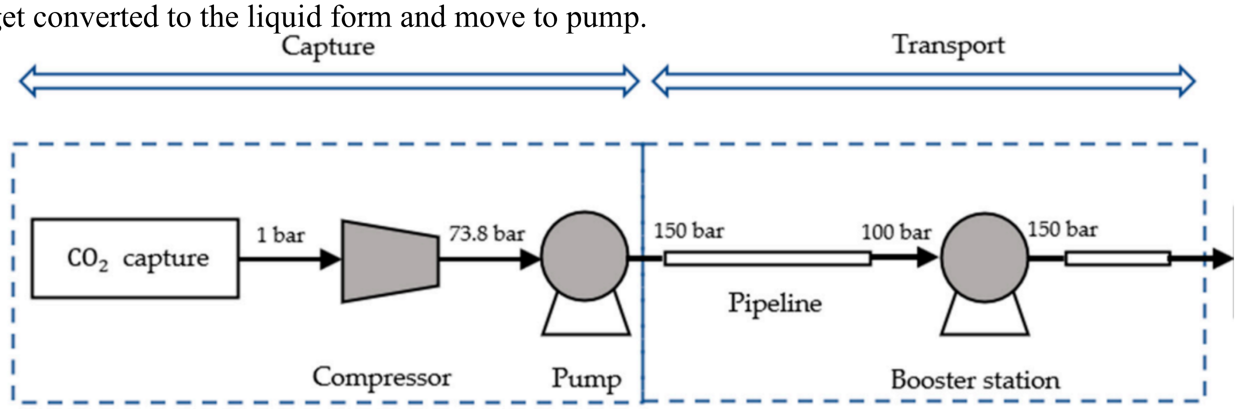

Figure 2.9 – CO_2 processing (Solomon, 2024).

In practice, pipeline transportation of liquid and gas distinguishes two transportation modes – steady-state and transient. Steady-state flow in pipeline transportation refers to a condition where the fluid properties, such as pressure, temperature, density, and flow rate, remain constant at every point along the pipeline over time. This means that there are no fluctuations or changes in these parameters as the fluid moves through the pipeline. Whilst transient flow shows when some operational processes arise – like, startup, shutdown and accidents with pumps or compressors.

As it said before, generally, transportation of CO_2 in dense-liquid form is preferable as it saves more energy to process. Unfortunately, because of the transient flow condition in pipe is not stable.

So, CO_2 may change phase from dense liquid to two-phase – liquid and gas (Aursand, 2013). Physically, in pipe should be gravity-induced segregation – gas will be on the top of the pipe.

In pipeline theory all equations are built on the 3 main laws: conservation of mass, moment and energy across the cross section in the pipe. In multiphase pipe flow, there are flow regimes where the velocities of the individual phases are highly correlated. For two-phase flow, the relative velocity between the phases can be expressed as a slip relation.

$$u_1 - u_2 = \Phi(\alpha_1, P, T, u_1)$$

Where u_1 – velocity of the phase 1 (m/s), u_2 – velocity of the phase 2 (m/s), Φ – Slip-correlation function (m/s), α_1 – volume fraction of phase 1 (-), P – pressure (Pa), T – temperature (K).

The behavior of two-phase flow can change dramatically depending on the amount of gas in the flow and the velocity of each phase. This behavior flow can typically be divided into flow regimes, such as bubbly, stratified, slug, churn, annular and dispersed/mist flow. These flow regimes are presented in figure 2.10 and table 1.

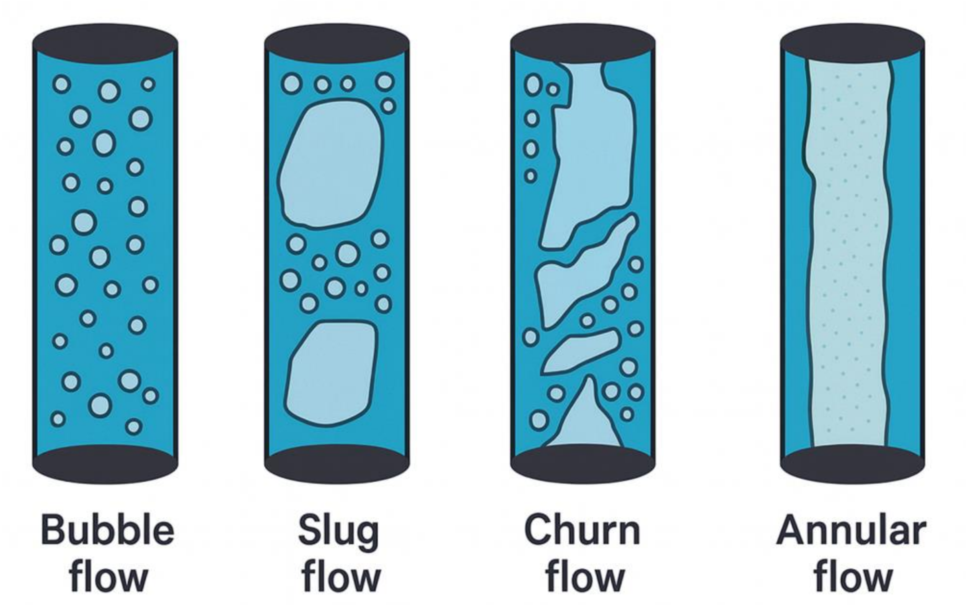

Figure 2.10 – Different flow regimes in two-phase flow.

Table 1 – Flow regime description.

Flow regime	Description
Bubble	Liquid-continuous flow with entrained gas bubbles
Slug	Bubble flow where small bubbles have coalesced into larger cap bubbles
Churn	Bubble flow with larger, “chaotic” gas structures
Annular	Liquid-rich near the wall with a gas-rich core, not necessarily gas continuous

Based on the 3 conservational laws and assumptions that pressure and temperature in liquid and gas phase is equal we can get drift-flux model. Drift-Flux Model (DFM) is an approach used to describe and model two-phase flow (e.g., liquid and gas) in pipelines. It is particularly useful for systems where CO_2 can exist in two phases simultaneously (liquid and gas) under certain temperature and pressure conditions.

So, this model can be described in the following equations (Aursand, 2013):

1. Conservation of mass:

$$\frac{\partial}{\partial t}(\rho_g \alpha_g) + \frac{\partial}{\partial t}(\rho_g \alpha_g u_g) = \Gamma;$$

$$\frac{\partial}{\partial t}(\rho_l \alpha_l) + \frac{\partial}{\partial t}(\rho_l \alpha_l u_l) = -\Gamma;$$

2. Conservation of momentum:

$$\frac{\partial}{\partial t}((\rho_g \alpha_g u_g + \rho_l \alpha_l u_l) + \frac{\partial}{\partial x}(\rho_g \alpha_g u_g^2 + \rho_l \alpha_l u_l^2 + p) = (\rho_g \alpha_g + \rho_l \alpha_l) f_x - M_w$$

3. Conservation of energy:

$$\frac{\partial}{\partial t}(\rho_g \alpha_g E_g + \rho_l \alpha_l E_l) + \frac{\partial}{\partial x}\left(\left(\rho_g \alpha_g u_g \left(E_g + \frac{P}{\rho_g}\right)\right) + \left(\rho_l \alpha_l u_l \left(E_l + \frac{P}{\rho_l}\right)\right)\right) = (\rho_g \alpha_g u_g + \rho_l \alpha_l u_l) f_x + Q_w.$$

Where t – time (s), x – axial coordinate along the pipe (m), ρ_g – gas-phase density (kg/m^3), ρ_l – liquid-phase density (kg/m^3), α_g – gas volume fraction (-), α_l – liquid volume fraction (-), u_g – gas-phase velocity (m/s), u_l – liquid-phase velocity (m/s), Γ – Interfacial mass-transfer source term (kg/m^3·s), P – pressure (Pa), E_g – gas-specific internal energy (J/kg), E_l – liquid-specific internal energy (J/kg), f_x – body-force term along x (m/s^2), M_w – wall-friction momentum sink (N/m^3), Q_w – wall heat source (W/m^3).

In spite of the fact that the field of modeling multiphase flows can be discussed as the well-established discipline, in fact modeling of closures does not exist allowing to apply the similar approach in the case of any fluid. Flow maps and correlations must be validated, revised or established with every new working fluid or fluid composition. This is one of the main issues of modeling the CO_2 flow in pipes. There are existing correlations and models that have been applied in research and industries in the oil-gas-water mixture, but they cannot be valid in CO_2 which contains impurities. The new use of these models needs experimental contribution towards the validation of these models.

The other challenge is hydrate formations of CO_2. Numerous studies have been conducted so as to have a better idea on which parameters (composition, temperature and pressure) cause the formation of hydrates with CH_4. In the case of CO_2, enough data are still deficient. This is an open door to the study of synthesis of pure CO_2, impure CO_2 hydrate formation.

In the article (Lu et al, 2020), scientists do research in the field of optimization of CO_2 transportation in a more economical and energy-saving manner. Pipes with different diameters, rates and pressure were considered. In conclusion of the work, it is stated that the optimal diameter of the pipeline in which CO_2 is to be transported comprises factors such as mass of something to be transported, distance to be covered, temperature during transportation, pressure drop throughout the pipeline, and the amount of booster stations. There must also be special reflection as regards pipeline investment costs, costs of operations, energy costs and interests rates in order to determine the best method of transportation.

Associated with petroleum transportation, CO_2 transportation also need pump stations in each 70-150 km (depends of profile, material, power). For understanding of this distance, one need to know the pressure drop along the distance between pump stations.

To calculate the pressure, drop along pipeline one might use the based Darcy – Weisbach equation (Darcy, 1857):

$$\Delta P = f \cdot \frac{L}{D} \cdot \rho \cdot \frac{v^2}{2}$$

Where ΔP – pressure drop along the pipe (Pa), f – coefficient of pressure loss because of friction (-), L and D are length and diameter (m), ρ – density (kg/m^3) and v – CO_2 flow velocity (m/s).

To calculate temperature distribution along pipeline one might use Shuhov's equation (Moiseev et al, 2016):

$$T_L = T_{amb} + \left(T_q - T_{amb}\right) \cdot e^{\left(-\frac{\pi \cdot d \cdot k \cdot L}{C_p Q_m}\right)} + u_{JT} \cdot e^{\left(-\frac{\pi \cdot d \cdot k \cdot L}{C_p Q_m}\right) \cdot \frac{dP}{dx}}$$

Where T_L – temperature at the length L (K), T_{amb} – ambient temperature (K), T_q – inlet temperature of CO_2 (K), d – pipe diameter (m), k – heat-transfer coefficient (W/m^2·K), C_p – specific heat capacity (J/kg·K), Q_m – mass-flow rate (kg/s), u_{JT} – Joule-Thomson coefficient (K/Pa), $\frac{dP}{dx}$ – axial pressure gradient (Pa/m).

Based on (Lu et al, 2020), it can be said that a pressure drop along pipeline can range between 0,5 and 1,5 bar/km. Among the most significant ones, there is the need to preserve the pressure over critical point (73,8 bar) to maintain the dense liquid state.

Regarding CO_2 injection wells, the flow of fluid can be in supercritical or liquid phase that depends on pressure, temperature and flow rates. Recent experiments by Hammer et al. (2021) presented that CO_2 passes in vertical wells as homogeneous mixture, with minimal gas-liquid slip. According to figure 2.1, gas phase can exist in the well till 72,79 bar, so if the pressure is hydrostatic in the well, it means that there exists double-phase flow up to 730 m MD (Measured Depth). It should be noted that Hammer et al. (2021) observed that the CO_2 remains well-mixed with little phase segregation. It yields flow regimes of dispersed bubbles or droplets rather than stratified flow.

There can be two types of injection wells – mostly used vertical wells and horizontal wells. The choice is matter for flow regime and pressure drop. In vertical flow gravity opposes the movement of the lighter gas phase, causing co-current flow in the middle (annular flow). However, as noted above, near critical conditions often get well-mixed flow. On the other hand, horizontal wellbore flow causes the segregation of phases. In case if the wellbore is under the critical pressure – two phase segregate by gravity – lighter gas phase tend to collect at the top of the pipe, while liquified CO_2 collects at the bottom. Research on horizontal well indicates that multiple sub-regimes may develop and transition between them depends on gas fraction and velocity (Greskovich et al, 1972). In the context of CO_2 injection, the horizontal wells might experience stratified flow near the well heel and more mixed flow towards to the toe. It can be useful to use inclined sections to avoid slugging that could cause oscillations in pressure.

In the context of CO_2 injection, two-phase flow dynamics become especially important as CO_2 often transitions between gas and liquid states depending on the temperature and pressure conditions within the wellbore. Additionally, the presence of gravity-induced segregation, viscosity differences, and potential interactions with impurities or other formation fluids can further complicate flow behavior.

Several models for two-phase flow have already been developed (Hammer, 2021):

1. Homogeneous model. In the homogeneous friction model, two-phase flow is treated similarly to single-phase flow, but the properties of the gas-liquid mixture are used. This assumes that both phases move at the same velocity, neglecting any slip between them. While this model simplifies calculations, it may lack accuracy in cases where significant phase separation or slip occurs, such as in CO_2 and water flows in wellbores.

2. The no-slip model assumes that the gas and liquid phases travel at the same velocity, ignoring the slip between them. This is essentially the homogeneous model but with an emphasis on equal phase velocities ($u_l = u_g$). While simplistic, this model might serve as a baseline comparison in simulations, though it may not capture the complexities of phase separation observed in CO_2-water systems.

3. The Friedel friction model (1979) is a widely used empirical correlation for calculating two-phase friction factors. It accounts for the complexities of gas-liquid interactions, providing a more accurate representation of pressure drops compared to homogeneous models. This model is useful for various flow regimes but is based on extensive experimental data, making it less flexible for unique wellbore conditions, like CO_2 injection.

4. Friedel-Haaland model combines Friedel's correlation with the Haaland (1983) friction factor, which improves predictions for rough-walled pipes. The Haaland factor is particularly useful in practical applications involving CO_2 injection wells, where wellbore roughness may affect flow dynamics.

5. The DFM is a two-phase flow approach that accounts for the slip between phases, meaning the gas and liquid can travel at different velocities. It introduces a drift velocity term to describe the relative motion between phases. This model is widely used for predicting flow patterns and phase distributions in vertical wellbores, such as CO_2 injection systems, where gravity and density differences lead to phase separation.

6. The Shi model is a drift-flux correlation based on experimental data from large-pipe flows, specifically for oil, gas, and water systems. It provides a more realistic estimation of phase distribution and velocity differences (slip) between the phases. The Shi model is particularly suitable for large-diameter wellbores, like those used in CO_2 injection, where drift-flux effects are prominent.

Nowadays, DFMs have been widely used to simulate two-phase flow in wellbores. These models can account for the relative motion between phases and are particularly useful for predicting flow regime transitions.

The paper (Hammer, 2021) studied downward flow regimes in an experimental lab. One of the results is presented in figure 2.11.

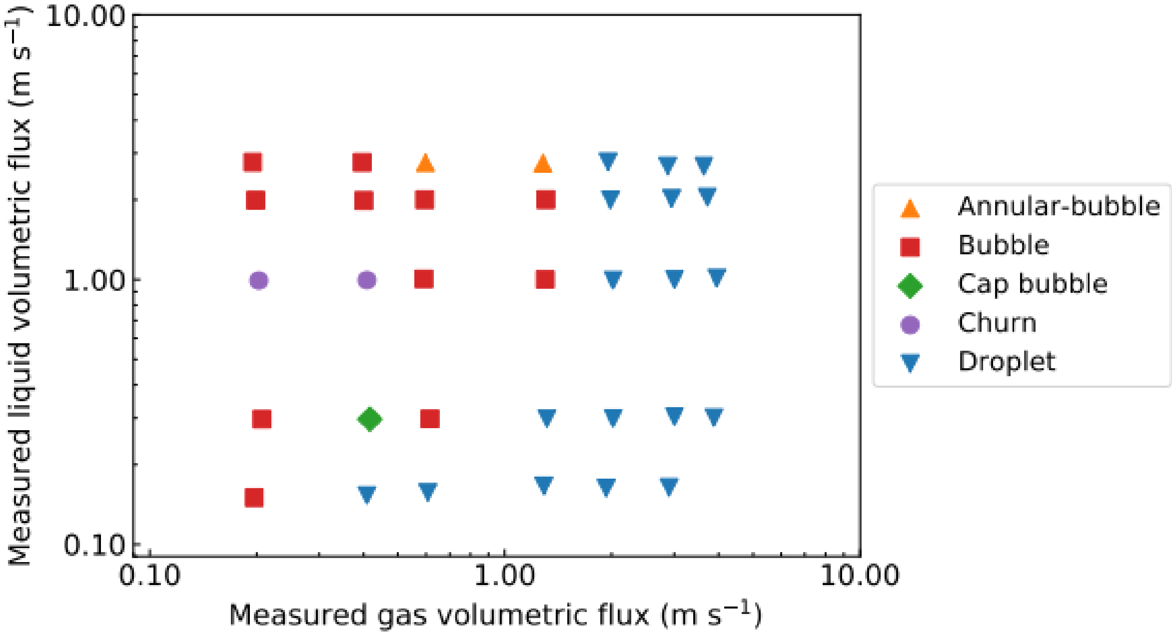

Figure 2.11 – CO_2 Flow regime observed in experiments with downward flow (Hammer, 2021).

The figure 2.11 illustrates gas-continuous flow with entrained liquid droplets/drops at high volumetric gas flux. For low volumetric gas flux, the flow is mostly liquid continuous or a chaotic gas-liquid mixture.

CO_2 can undergo phase transitions in the wellbore, which can dramatically affect the flow regime. Research has shown that regardless of the initial injection state, CO_2 typically reaches the reservoir in a supercritical phase due to phase transitions occurring in the wellbore

A scientific work by Thu (2019) has focused on modeling CO_2 injection in various fields such as Sleipner, Snøhvit, In Salah, and Ketzin using the OLGA simulator. This research primarily aimed to study transient flow behavior under conditions like shut-in and blowouts. Steady-state solutions were obtained first, followed by dynamic modeling to simulate real-life operational scenarios. Similar studies on depleted gas reservoirs have explored the thermodynamics of injecting liquid or supercritical CO_2, highlighting challenges in the near-wellbore zone due to phase behavior, which can complicate injection performance (Hoteit et al, 2019).

Phase behavior plays a critical role in CO_2 injection, as highlighted by studies like the Peterhead CCS project, which injected CO_2 into the depleted Goldeneye hydrocarbon field. This study emphasized the importance of understanding carbon dioxide's phase dynamics to optimize injection well design (Acevedo & Ajay, 2017). Moreover, models developed for vertical wells account for the complex thermodynamics of CO_2 flow and include heat conduction effects in the surrounding layers, which are essential for operations like blowouts and shut-ins (Linga & Halvor, 2016).

The integration of reservoir and wellbore models is crucial for a comprehensive understanding of CO_2 injection. A coupled model presented in one study explored interactions between the wellbore and reservoir, focusing on two-phase flow behavior. This model integrated heat transfer effects and described various flow regimes that occur along the well construction (Doughty & Karsten, 2004). Another study, using TOUGH2, simulated multi-phase flow in brine formations and addressed key challenge – phase interaction during CO_2 sequestration (Strpić et al, 2021).

Operational challenges such as phase changes during transient flow periods and injectivity issues have been thoroughly studied. For example, the T2Well simulator, coupled with a modified ECO2M EOS, was developed to detect operational problems caused by phase changes during CO_2 injection (Strpić et al, 2021). Similarly, studies using OLGA multiphase flow simulators examined the dynamics of wellbore flow regimes and addressed concerns like hydrate formation and injectivity changes (Pekot et al, 2011). The DFM, widely used in coupled reservoir/wellbore simulators, has been applied to capture these interactions effectively (Peng et al, 2022).

All these studies concludes that coupling process and integrated modeling of CO_2 injection is important for analyzing steady-state and transient processes during injection.

In terms of subsurface flow, after CO_2 leaves the well, vertical movement is governed by buoyancy effect. Horizontal movement is mostly governed by the pressure gradient. In a homogeneous reservoir, CO_2 will initially moves radially from the well and then it will redistribute vertically to the caprock. In a layered or heterogeneous reservoirs CO_2 moves by channels along more permeable layers. From the storage efficiency point, promoting horizontal spread is much preferable than vertical escapes (Machado et al, 2023). This can be achieved by well placement and injection rate control. The last suggestion means that operator can enhance storage efficiency by controlling injection flow rate. Higher rates favoring lateral spread before buoyant segregation.

Figure 2.12 presents this effect for three different injection strategies with the same cumulative. Study by Machado et al (2023) confirms that horizontal wells naturally encourage lateral CO_2 movement than vertical wells. They have a larger swept area in the reservoir, so it can be beneficial to increase the contact with brine than will enchase solution and mineral trapping.

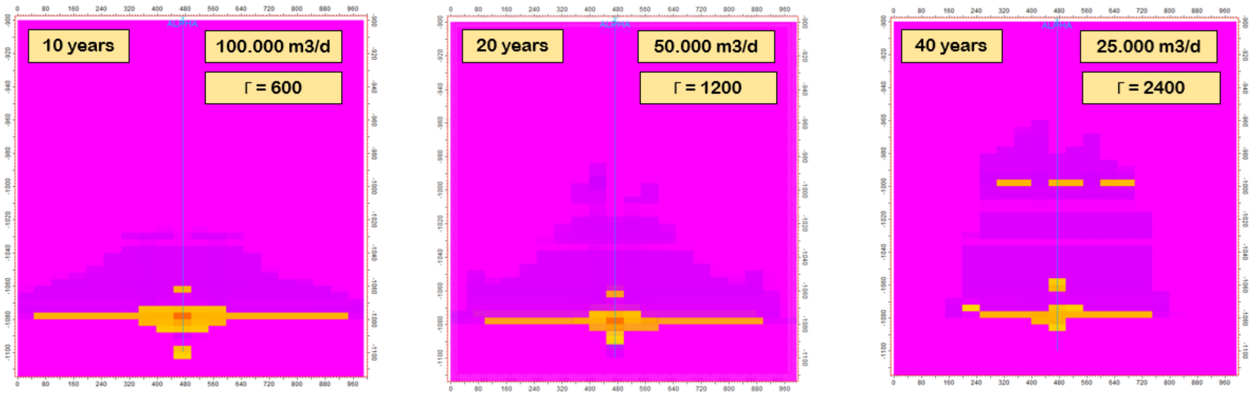

Figure 2.12 – CO_2 saturation for vertical wells injection among different injection strategies for the same reservoir and cumulative amount of CO_2.

After the beginning of CO_2 injection, the fluid pressure in the near-wellbore region increases. Then, this pressure increase propagates outward as plume migrating in the reservoir. The brine is slightly compressible, so the injection-induced pressure goes through the brine rapidly. Some studies have underscored that the induced pressure plume moves even faster than CO_2 saturation plume (Das et al, 2021). This has important implications for the CCS since even if CO_2 became trapped in the structure, the pressure wave still could reach the legacy wells or fractures. During active injection, the bottom-hole pressure (BHP) rises to overcome the pore pressure and friction losses. Field and simulation studies put large attention to keep the injection pressure below the formation fracture pressure for safety reasons (Shchipanov et al, 2023).

Regarding phase distribution, the rule is the same as for CO_2 well flow – if the condition in the figure 2.1 satisfies – double phase flow exists. The two-phase flow in reservoir can be in the following conditions (Vilarrasa et al, 2013):

— Cold-liquid injection (e.g. 6-8 MPa and -50 °C from the ship-borne). Fluid warms as it enters the warm structure, while it still staying below the dew point line.

— Near-wellbore Joule-Thompson cooling effect during high flow rate injection cases. Rapid expansions through small orifice in the perforation might cause the temperature and pressure fall below 73 bar and 31°C. However, it occurs only for short-time period, since CO_2 immediately warmed by reservoir.

— Shallow (<800 m) saline aquifers. Static pressure could be less than 73 bar that is bellow critical pressure.

The study of flow regimes in two-phase for each aspect of CO_2 injection is a complex and evolving field. While significant progress has been made in understanding and modeling these phenomena, there is still a need for further experimental data and improved models to accurately predict and optimize CO_2 injection and storage processes.

To sum up, two-phase flow could occur rather in pipes after the passing through wellhead choke than in wellbore or reservoir. It can be explained because of Joule-Thompson effect that lowering the temperature of CO_2 after passing through hydraulic resistance element. After the wellhead choke, gas volume is rapidly increasing, then, going deeper to the reservoir the condition is changing and CO_2 shifts to supercritical state after ~800 m MD. In the next subchapter will be presented detailed characterization of Joule-Thompson effect for CO_2 for better understanding of the nature of two-phase flow during CO_2 injections.

2.3 Thermal Effects During CO_2 Injection

The phenomenon of the cooling behavior of CO_2 through a choke is very important in CCS, as well as in the EOR. This process is critical in optimization of CO_2 injection, wellbore control mechanism, stabilization of pipelines and surface facility. Chokes are flow-restricting devices which control the pressure in wells and very rapid expansion of CO_2 through the devices causes intense cooling through Joule-Thomson effect. Such cooling may be profound, resulting in temperature reduction that can lead to the formation of hydrates, thermal strains, and issues with assuring the flow.

The knowledge of CO_2 cooling effect is important in the phase changing processes that is analyzed prior to injection. Due to the rapid decrease of pressure through the choke, large temperature decreases can be reached which can cause a change of phase of the CO_2 to liquid or even into solid CO_2 (dry ice). These phase transformations may be of critical influence on the process of injection because it affects the density of CO_2, its viscosity, and the total pattern of flow processes. In addition, the phase shifts in CO_2 can have an impact on the interaction of CO_2 with the fluids of the surrounding reservoir by worsening displacement efficiencies as well as the effectiveness of the whole storage process.

Due to Joule-Thompson effect the temperature changes. A thermodynamic phenomenon known as the Joule-Thomson effect involves the temperature change of gas or liquid as it travels through a component of hydraulic resistance (nozzle, valve or porous baffle) without performing a work or conducting a heat transfer with the environment.

This effect can be described by the following equations (Gao, 2021):

$$\mu_{JT} = \left(\frac{\partial T}{\partial P}\right)_H$$

$$\left(\frac{\partial H}{\partial P}\right)_T = V - T\left(\frac{\partial V}{\partial T}\right)_P$$

$$\left(\frac{\partial H}{\partial T}\right)_P = C_p$$

Where μ_{JT} – Joule-Thompson coefficient (K/Pa), $\left(\frac{\partial T}{\partial P}\right)_H$ – temperature change with pressure at constant enthalpy (K/Pa), $\left(\frac{\partial H}{\partial P}\right)_T$ – enthalpy change with pressure at constant temperature (J/kg·Pa), V – specific volume (m^3/kg), $\left(\frac{\partial V}{\partial T}\right)_P$ – change of specific volume with temperature at constant pressure (m^3/kg·K), $\left(\frac{\partial H}{\partial T}\right)_P$ – enthalpy change with temperature at constant pressure (J/kg·K), C_p – specific heat capacity (J/kg·K).

It should be noted that the Joule-Thompson coefficient, generally, for gas is positive, while for liquid is negative. In other words, passing through flow-resistivity element cool gas and heat up liquid. This feature is widely used in the ship transportation of gases – for example – liquefied natural gas, C_2H_6 and others. After pipeline transportation, where such gases have huge pressure, valve or choke reduce it and decrease the pressure and temperature – to reach liquid or solid phase.

This phenomenon is also useful for liquid. For example, oil passing through choke lead to increase temperature. The higher temperature – the lower viscosity and chance of formation of hydrates and paraffins.

In case of CO_2, the effect should be considered as the gas has quite low critical temperature (30,98 °C). Joule-Thompson coefficient depends on temperature and pressure. It can be calculated in the labs by using formula (Gao, 2021):

$$\mu_{JT} = \frac{T_2 - T_1}{P_2 - P_1};$$

Where μ_{JT} – Joule-Thompson coefficient (K/Pa), T_1 – temperature of the fluid at upstream (K), T_2 – temperature of the fluid at downstream (K), P_1 – upstream pressure (Pa), P_2 – downstream pressure (Pa).

The study by Gao (2021) presents values of the coefficient under different conditions. The output is illustrated in figure 2.13.

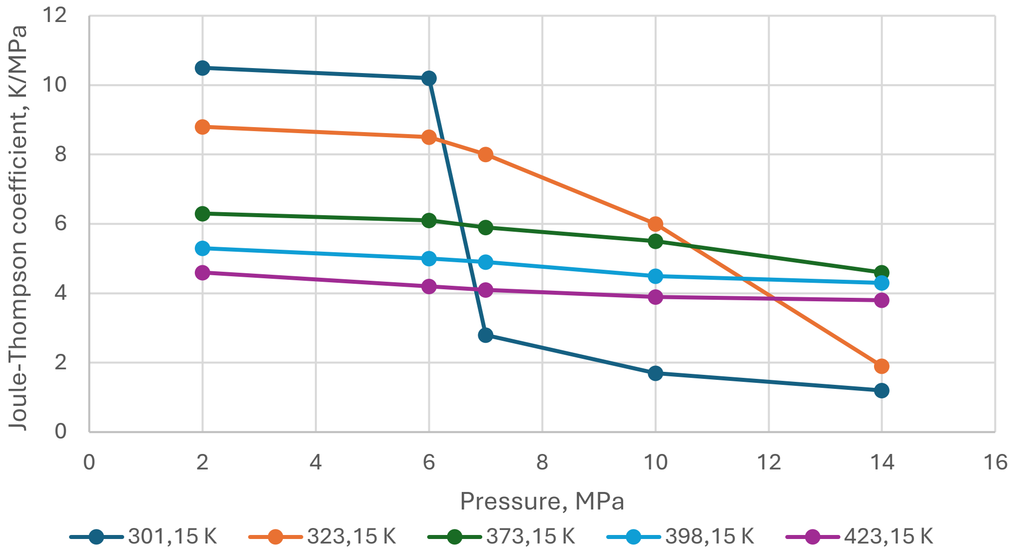

Figure 2.13 – Joule-Thompson’s coefficients for CO_2 under different conditions (Gao, 2021).

The phase transition during steady-state and transient flow was researched in the work by Li et al, (2020). The research group constructed a CO_2 throttling test. The cooling effect in gaseous CO_2 steady choked flow is much stronger than that in supercritical CO_2 choked flow while the liquid CO_2 has the lowest.

The analysis of scientific literature on CO_2 cooling in chokes reveals that research in this area is currently limited. While some studies have explored the basic principles of CO_2 cooling through the Joule-Thomson effect, there is a notable lack of comprehensive investigations, particularly concerning the practical implications for large-scale CO_2 injection and transport. Recent progressive studies have begun examining the cooling behavior of CO_2 mixed with other components, which could provide valuable insights into improving operational efficiency and safety. However, further research is needed to fully understand and optimize this phenomenon for real-world applications.

Beyond the wellhead, thermal effects appears near the wellbore zone – as the CO_2 expands into the formation. When warmed (from the formation heat through the well wall) CO_2 reaches the bottomhole, it enters the reservoir via cased-hole perforations. Some studies presented that the temperature drop can be significant and yield very low values around the wellbore (Tweed et al, 2024). This cooling effect in the formation has few implications. Firstly, the surrounding formation area rock and cement experience thermal load – it may lead to fractures and stresses (Tweed et al, 2024). Some other aspects include the risk of ice and CO_2 hydrates close to perforation. This may lead to the reduction in injectivity.

Importantly, studies that focuses on the integrity underscores that Joule-Thompson effect influence rock stability. Numerical modeling by Younessi (2024) found that under typical condition of CO_2 injection, the temperature drop does not generate additional compressive stress to crush or destroy the perforation walls. While thermal contrast for the rock can induce tensile stresses that might cause to potential fractures. In other words, thermal stress can have an impact on casing cement and formation rock, but not on perforation and tubing.

In summary, thermal effects in the completion zone need significant consideration. Expansion of cool CO_2 that passing through small-sized orifice can even cool more the wellbore zone. This aspect does not have lots of case studies in literature. This effect can lead to positive and negative events for CCS, particularly positive:

- Thermal stresses in the formation could result in thermal fracture that increase the injectivity and lower the needed pressure for injection.
- Cooled CO_2 has higher density that lower buoyancy effect that enhancing storage efficiency.

Negative effects include:

- Cooling near wellbore zone might lead to ice and hydrate formation that can lower the injectivity of well by closing the perforations.
- Thermal stresses in the wellbore might lead to potential fractures and damage for casing cement. It highlights the leakage potential.

Another aspect arise when CO_2 is injected into warm formation, since temperature in the reservoir changes leading to the existence of temperature differences that can alter the fluid and rock behavior. The Joule-Thomson cooling effect will occur when CO_2 is expanded, though high-pressure wells into lower-pressure underground storage passing through small-size orifices in the perforation zone. Because of this, temperature may reduce drastically at the perforation zone and a cooled zone may be generated. The warmer rock raises the CO_2 temperature as the cold plume of CO_2 extends further away up to the temperature level it had previously.

According to analytical models, temperature will decrease, but rapidly close to the well, and increasing with distance, and finally steady, because the loss of heat on the surrounding rocks is equal to loss of heat around the drill hole (Ramey, 1962). The thermal front close to the injector well has the highest influence during injection.

Effects of thermal variations are observable in the behavior of fluids and in the functioning of the storage facility. The decrease in temperature causes a thicker aggregation of the CO_2 particles which causes them to be slightly less buoyant, as Bachu (2008) reveals. In most cases as CO_2 goes further into deep formations, the pressure on CO_2 grows faster than temperature hence making CO_2 supercritical at the mentioned depths (Bachu, 2008). CO_2 becomes denser by cooling to these depths by further expansion Joule-Thomson expansion. Increasing the amount of liquid CO_2 that could be stored in the reservoirs may enhance the ability to hold it in place since it takes more space in the pore volume and it would also slow down plume migration.

Nevertheless, under low temperatures, the formation fluids might partially thicken, such as CO_2, hence necessitating more pressure to flow them. This net effect is that increased density enhances flow of the CO_2 during injection, but increased oil viscosity and increased water viscosity may limit this benefit. In practice, simulations of fields imply that deeper (high-pressure) reservoirs are desirable for storage due to the fact that CO_2 is denser at those pressures.

It is not only the fluid behavior properties that should be known but also thermal stresses of reservoir rocks. Cold that comes with CO_2 injection into the formation at a significant temperature lower than the formation temperature may also lead to expansion and contraction of flowing fluid and the rocks. In case the CO_2 is colder than the reservoir, neighboring rocks will contract with the tendency of stressing them and possibly breaking them. In some instances, only a sub-zero temperature of 10–20°C near the well is enough to produce a fracture stimulation (Samaroo, 2024). The above calculations have revealed that the injected CO_2 having the temperature of 15°C to about 0°C significantly increases the chance of having the following; thermal fracturing and opening of faults at the wellbore. Thermal cracking will be avoided when the CO_2 is introduced laterally to the reservoir into the vicinity of the reservoir temperature (Nguyen, 2016). As seen in research, increasing the injection temperature to an extent of approximately 40°C, produced no further fracturing hence, it testifies that keeping the injection temperature below the formation temperature will help avoid the damage of rocks through the effects of heat (Salimzadeh, 2018).

An aditional heating issue that is related to thermal effects is a potential formation of solid hydrate during CO_2 injection into the reservoir. Gas hydrates composed of CO_2 and water (very cold, but slightly solid) will be obtained at low temperatures and high pressure. In cases of reservoirs of deep North Sea aquifers (where temperatures at the aquifer leves are commonly between 30 and 100°C), the temperature of the bedrock is virtually always more than that of the CO_2 hydrate stability boundary. But, at times when the injection occurs at a very high rate or in shallow areas then local chilling may lead to a reduction in the temperature below that of the hydrate formation hydrate condition. Ice or surplus water raised towards the well may be very destructive, congesting the pores and tubulars and severely reducing how much extra fluid is able to take the well. That is why both wellhead and bottomhole temperatures are regularly measured by engineers and it is possible to add the elements of dehydrators or heaters to the injection equipment to prevent the formation of hydrates and maintain the structure of the reservoir during the injection process.

To sum up, to foresee the behavior of CO_2 and make the process safer and more productive, it is worthy knowing how the effects of thermodynamics work, and how they influence the properties of fluids and formation rock.

2.4 Outflow Control Technologies for CO_2 Storage

CCS combined with EOR represents one of the most promising technologies for both increasing hydrocarbon recovery and mitigating rising concentrations of CO_2 in the atmosphere. However, CO_2 injection in heterogeneous reservoirs faces some significant challenges including early breakthroughs through legacy wells and faults, poor sweep efficiency and uneven distribution of fluid (Aakre et al, 2018). For struggling these problems new concept of OCD were developed. The idea of these devices came from the concept of Inflow Control Devices (ICD) that mainly installs now in intelligent wells.

OCDs are completion tools that were designed to restrict flow in a fixed manner, since there is no moving parts as well as surface control over them. They were created to achieve more uniform fluid distribution in subsurface reservoirs across multiple layers with different geological properties. By adding additional pressure drop to high-permeable zones, an OCD forces CO_2 flow to move into lower-permeability layers (Rezvani et al, 2023). This advanced devices secure to avoid problems such as early gas breakthrough into producers (in case of EOR) and thief layers (in case of CCS) (Rezvani et al, 2023).

Most OCDs represents a calibrated flow restriction such as small-sized nozzle or orifice. These devices are integrated typically with sand screens and packers. As CO_2 flows through OCD, it experiences a pressure drop. These devices can be adjusted for individual cases by selecting the appropriate flow area. As an example – CO_2 in gas state requires smaller area, since it has low density and viscosity – high chances for breakthrough (Rezvani et al, 2023).

Their principle of working is based on the following equation:

$$\Delta P = \frac{\rho v^2}{2{C_v}^2}$$

Where ΔP – pressure drop (Pa), ρ – fluid density (kg/m^3), v – flow velocity (m/s), C_v – flow coefficient (-).

$$C_v = \frac{C_D}{\sqrt{1 - \left(\frac{D_2}{D_1}\right)^4}}$$

Where C_D – discharge coefficient (-), D_2 – resistance element's diameter (m), D_1 – up-stream pipe diameter (m).

OCD has shown to be great tools for EOR applications. In practice, these EOR projects mainly consists of miscible flooding and Water-Alternating-Gas (WAG) injections. Heterogeneity as well as early CO_2 breakthrough to producers are well-documented in CO_2 injection. High permeable layers and fractures can cause CO_2 to shortcut or destroy oil production wells, leaving large volumes of oil uncontacted.

Therefore, engineers has suggested to use OCD for solving these problems. These devices have been employed for one of the largest CO_2 WAG case in Canada – Midale Field (Kais et al, 2016). After years of WAG, CO_2 and water were channeling rapidly from injectors to producers, leading to early breakthrough. To combat this, the multi-zone completion with OCD were designed (Kais et al, 2016). The result was a tailored OCD design predicted to improve producer's performance and overall sweep in the WAG flood. Controling the injection profile led to lower production of unwanted fluids. The study by Taghavi et al. (2023) found that compared to a fully perforated completion, an OCD completion could lower the produced CO_2 gas fraction. Even though passive OCDs cannot shut the gas flow completely.

Using these advanced devices for the application for saline aquifers is quite similar to its application for EOR. Unfortunately, field examples are still scant to date. Most large-scale carbon sequestration fields have utilized relatively simple well constructions – budget vertical wells with simple completion – single open interval. The reason can be that these fields have quite homogeneous highly permeable aquifers. Therefore, in these cases the injection strategy does not require complex flow control. However, as CO_2 storage projects moves from easier homogeneous applications to heterogeneous cases – the actuality of these devices can increase.

Research has begun considering the application of OCD for saline aquifers relatively recently. Rezvani et al (2023) address the OCD design for CCS projects. In this study were also noted that proposed method for searching optimized area in CO_2-EOR cases is the same as in CCS application. The goas is clear – to balance the injected CO_2 front in all layers of saline formation, preventing situation where CO_2 would fingers through the highly permeable structures. By evening the injection profile, OCDs can maximize the efficiency of storage utilization. Simulation studies shows that this concept would yields more CO_2 stored for the same injected volume (Taghavi, 2023). In other words, what uniform sweeps and make even distribution for EOR cases translates to more uniform plume distribution for carbon storages in aquifers.

Another significant advantage for carbon storages can be pressure build-up. A long horizontal injection well with segmented OCD intervals could distribute CO_2 as well as pressure over a wide area. It means that it would reduce local pressure hot spots and lowering the risks of fracturing the caprock or induce seismicity. While not yet demonstrated in the field application, this concept has been only discussed in the CCS engineering communities. Unfortunately, there is still lots of debates, as some of engineers suggests keeping injectors simpler and more robust as there is still not enough records and studies about plume distribution.

In summary, the application of OCD for CO_2-EOR is performed perfectly – decreasing the presented of unwanted fluid in producers – CO_2, while for CCS cases, it is only in an early, conceptual stage. The studies indicates that the benefits for CCS will be analogous as for EOR cases. As CCS projects scales up, particularly involving cases with huge heterogeneous aquifers and horizontal injection wells, OCD are a potential tool for making CO_2 injected safely and efficiently.

2.5 Gaps in Existing Research

The study of the injection behavior of carbon dioxide in saline aquifer has progressed but there are still fundamental gaps to fill. Multiple scientific procedures such as systematically conducted research of two-phase flow dynamics and a buoyancy mechanism of migration and deep saline geological trapping can enable scientists to formulate their comprehension (Celia, 2015). Based on the North Sea Sleipner project and other related projects, the injected carbon dioxide develops an independent buoyant phase below brine density thereby developing a significant buoyant force (Celia, 2015).

Dynamics of large scale can be appropriately described in the process of single-phase simulation reservoir with the help of normative models nowadays but together with these, there are flaws in describing complex transient interactions as well as coupled processes. It contains a brief review of the current developments in the area followed by the in-depth discussion of the research gap in the two-phase flow modeling: thermal effects and wellbore-reservoir interactions with flow control technologies as applied to saline aquifers.CO_2 is pumped deep into the underground reservoirs which is converted into fluid that displaces brine as it moves up due to buoyancy (Celia, 2015). The gravity-driven segregation observed and modeled indicates that the dissolved CO_2 accumulates to the bottom of the caprock leaving the brine with a higher density in the top (Wang et al, 2024). Implementation of this procedure encounters various significant challenges when it comes to modeling and control operations.

Field-scale models are found on the thought that there is an instantaneous difference to carbon dioxide that creates focus on the top highest part of this formation. It encompasses the simulation models that are generally applied in case of large-scale modeling of buoyant plumes, and yet, vertical flow should be small, which is not the case of early stages or non-stratified settings (Celia, 2015). The rapid cloud warming that causes movement and mixing could not be simulated in the model since this is not valid in the case. The modeling stage is transient where appropriate approaches are not present in analyzing the time prior to gravity segregation becoming vertical.

This issue can be seen as the basis of the problem which arises because of the inability to find a match between the distribution of aquifers and the complexities of buoyancy. Sleipner reservoir in North Sea Utsira formation illustrates how the CO_2 spreads across various thin layers under the seals due to the effects of the gravity and small influences of heterogeneity. The generic models must modify their parameters that involve relative permeability and capillary pressure using plume configuration datasets available. The variations between the model simulation results and the behaviors points out how little scientists know of the relationship between heterogeneity, capillarity and gravity-driven effects. The uncertainties to the spread and movement of the CO_2 largely rely on the model of choice during the prediction. The divergence of results based on different presumptions on the underlying principles are in increase. There is uncertainty in the accuracy of hydrodynamic simulation that is performed to be injected into the underground reservoirs as small trapping mechanisms or material parameter may result in significant changes in results. Due to unreliability in parameters, which influence residual trapping and permeability averaging, scientists are faced with difficulties to predict plume behavior during the large-scale CO_2 storage exploitation.

In modern operation, the reservoir simulators and the wellbore/pipeline simulators can merely exchange simplified boundary conditions (i.e. steady inflow performance relationship (IPR) tables or fixed pressures) instead of directly interacting with each other (Peng et al, 2022). The majority of commercial tools (e.g. standalone reservoir or well simulators) have them fixed, e.g. reservoir models have bottom-hole pressure, or field (pore) pressure fixed, well-bore models have inflow rate fixed – all of which disregard feedback between the two (well and reservoir), as well as the effect of choking in a wellbore choke to the reservoir response (Peng et al, 2022). Such a discrepancy implies that the complex interaction (pressure, temperature, and flow transients) is not accurately modelled by isolated models.

Indeed, recent works enhance that only the coupled wellbore-reservoir simulation will allow making proper prediction of CO_2 injection system behavior (Burachok et al, 2022). There are very close interconnections of the wellbore and reservoir process, such as the wellbore flow mechanics, thermodynamics and phase change process have a direct impact on the injectivity. In other words, integrated modeling solves the gap by accounting for how surface injection conditions and subsurface responses evolve together in time. This integrated approach is broadly recognized in modern CCS engineering as critical for accuracy, integrity and safety.

The CO_2 injection behavior could be erroneous in a scenario where a case of wellbore-reservoir simulation is simulated independently through usage of static tables. Decoupled models may incorrectly produce a low bottom-hole pressure, or incorrectly high injectivity, as such models do not look at the pressure losses, and multiphase flow occurring within the well as reservoir conditions change. They are also unable to present temperature changes, e.g. Joule-Thomson cooling and thermal front time moving into the reservoir – that can vary fluid properties and rock stress.

Literature also says that steady-state assumptions result in the consideration of commercial simulators missing the dynamic relations and, thus, will show false results (Peng et al, 2022). Conversely, the feedback loops will be noticed with respect to a coupled model: e.g. an increase in reservoir pressure will be felt in the coupled well model in the form of the increased back-pressure, and the reduced CO_2 flow, which, in its turn, will also lead to slower progress of the pressure build-up. In the absence of this, the operators could be provided with false information concerning the attainable rates of injection or safe operating pressure which may result in either a failure of design or operation. Therefore, the integration gap is significant to bridge in a bid to de-risk CO_2 injection operations.

The gravity override causes the CO_2 distribution of CO_2 plume to decrease and most of the CO_2 as free gas is driven to the caprock. The scientific basis of injecting CO_2 to the bottom sectors of salty aquifers and bifurcation of the injection process to ensure segregation through gravity is not well exploited in science. The most of these computer models presuppose, inevitably, a layer of accumulated CO_2. The first issue of engineering is creating methods that could enhance CO_2 vertical migration across the aquifer to allow more contact with the brines and consequently adhering to the rock. Researchers should study further regarding the effects of the gravitational forces on the processes of dissolution and mechanisms of capillary trapping. Researchers cannot ascertain the level at which the two major types of behavior of carbon dioxide interact when carbon dioxide is acted upon by rock formation since the two parts of the substance remain caught in the pores and other sections of it behave in a chemical manner with brine.

Initial CO_2 storage models assumed an isothermal system but now scientists have identified how important thermal effects are on injection processes. The CO_2 injected through surface injection points is usually cooled to a low temperature compared to the natural reservoir temperature, and any further cooling process will occur in the form of the Joule-Thomson effect as the CO_2 zone expands down wellbore pressure into the reservoir. There is an alternation of temperature around the wellbore which may be many tens of degrees Celsius depending on the pressure situation. Extreme cooling is produced by the valve because of Joule-Thomson through provision of CO_2 with high rate (Ziabakhsh-Ganji, 2014).

The results of thermal cooling go beyond developing the temperature patterns. The fluid density and viscosity alteration together with the transformation of the pattern of mechanical stress owing to the cooling process that takes place in the reservoir rock. Thermal stress by cooling is manifested in contraction of the rock, which may lead to fault slip and fracturing (Peters et al, 2013). development of thermal fractures may enhance injectivity due to increased permeable pathways but concerns are raised on cement bonding of the wellbore and caprock integrity (Roy et al, 2018). most large-scale reservoir models have no explicit thermal-geomechanical coupling despite these implications creating a research gap with respect to thermo-mechanical coupling. The computational complexity of complete thermal simulators drives researchers to solve fluid problems through isothermal approximations instead of fully coupled thermal models. The research conducted by Pruess et al. (2008) demonstrates that isothermal modeling produces incorrect predictions about CO_2 migration extent and leakage when compared to thermal models according to Celia (2015). The exclusion of thermal transients from models results in incorrect calculations of both pressure buildup and CO_2 phase states in the vicinity of the well.

Thermal effects become insignificant to the North Sea aquifer analysis due to offshore environment and injection processes. The fluid gets injected into the CO_2 injection well at a relatively low temperature that cools along the way or under compression to rise in performance as it passes the wellbore and lowers down the temperature as compared to the formations. Northern Sea bottom seawater injected into Utsira and Bunter Sandstone formations at high rates of injection would offer widespread cooling in both high permeability rock systems. Scientific literatures present minimal studies concerning thermal behavior in such specific environments. The ongoing studies do not have knowledge on the spread distance and velocity of thermal fronts of saline aquifers and how they interact with two-phase fluid transport. This paper will fill this gap by non-isothermal modeling of the two-phase flow by considering the Joule-Thomas cooling after the wellhead choke. The question of the impacts of temperature variations on injection performance and containment in a North Sea reservoir will be answered.

A majority of the CO_2 injection studies done on reservoir scale limits the injection rate or bottom-hole pressure control to the wellbore boundaries but connection between the reservoir and the wellbore flow is multi-faceted and needs additional research. The injection well undergoes rapid decompression and two-phase fluid flows particularly in the situations where it is in the operations of depleted or offshore reservoirs owing to the fact that such factors influence the sandface reservoir entry conditions. By using a well-reservoir model, Paterson (2010) revealed that at low-pressure injection of CO_2 into a gas-reservoir in the North Sea, it would vaporize into a gas within the well and close to the perforations. A reservoir simulator does not have the capability of simulating such behavior. Transient wellbore conditions cause the injectivity of system to be dependent since they influence the pressure drop and temperature loss to strata and phase transition in the tubing that will cause either dense-phase CO_2 to enter the reservoir or it will cause the gas to leak early.

An overview of modeling strategies shows that the fully-coupled wellbore and reservoir systems represent the most accurate technique of modeling CO_2 injection phenomena in depleted North Sea fields (Tavagh Mohammadi, 2025). Multiphase flow between wells and reservoirs is still supposed to challenge since little work has attempted to unify these two areas yet there is need to simultaneously solve the high-velocity one-dimensional well flow equations and the three-dimensional porous flow equations in the reservoir.

OCD and the other similar technologies are parts of flow control completions and within this scenario, the outflow control is regarded as an innovative method of CO_2 injection wells. ICDs have been used widely in oil production wells to maximize the oil production and to delay unwished fluids in the production (water), but the application of same structure devices – OCD, on CO_2 storage injection wells is not tested. Improved distribution of CO_2 throughout the well can be obtained using the same technology but for the injection – OCD, or flow control valves installed in vertical or horizontal CO_2 injectors in order to avoid premature breakthrough of CO_2 into high-permeability streaks that increases the sweep area.

These devices aid the prevention of creation of thief zones as they target CO_2 concentration and divert it towards specific layers. When CO_2 is in use with OCDs, there is limited documented performance since this fluid is non-compressible and two phases in nature; it does not behave in a similar way as oil. Simulation and laboratory studies associated with CO_2-enhanced oil recovery prove that the CO_2 flow can be self-regulated partly due to a particular OCD design (such as orifice or labyrinth-type devices) (Stian, 2022). Determination of design requirements of OCDs in pure storage applications (saline aquifers without production of oil) is not definite due to the lack of clarity in terms of the long-term performance behavior of OCDs as well as the effects of fluid phase changes liquid CO_2 to gas or discharge brine co-injection effects. The latest technology shortage lies at the injection well design concept of CCS.

The well-reservoir coupling gap combines wellbore integrity with thermal interrelationships, which exist between the well system and reservoir system. The above section detailed why cold temperatures of CO_2 cool down the wellbore tubulars and near well areas of the formation. When the thermal stresses are not controlled, well casing and cement may be damaged. The well is the channel of transmission of pressure waves that move through the well into the reservoir and these waves may have an effect of influencing the risk of fracture or improve chances of injectivity.

There is a lack of sufficient information in the present available scientific literature on wellbore transient response when CO_2 is injected in terms of bottom-hole pressure change and time of thermal equilibrium. Wellbore-reservoir modeling techniques serve the purpose of the thesis because they can be used to simulate CO_2 injection activities, hence covering this deficit in knowledge. This paper undertakes a pressure and temperature sensitivity study of the well and the reservoir in terms of flow characteristics in order to find the OCD arrangement in terms of stable injection and enhanced conformance. The analysis is the crucial step in the development of the best completion guidelines at North Sea CO_2 storage facilities as field learning in the field is minimal so far.

None of both steady-state and transient flow conditions are taken care of appropriately in scientific literature. A simplified approach in research models of CO_2 injection involves constant conditions like constant rates of injection or pressures to understand long term outcomes like plume radius and stabilized pressures. Steady-state simulations assist in limitation determination but cannot simulate the ephemeral patterns of operation that occurs in reality in injection operations. The rate of injection in working fields is gradually increased with the occasional variation and the wells need to be stopped at certain frequent intervals and the setting of reservoir adopts various forms during the ongoing project time regarding the dynamics of the project development. The temporary activities will result in a complex system response since the local pressures and temperatures will change quickly as the injection is operated whereas the CO_2 still does a redistribution process after the injection process is halted in the form of the pressure reduction and the thermal recovery protocols.

Multiphase transient flow modeling is a challenging task since it involves time relations among various processes inside and outside the wellbore region. The results of scientific observations based on laboratory tests and field measurements indicate that transient injection operations are associated with the co-flow of gas and liquid phases, in connection with the accompanied significant Joule-Thomson cooling effects and unstable thermal contact between the formation and the phases. These effects have been restricted to little research since it required high resolution in time-stepping and state-of-the-art models.

A majority of case studies do not clearly examine the pressure transients within the reservoir at ramp-up injection and post temperature recovery after injection shutdown. The models that ensure constant conditions do not offer any answers concerning the way injectivity changes in the course of the first several weeks of injection. There are two contrasting reactions on the injectivity relocation reaction in the reservoir as CO_2 changes in viscosity gets lower due to fracturing and evaporative cooling that causes salt precipitation. The above problems are but temporal dependence.

There must be model adjustments to fit monitoring data like bottom-hole pressure over the time period compared to only paying attention to the final location of the plume in historical matching of transient phenomena. The investigation of early injection transients in the saline aquifers has been sightlessly explored owing to the unavailability of the respective datasets. North Sea storage business ensures seismic survey checks on post injection plumes but not much is publicized on the data of wells lying under the injection business. The current knowledge of the dynamics of transient flow is limited and it poses challenges in providing decisions in the operations of controlling injection pressure surges.

Transient issues are addressed by the thesis via time-varying simulative options that can monitor the injection processes rather than achieve the instant equilibrium status. It is a research study evaluating three major phenomena in a North Sea reservoir model such as the early part of injectivity formation, Movement of a thermal front and diffusion of pressure waves. When analyzing the process of developing gravity segregations, the study explores the time consumption of the process and creates analysis on thermal-pressure effects when analyzing the possibility of the near-well flow instabilities during the ramp-up activities. The realization of the difference between steady-state and transient condition in this study will generate invaluable content that can be used to come up with guidelines that guide regulation of injection rates and well control measures using OCDs and pressure limitation during CO_2 storage projects development.

The main barriers in simulating two-phase flow dynamics with gravity segregation under all conditions together with the incomplete incorporation of thermal processes and their geomechanical impacts and the sparse understanding of impurity-laden CO_2 behavior and insufficient wellbore-reservoir model integration including novel completion tools and the lack of detailed transient flow analyses.

The knowledge gaps are particularly important for North Sea large-scale storage operations because their operational conditions (offshore wells and high injection rates) differ from the typical scenarios examined in literature. The present thesis addresses these knowledge gaps through a comprehensive modeling system that solves these problems simultaneously. The work delivers an improved CO_2 injection physics representation through the combination of a compositional two-phase flow simulator with thermal modules and wellbore flow modeling. The research delivers novel information about hydrodynamic flow segregation patterns together with improved vertical sweep strategies for a North Sea aquifer while assessing Joule-Thomson cooling effects on the temperature and pressure profiles. The research identifies existing study limitations while providing direct solutions to these problems. This thesis delivers outcomes which bridge the gap between basic models and actual CO_2 injection projects to enhance the reliability of saline aquifer storage performance predictions. Advancement represents a critical requirement to ensure safe carbon storage expansion in both the North Sea and worldwide because it enables the development of efficient and secure long-term injection operations.

Chapter 3. Methodology

In this chapter will be discussed the chosen case for study – Smeaheia site, choose of simulation tools for performing modeling, models development and suggested loose-coupling flowchart.

3.1 Case Study Overview: Smeaheia Site

Smeaheia is a north-south oriented fault block forming the northwestern part of the Horda Platform in the northern North Sea (Mulrooney, 2020). The Smeaheia CO_2 storage project represents one of the most ambitious and technologically advanced project for carbon sequestration. The development process includes essential knowledge and applicable lessons that were learned from Norway's Nothern Light project that established indusital standards. The project incorporates multiple advanced methods that were specifically designed to overcome geological issues that was faced on the Horda Platform.

This project implemented two CO_2 transportation systems:

- CO_2 Highway Europe: The project includes a 1000-kilometers pipeline connecting the northern Europe's countries to huge CO_2 storage on the Norwegian Continental Shelf (including Smeaheia). The 24-inches diameter pipeline will operates under the 150 bar pressure and will be able to handle around 20 million tones of CO_2 in its final stage (Equinor, 2024). The map of the project presented in figure 3.1.
- Smeaheia Norwegian Hub: Few dedicated tankers for CO_2 serve as transportation system that will carry it to special novel offshore loading buoy that will be 12 km north to Smeaheia (Ministry of Petroleum and Energy). Each of these tankers will have a capacity of around 160000 m^3. They will discharge liquified CO_2 (-50°C, 6.5 bar) into converted offshore platform before the subsurface injection. This scheme is presented in figure 3.2.

Figure 3.1 – CO_2 Highway Europe project map (Equinor, 2024).

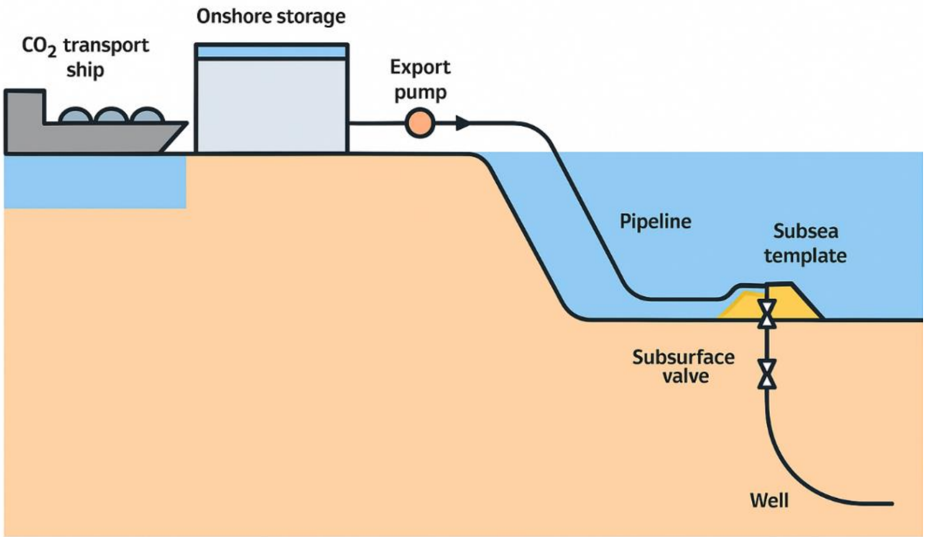

Figure 3.2 – Land-based terminal at Smeaheia.

The current schedule from the Equinor states that final investment decision will take place in 2025, with first injection targeted in 2027-2028 and full load achieved by 2030s (Mulrooney, 2020). The subsurface evaluation by Mulrooney showed that the fault-bounded Smeaheia can safely store hundred Mt of CO_2 maintaining injection pressure below fracture limits. The planned starting injection is around 1,5 Mt/year (Mulrooney, 2020).

So, the Smeaheia site is a north-south oriented fault block forming part of the Horda Platform on the Norwegian Continental Shelf (Mulrooney, 2020). The Horda Platform itself is a 300 km north-south wide and 100 km west-east wide structure that is placed east to Viking Graben. The primary structural map of the Horda platform and other basins is shown in figure 3.3. The Smeaheia block has sufficient features – it is formed with two faults systems – the Vette Fault Zone (VFZ) to the west and the Øygarden Fault Complex (ØFC) to the east.

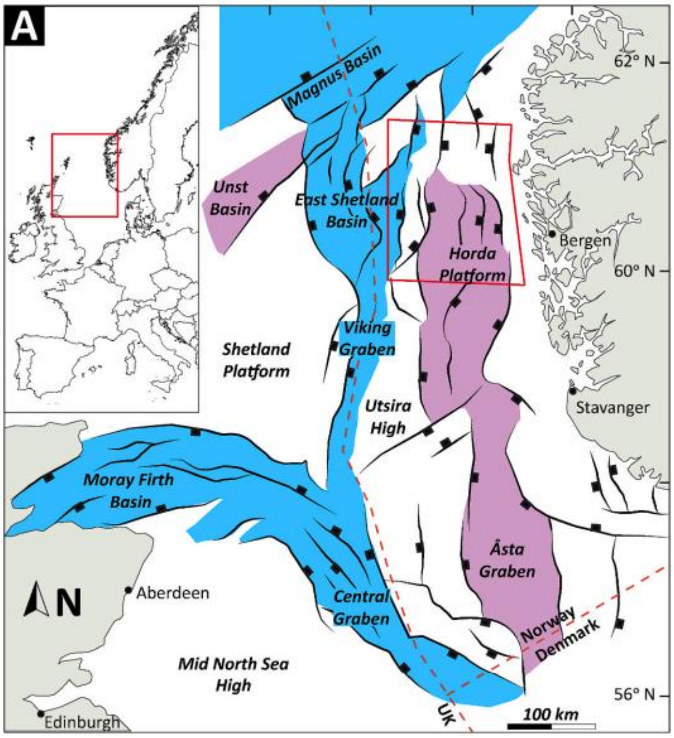

Figure 3.3 – Primary structural elements map of the North Sea (faults, basins, and structural highs) (Mulrooney, 2020).

This potential structure for storing CO_2 formed during the early stages of Permian-Triassic rifting, though major shifts happened in the late periods. The highest rates of rifting in that region were found during the Early Cretaceous and it then experienced smaller fault activiations from the Paleocene through to the Eocene (Mulrooney, 2020).

During the operational drilling wells for the Troll field there were found two potential structures for storing CO_2 – Alpha and Beta, that are two clear structural closures. Those drillings showed that water lay underneath every one of the earlier targeted sites for hydrocarbons (Mulrooney, 2020). Thus, these structures has proven to be good spots for storing carbon dioxide. These Alpha and Beta structural closures are shown in figure 3.4.

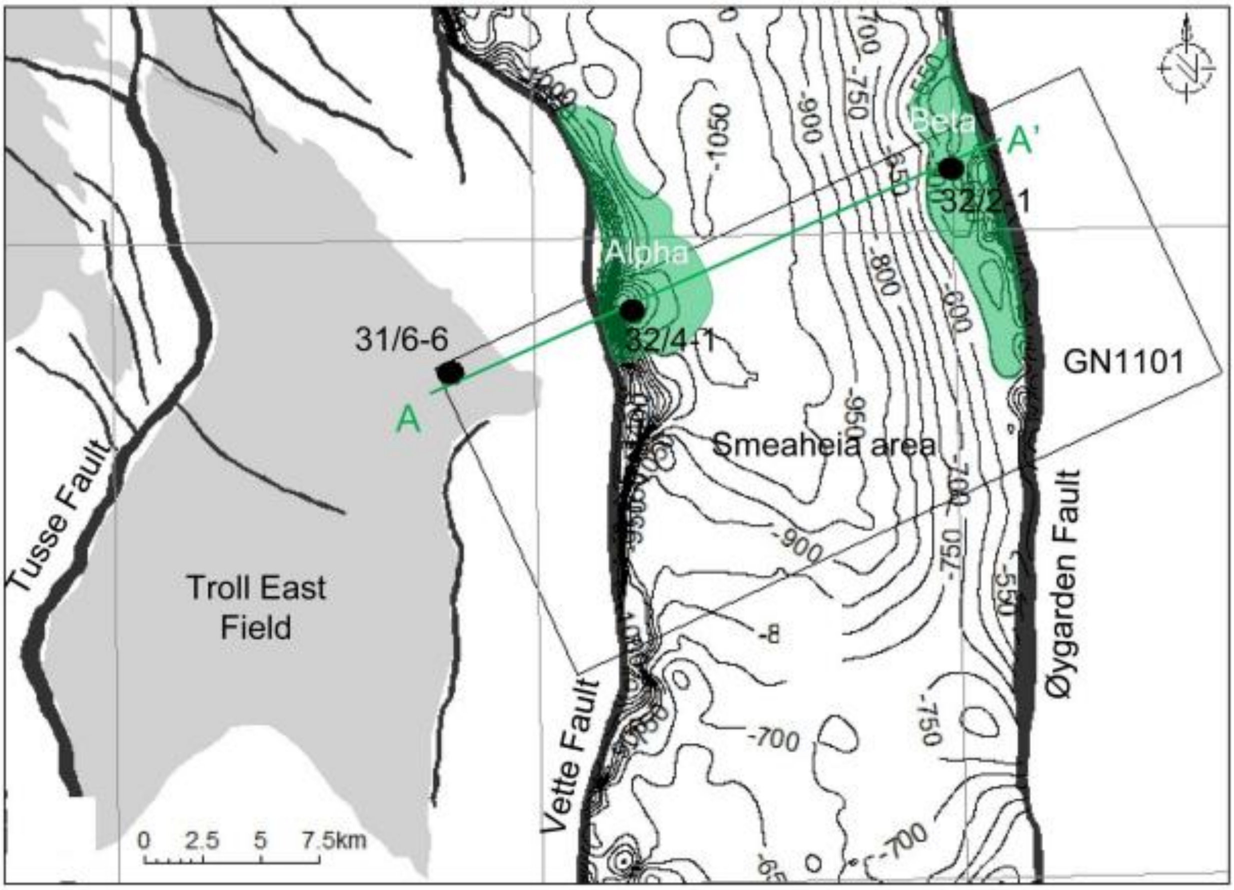

Figure 3.4 – Structural map of the Smeaheia block (Mulrooney, 2020).

The main storage rock at Smeaheia is the porous and highly permeable Viking Group sandstone from the Jurassic era which was formed in shallow seas that were near the coast. Sandstones are proven to be good structure for successful and safe CO_2 storage. The geological intersection for the Horda Platform is presented in figure 3.5.

Caprock security on the Horda Platform comes from mud-rich successions in the Upper-Jurassic to Lower Cretaceous. The main caprocks in this region, such as the Draupne and Heather formations, formed because of the second rifting event. They are necessary to stop CO_2 injected underground from moving upwards.

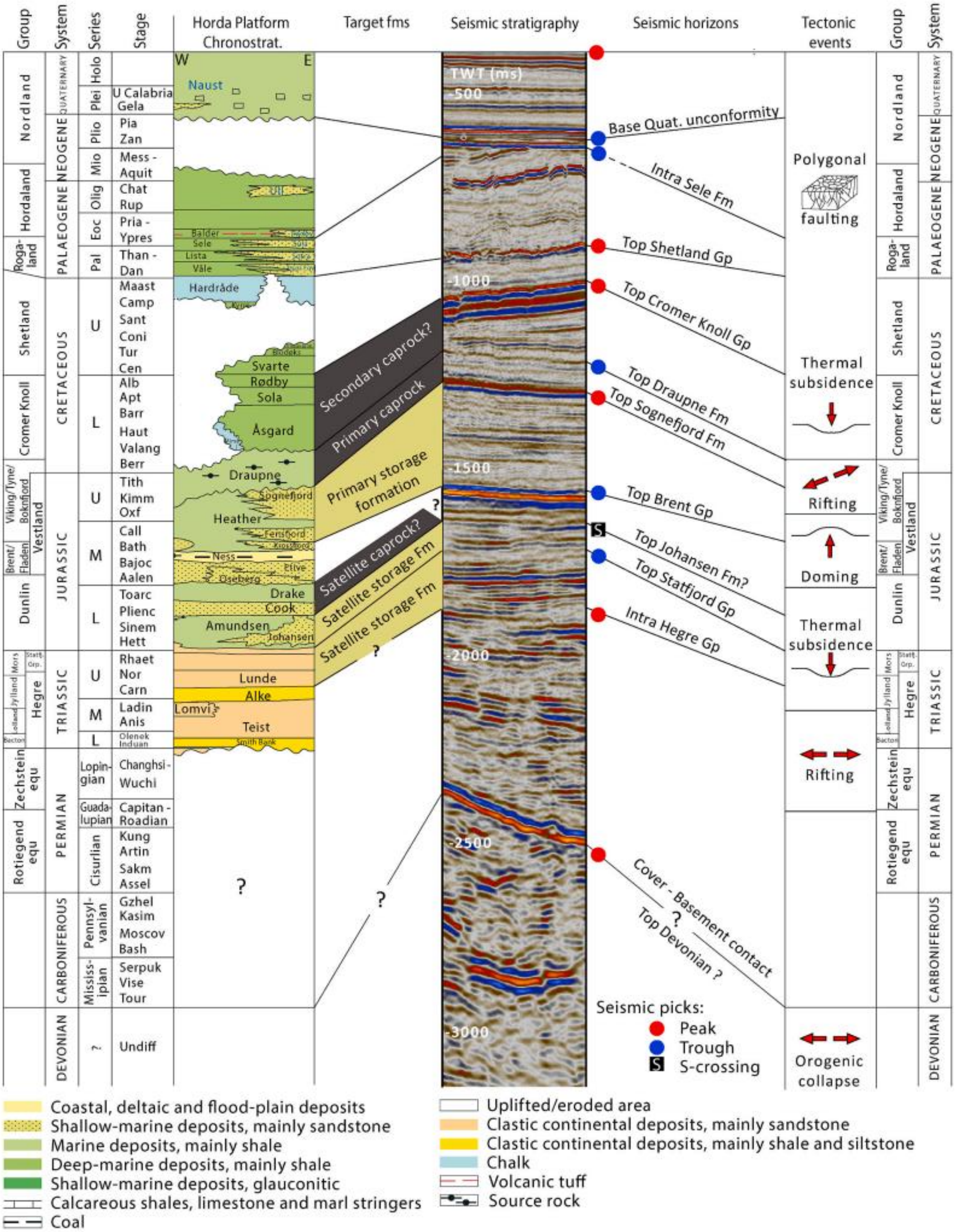

Figure 3.5 – Geological Intersection of Horda Platform (Mulrooney, 2020).

The western side of the Smeaheia block is formed by the FVC and its eastern boundary is formed by the ØFC. Some studies shows that those faults can be dangerous since they present chances of leakage to the surface (Mulrooney et al, 2020). The Smeaheia Fault is shown in a seismic cross-section view in figure 3.6.

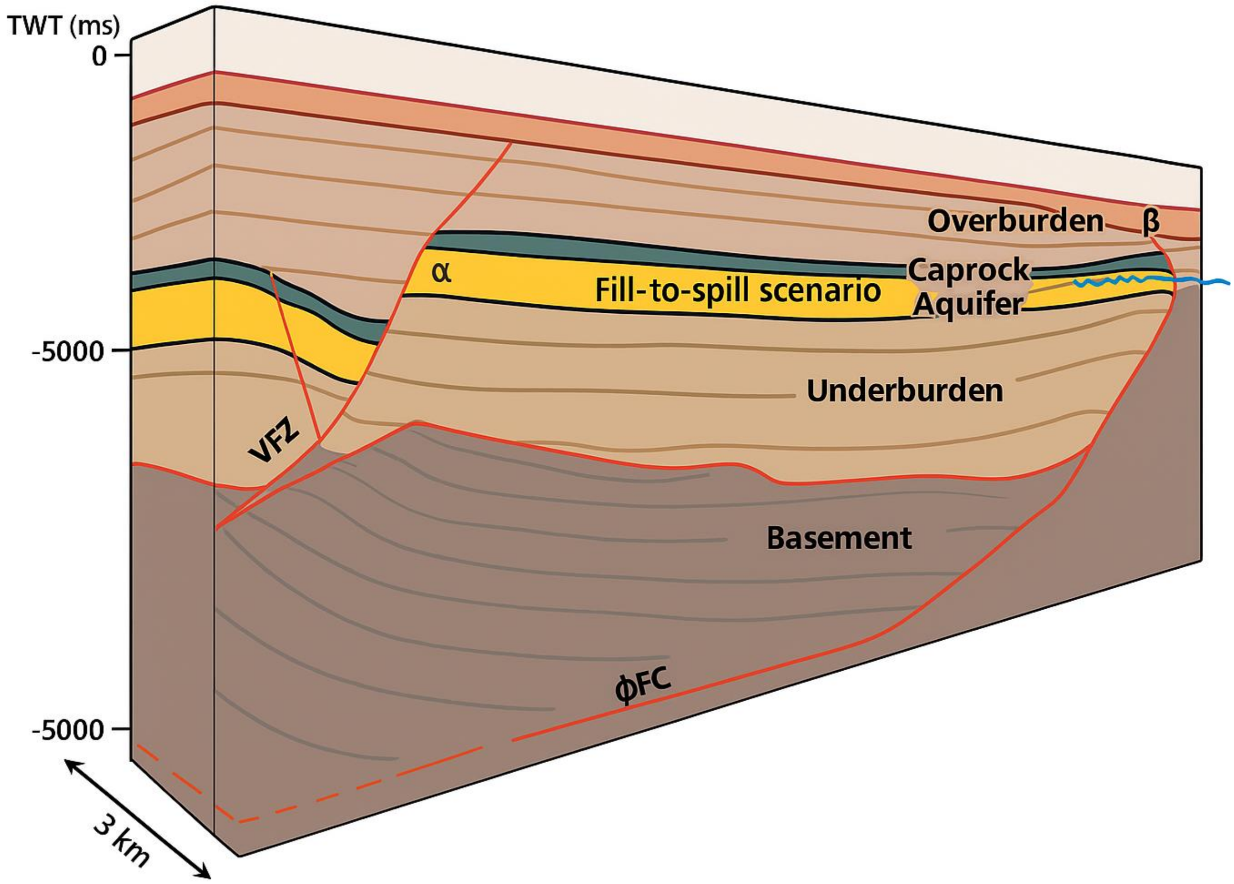

Figure 3.6 – Seismic cross-section view of the Smeaheia Fault blocks.

There are dangers tied to the Vette Fault Zone. According to probabilistic geomechanical calculations, the probability of the VFZ failing under ordinary conditions is 10 million times lower than 1 in a million or about one in ten thousand (Mulrooney, 2020), demonstrating "good-to-average" containment capability at typical injection levels. In spite of this, continuous pressure build-up might wake up certain areas, particularly those areas where the aquifer intersects the fault and water from the depleted Troll East field could reach them.

At the same time, the ØFC does create some risks. In the Oman Fault, the reservoir is situated against crystalline basement and laboratory tests indicate that faults in similar environments have low friction angles (17–31°). This soft and clay-filled gouge can seal fluid or move without causing earthquakes; but when pore pressure rises to more than the minimum principal stress, it could allow fluid to flow through. For this reason, it is still likely that salt would leak out from damage zone fractures, mainly when a late-stage plume reaches shallower regions (Bjørnstad, 2022). For this reason, basement penetration and stress transfer during flow from Alpha to Beta should be part of the coupled flow–geomechanical simulation.

The wellbore infrastructure is another major way for leakage, following the faults. The wells 32/4-1 and 32/2-1 stopped in the storage section, so problems like debonded cement sheath or corroded tubulars could leave micro-gaps that allow the reservoir to be polluted by aquifers above. The 2022 review on Smeaheia proposes orderly ranking of old wells, use of high-definition cement-bonding logs and, in the absence of suitable main barriers, the use of mechanical side-track plugs or sectional milling before starting CO_2 operations (Romdhane et al, 2022). In order to prevent new risks, Equinor must use the same high safety standards during this period wells for its CCS licence as it did during its early wells.

3.2 Simulation Tools and Workflow

This section reviews three commercial simulation tools that were used in this study. Simulating the whole operational process of CO_2 injection results in predictions of main technical parameters – pressure, temperature and CO_2 plume migration inside the Smeaheia aquifer. It includes details about information on using the software in practice and guidelines for typical use and important results.

3.2.1 Ledaflow

Transient multiphase flow simulators Ledaflow is a jointly developed tool by KongsbergDigital and SINTEF, developed to simulate CO_2, oil, gas, water steam and hydrogen in wells and pipelines (SINTEF, 2015). There is a complete conservation scheme of the mass, momentum and energy meaning that the code solves the slip between droplets, bubbles and the carrier phase. This scheme is proven to be quite effective for such calculations (SINTEF, 2015).

Ledaflow is unique, as it applies the specific precise modeling framework to imitate the multiphase flow. Mass and momentum are always conserved in wells and pipes of the system regarding oil, gas and water phases. Ledaflow address the problems of terrain and slugging in the pipeline, and they also inventory the emergence of the hydrates and transfer of hydrates and wax through pigs.

The individuals applying the system can configure steady-state and transient flow simulations. The initial part should be using steady-state modeling to determine the required starting positions and then transient modeling assists in verifying time-dependent activity, which will cause the system to alter its production scheme in easier unloading and shut-downs and to allow various features.

Ledaflow for modeling requires specific conditions inputs – so called boundary conditions, which define the physical system and operational parameters of a system. The inputs include:

- Nodes, pipes, wells, their detailed geometries and parameters (such as diameter, length, roughness, k-value (the equilibrium thermodynamic constant), material).
- Fluid properties, which include defining the compositional data (choosing from the database).
- Boundary conditions, such as inlet pressure, temperature or flow rates, end pressure and so on.
- Environmental parameters, such as ground or sea temperature, geothermal gradient.
- Computational settings – it can be Courant-Fredrich-Lewy number, time step or number of meshes.

For advanced simulations there also can be added complex elements, such as pumps, compressors, heaters, coolers, valves, leaks and other elements.

The simulator integrated with external pressure-volume-temperature characteristics of single element. In Ledaflow there is instilled special packages – Multiphase to provide precise fluid properties. The tool also exploit advanced thermodynamical models package – PR, CO2PURE, CPA, CSMA, GERG-2008 and others. Unfortunately, the student license version for the simulator offers limited PVT capabilities, but it can be expanded by linking Multiphase software which provide these thermodynamical packages.

The simulator provides an extensive database of output which deliver essential details about dynamic behavior. Outcomes include:

- Time dependent pressure and temperature profiles alongside with phase distribution that occur in the pipes. It also present different phase mode descriptions (sluggy, charn, bubbly).
- Mass or volume flow rates for each phase and component
- Saturation pressure graph and phase diagram
- Unstable flow behavior, slug formation, hydrate risks and wax deposition

The output data are in a structured database (MariaDB or SQLite) creating the convenience of easy retrieval and viewing of the data afterward. The user can also employ simple integration functions to tailor graphs and trends to his specific requirements to carry out detailed analysis and reporting. The output way of the simulator is beneficial in both study of engineering and real-time decision making that justifies the use of the simulator all through the project.

Ledaflow is an advanced platform that has been used especially to model multiphase flow particularly in this CO_2 injection case. This site is differentiated by its ability to build a complex model that is properly developed, the capacity of advanced physics, flexible input structure which can be changed depending on requirements, and outputs that are comprehensive and detailed to give sufficient information. Ledaflow is the most effective choice when it comes to engineering teams that want to overcome the various technical hindrances that are brought about by contemporary technological breakthrough in their area of operation (SINTEF, 2015).

3.2.2 Pipesim

Pipesim is an industrial tool that was invented by the SLB to model the various fluids transportation in pipes, wells as well as surface networks. This software has become one of the main industrial standards for oil and gas simulations. The main active in which this software is utilized in designing, analyzing and optimization of productions, injection systems with specific reference to assurance and network performance. The modular nature, solid physical models and graphical interface of Pipesim made it a superb tool in the oil industry.

Pipesim modeling process is constituted by the steady-state conservation equations of mass, momentum, energy, as they describe the behavior of the interactions of the various phases. It should be noted, that apart of Ledaflow, Pipesim can operates only in steady-state modem while Ledaflow can present complex transient mode and events (shut-in, leakage and others). These calculations are performed on empirical and mechanistic correlations that define a multiphase flow. Pipesim is flexible enough to be able to accommodate the homogeneous, separated and mechanistic models of flow and therefore a user will be able to use the most suitable modelling technique among those available in use.

Among the most important possibilities of Pipesim is its ability to represent complex surface structure built of manifolds, pipelines, surface facilities (valves, separators, storages). The program can also support compositional modelling by using of internal PVT packages within Pipesim. The lists of the PVT models are PR, CPA, Van-Der-Waals. This process is especially essential in systems that entail the usage of condensates, volatile oils as well as CO_2 systems.

Construction of a Pipesim model will need specific input data which characterize the physical system and the operation mode. The primary inputs are standard geometrical data of pipelines and wells (pipeline length, diameter, elevation profile, roughness, k-values), fluid details (composition, PVT data, phase envelopes, viscosity, density), the boundary conditions (inlet pressures and temperature or ends-up pressure and temperatures with flow rates), and the environmental conditions (ambient temperature, insulation properties and formation temperature). In network models, users specify the connections between the network nodes (wells, pipeline and surface facilities) exploring the operational constraints at each node.

Beside the Ledaflow solution, the Pipesim has also the ability to generate massive data that describes the pressure, temperature and phase fraction within the pipes and wells, phase flow rates and identification of various flow regimes (slug, annular and others).

In network models, Pipesim will give system performance data at the system level, i.e. system wide production rates, pressure drops throughout the network and the effects of changes in operations (e.g. well shut-ins or choke adjustments) and the overall system response. It is possible to use scenario analysis and examine how different inputs parameters are affecting the performance of the system too.

Conclusively there is a strong, beneficial, and convenient platform/grid that provides steady-state modeling of a multiphase flow in the oil and gas production systems, and this is Pipesim. Solely due to its licensing model, thorough physical modeling, flexible input structure, and the detail of its outputs, it is now considered as a core tool by production and flow assurance engineers.

3.2.3 Eclipse (E100 and E300): Black Oil vs. Compositional Models

Eclipse is a software that simulates a reservoir, which was developed by SLB. It is largely used as an industry standard in modeling fluid flow in porous media. The software demonstrates the capability of operating with 2 primary model types: E100 as software to accommodate black-oil approaches and E300 as software that represent compositional approach. Due to it, it is widely applied in the designing, optimization, and administration of oil, gas industry, hydrogen and CO_2 storages.

The physics governing Eclipse is model-specific, it depends on the model selected and the numerical schemes applied in integrating the conservation equations of mass, momentum, and energy in the reservoir. Eclipse E100 uses the black oil model that models the reservoir fluids with 3 pseudo-components which are gas, oil and water. Therefore, it supposes that every phase is constantly composed. The special PVT tables establish the PVT properties of each phase with the user specifying gas-oil-ratio (Rs), oil formation volume factor (Bo) and viscosity. The method is computationally inexpensive, and suitable to compositional effects in reservoirs that are of secondary importance.

Conversely, E300 is a fully thermal compositional simulator. It represents each of its components by attaching thermodynamical properties as well as opting line of equation state. Consequently, it follows the composition of every step of the simulation. The method is needed in systems where phase behavior is complicated, e.g., volatile oil, gas condensates and CO_2 injection conditions. E300 uses an EOS, usually the PR or Soave-Redlich-Kwong (SRK) equations to calculate phase equilibria and fluid properties as a function of pressure, temperature and composition.

Both of these approaches solve the governing partial differential equations by applying finite-difference methods, with support for a range type of grids (structured, unstructured or corner-point) and advanced numerical techniques. The simulator can model wide range of processes, including water or gas injection, chemical and thermal enhanced oil recovery methods, and other advanced techniques that applicable for oil and gas as well as CO_2 injection modeling.

For performing simulations with Eclipse, user have to define the following inputs:

- Geological model, such as grid geometry, rock properties (permeability and porosity), fault system.
- Fluid properties, in case of E300 – compositional data and thermodynamical data for each component. For E100 – simple PVT table is sufficient.
- Initial and boundary conditions – reservoir pressure and temperature, injection rates, water-oil contacts, saturation.
- Well configuration – location, completion, schedule and control strategies.

Major operational schedules, including injection and production rates, pressure limits, and well treatments are defined with the help of input decks. In more sophisticated cases, further inputs could be necessitated which could be geomechanical values, chemical concentrations, or thermal values. The flexible input structure of Eclipse enables modelling of a very broad spectrum of the reservoir models and development strategies.

Eclipse simulators produce detailed body of outputs which represent description on dynamic behavior of the fluids in the reservoir. The key products are time profiles of pressure, temperature, saturation, and composition at every grid cell and production and injection rates per well; also at the system level are cumulative recovery, sweep efficiency averages and breakthrough times. In the case of compositional simulations, E300 comes up with the close-monitoring of component distributions, compositions of phases, and miscibility influences.

Data related to the output can be either viewed in client post-processing tools or exported to other external packages. Eclipse allows generation of summary reports, cross section plots and three-dimensional plots of reservoir behavior. Through the detailed outputs, engineers are able to make an evaluation of the performance of the reservoirs, optimum development strategies and the effects of the changes in the operations.

It should be noted that in E300 exists huge number of modules that can be quite useful and applicable for CO_2 injection scenarios. They are:

- CO2STORE – special module for modeling CO_2 storage in saline aquifers. Mostly calculates all thermodynamic parameters by providing small amount of data – compositional data and salinity level.

To conclude, Eclipse E100 and E300 are the most skillful tools among the available ones that enhance the capacity of fluid flow simulation within reservoirs in the industry. Selection between black oil and compositional models is based on the complexity of the fluid system and the intentions of simulation. These two simulators are highly competitive because they have a flexible licensing, sound physical modeling, extensive input structures as well as a well-documented output that is essential requirements of reservoir engineers and asset managers.

3.3 Model Development

In this section will be presented the process of construction surface equipment and wellbore model in the descripted above software – Ledaflow, Pipesim and Eclipse.

3.3.1 Wellbore and Pipeline Flow Models (Ledaflow/Pipesim)

The Smeaheia storage site will get an injection rate obtained as reference-case 1,5 Mt CO_2 per year equivalent to approximately 47,6 kg/s. The chosen throughput defines limits of the designing of both a surface flowline (1 km) and a vertical injection well (1,5 km). The modeling process is focused on investigating the multi-decadal scenario of the model thermal-hydraulic coupled response of the well-surface of the system to ensure that over the planned multi-decadal storage campaign the containment of pressure and the thermal integrity and flow assurance remains within safe operating conditions.

The dense stream (4°C) leaves the tanker prior to entering a 0,16 m-internal diameter (ID) carbon-steel flowline, commonly referred to as a riser; the line is 1000 m long and leads to wellhead choke. In the various sensitivity tests the choke system has 98 bar inlet pressure, and the wellhead pressure varied between 20 and 40 bar. The temperature of the CO_2 reduces to a low temperature at the wellhead due to Joule Thomson cooling through the choke although outside the seabed was 4°C in the model. Such boundary conditions play an essential role in forecasting transient thermal stresses and possible risks of hydrate or ice occurring in the annulus. This scheme is presented in figure 3.7.

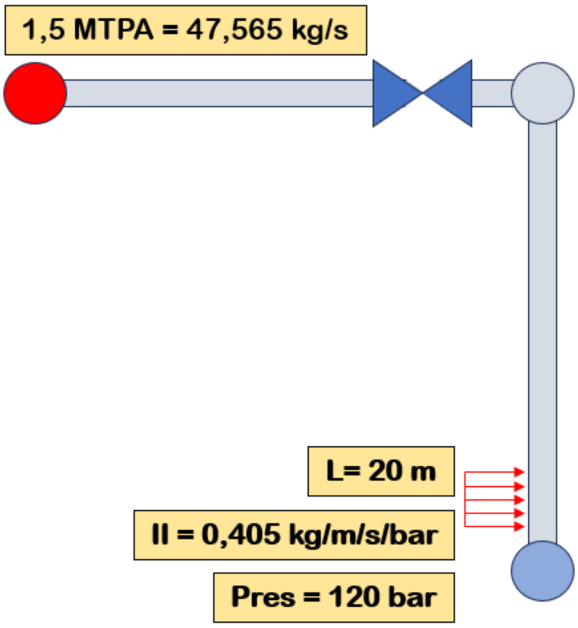

Figure 3.7 – Smeaheia's case description. Red node – pressure boundary. Blue node – flow boundary.

The details of the well construction are displayed in figure 3.8. The injector comprised a vertical well of 1500 m having one 0,16 m-ID in a four-concentric casing of 0,224 m;0,315 m;0,46 m;0,87 m with sections of conductors, surface casing, intermediate casing and production casing. The casings are completely cemented to isolate the zones and provide good thermal conduction to the involved formation. At the production casing bottom a 24 m perforation goes through directly to the storage formation. The simple two-tubing completion carries on the same advantage by lowering the pressure loss that allows the capability to carry out logging or velocity-string installation in the event of a drop in injectivity.

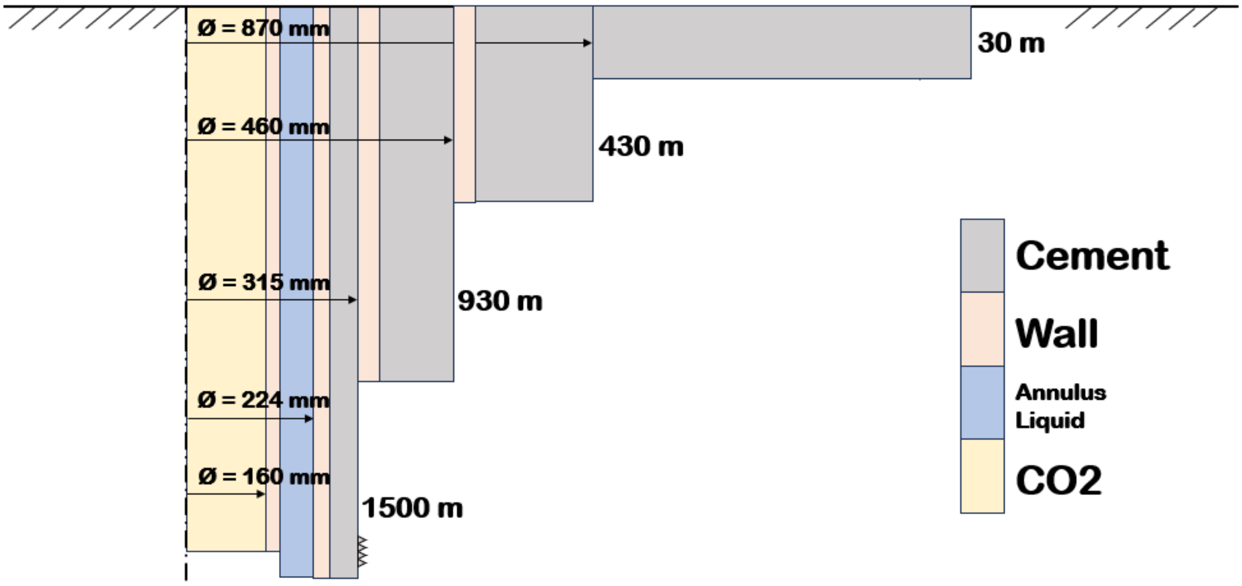

Figure 3.8 –The proposed well Smeaheia's construction.

The in-situ temperature at 1500 m depth reaches 45 °C because of a measured geothermal gradient of 2,73 °C per 100 m. The static reservoir (pore) pressure measures at 120 bar while the model predicts BHP of 125,8 bar during steady injection. The 5,8-bar over-balance pressure matches the measured injectivity index of 0,405 kg/s/m/bar which enables the design flow-rate of around 47,6 kg/s. The predicted bottom-hole temperature (BHT) will reach around 10-20°C under these conditions because the injected fluid causes strong cooling which requires temperature-dependent viscosity in the reservoir model.

Firstly, this case was decided to model in network simulators (Pipesim/Ledaflow). The integration of two specialized simulators into an integrated workflow requires precise descriptions of fluid properties and well hydraulics and completion parameters. The table 2 shows the main parameters used for Ledaflow and for the Pipesim.

Table 2 – Ledaflow and Pipesim settings comparison.

	Ledaflow	Pipesim
Thermodynamic model	CO2PURE	PR
Viscosity model	Pedersen	Pedersen
Volume shift correlation	Peneloux	Peneloux
Valve model	Perkins	Mechanistic, Ashford
Injectivity setting	Linear PI	Linear PI

Ledaflow utilizes CO2PURE EOS that is dedicated to dense-phase carbon dioxide and was developed and tested with high pressure low-temperature experimental data on offshore transport lines. Pipesim uses the PR EOS as a general-purpose third-order model in dealing with multi-component mixtures. The two formulations will have the same density above the critical point but CO2PURE will have slightly higher liquid densities at 0-10°C and therefore will produce a slightly higher line-pack during cold-start conditions (SINTEF, 2015).

Both simulators use the Pedersen viscosity model as well as volume-shift by Peneloux to minimize cross-platform uncertainty. Use of the same secondary correlations then eliminates any undesirable viscosity or Z-factor mismatch that is due to the EOS rather than the ancillary empirical alterations.

Ledaflow uses the Perkins critical-flow correlation to control the wellhead pressure due to the efficient homogeneous-equilibrium approach of this correlation allowing fast time-steps to be used. Pipesim presents a more mechanistic model of phase slips, but the variation is negligible with less than 0,5 bar during injection of thick-CO_2 phases without flashing relied on in the sensitivity tests.

First of all, this case was modelled in Ledaflow. The picture of the case is presented in figure 3.9. The concept replicates the information that was discussed in the text before. Carbon Dioxide produced on the ship is added to the riser at the Pipeline Start (PS) point that exists at 98 bar and 4°C. The fluid then travels through the riser then enters the valve. The valve is working on 20 percent opening with C_v= 0,2. Parameters of the choke were assigned because of various tests performed in the process of assembly of the model. The loss of well head choke pressure caused CO_2 to be injected into the 1.5 km vertical well prior to being injected back into the ground at 1500 meters below ground level.

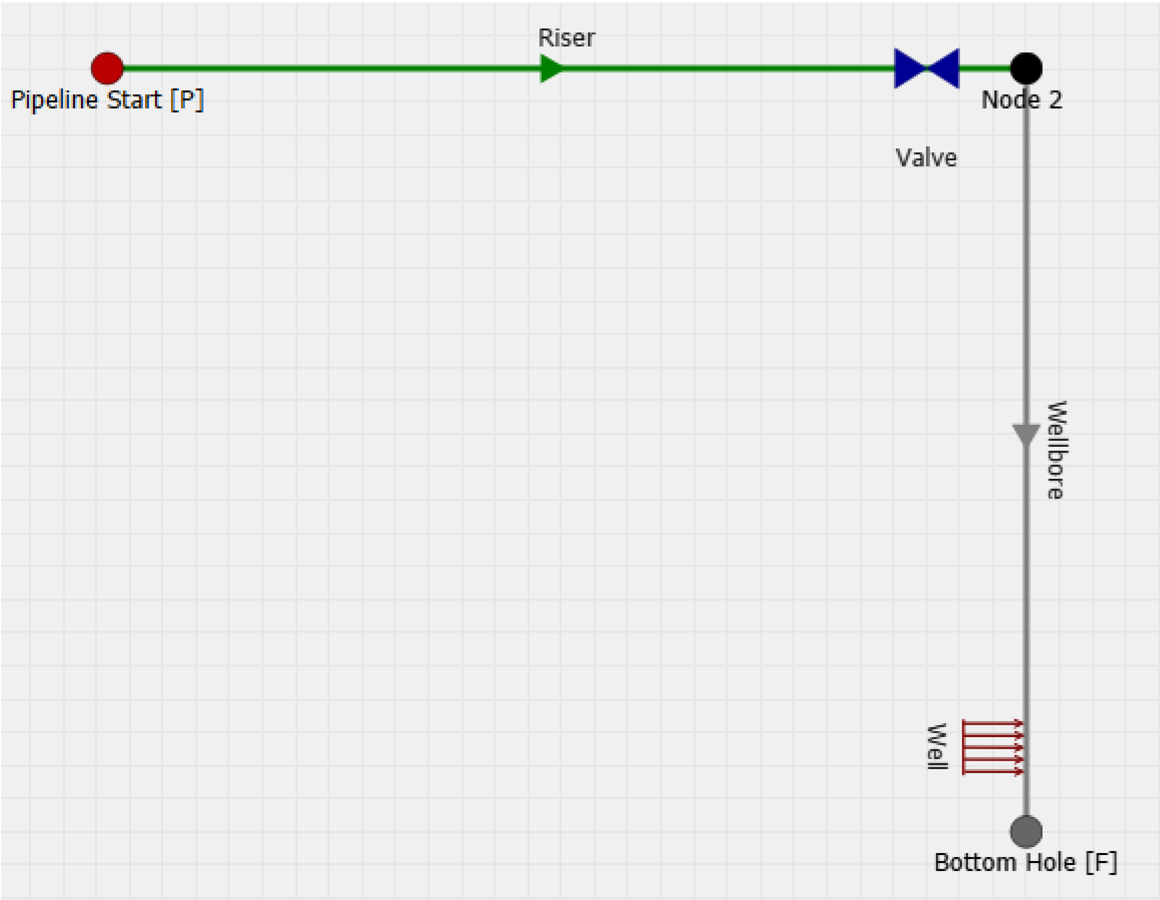

Figure 3.9 – Smeaheia's presentation in Ledaflow.

Secondly, to compare different available options the case were modeled in Pipesim. The process is quite different from the Ledaflow flow path. In the beginning, the user must define the construction well. The well construction is presented in figure 3.10.

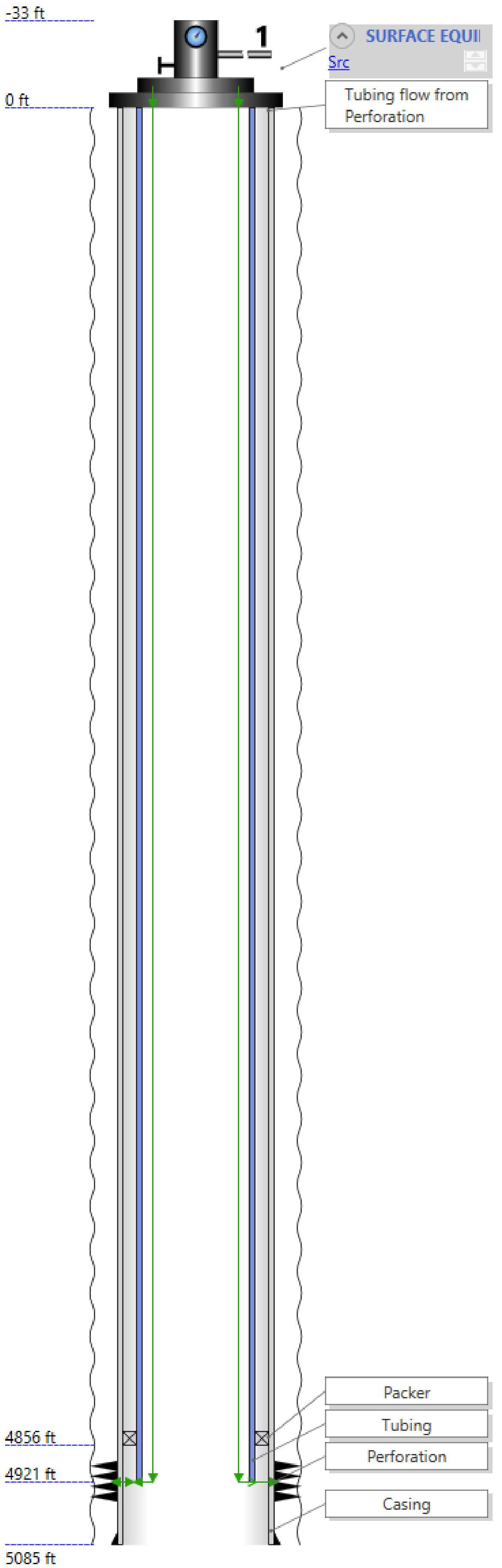

Figure 3.10 – Schematic of the Smeaheia well implementation in Pipesim.

After constructing the well, the main properties of the well should be specified. For the modeling of the riser and choke, network model should be used. Figure 3.11 represents the network model.

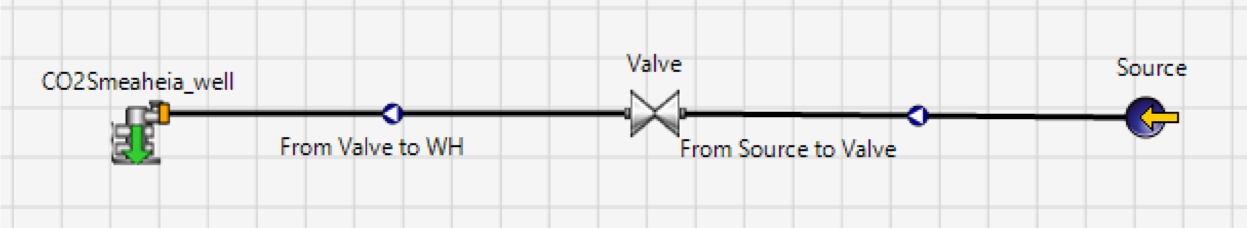

Figure 3.11 – Case presentation in Pipesim.

After validation and verification of the models' performance, they were calculated, and the simulation results will be presented in the next chapter 4.

3.3.2 Reservoir Models: E100 (Black Oil) and E300 (Compositional)

Two successive models were used in monitoring the Smeaheia injection project to capture subsurface responses during the whole period of the project. The E100 black-oil formulation provided numerical speed, simple approach and well controls. The model has a representation of brine as oil phase and CO_2 as gas. The model enables its user to perform rapid phase-behavior calibration of rock-physics parameters (permeability, porosity, Net-to-Gross, relative-permeability tables) and benchmarking the injectivity without incorporating density-driven mixing and phase-split processes.

The E100 model was downloaded from CO2DataSharePortal includes a full Eclipse E100 black-oil model to forecast the CO_2 injection and the long-term storage in the Smeaheia prospect on the Horda Platform. The model splits the Alpha and Beta potential storage structures along with the intervening saddle into a regular 200m x 200m mesh that is forty layers of around 4 meters each, with an overall foot print of around 20 km east-west by 34 km north-south which results in approximately two million active cells after removing inactive volumes. The grid of the model presented in figure 3.12.

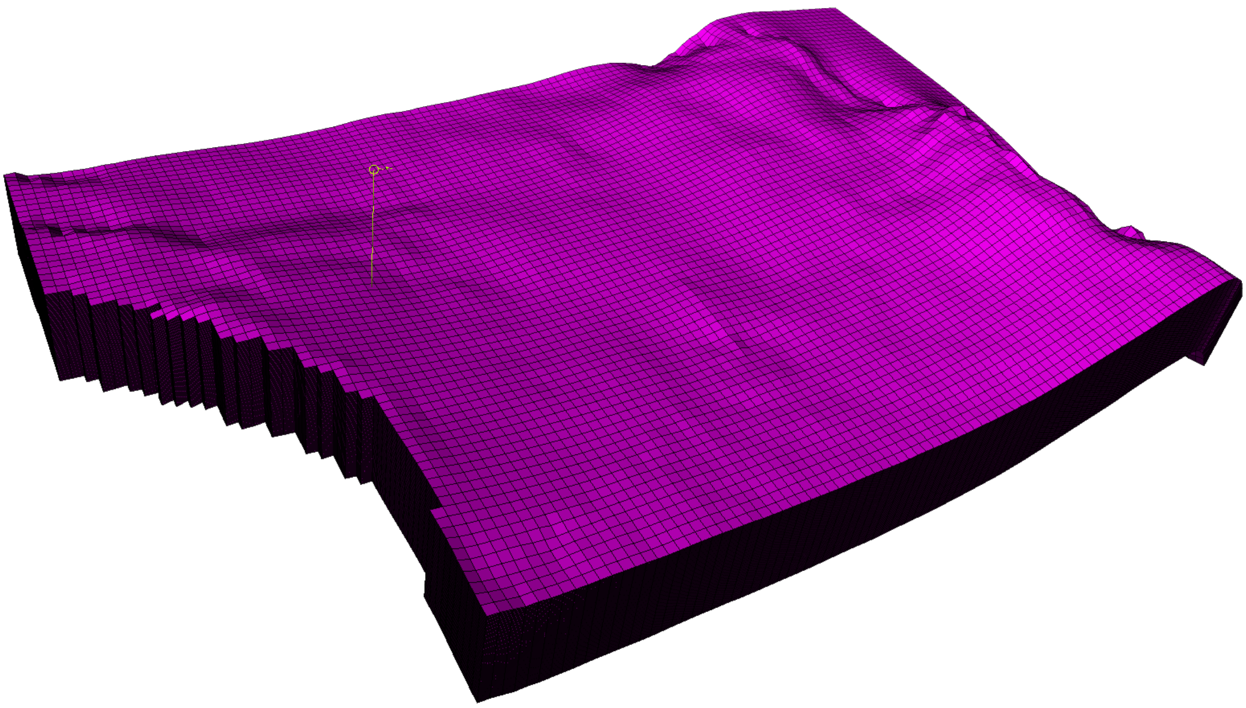

Figure 3.12 – Grid of Smeaheia model in Eclipse with “Alpha” well (yellow).

Black-oil PVT models dynamic behavior by assigning brine to the oil phase while treating CO_2 as the gas phase to allow various dissolution options. The reference reservoir temperature reaches 37 °C and it measures 45 °C in Alpha and 35 °C in Beta. A 50-bar draw-down reduces the density of CO_2 to about 183 kg/m^3 in Alpha and 87 kg/m^3 in shallower Beta while demonstrating how regional depletion affects storage capacity. The E100 model omits CO_2 dissolution in brine to maintain a conservative plume footprint.

The Smeaheia E100 grid shows it can effectively meet Northern Lights Phase 1 requirements with 2,1 million tons per year storage capacity for twenty years while offering additional storage potential when Alpha reaches its maximum capacity and Beta starts operations. Storage performance depends primarily on regional pressure history and accurate saddle mapping rather than injectivity or rock quality which are beyond the project requirements. As a result, the proposed well management plan for this study includes the following: The well in "Alpha" structure begins its injection operations on January 1st, 2029, with a loading curve that rises from 175000 m^3/day in the first month to achieve the full capacity of 2,1 million m3/day by the beginning of 2030. Then – 20 years of injection to 1st of January 2051. The well will be closed after injection, then the CO_2 migration will be evaluated for the subsequent 20 years.

The transition from black-oil model to thermal compositional model required the following steps:

A complete simulation transfer from the original E100 black-oil model to a new thermal compositional E300 model required sequential input deck rebuilding to ensure every crucial physical simulation could run without approximations.

Firstly, it was enabled the CO2STORE option within RUNSPEC to convert the compositional solver into a three-phase CCS engine which handles CO_2-rich gas and H_2O-rich aqueous phases and an optional solid phase. This option maintains tracking of CO_2-brine mutual solubility and brine density modifications from salts while also detecting halite or calcite precipitation beyond black-oil PVT capabilities. Then, it combined the THERMAL module with this setting because the energy balance in the module allows temperature variations throughout space and time while it modifies k-value calculations and enables the monitoring of temperature stresses around the injection point and the caprock. The THERMAL module provides users with heat-loss terms as well as wellbore heaters and temperature-based rate controls which are documented as fundamental capabilities of the module.

The COMPS section contained a four-component mixture that included CO_2, H_2O, NaCl and $CaCl_2$. The simulation used critical temperature, critical pressure, acentric factor and molar weight data from the user's input as well as standard salt property tables to make the PR EOS converge within the 20–80 °C, 50–350 bar temperature and pressure range.

The THERMAL module is active so the simulator cannot maintain an isothermal reservoir condition so it was added a true-vertical-depth temperature profile in RTEMPVD matches the 37 °C average data and maintains a 25 °C/km gradient until the seabed. The simulation starts every active cell at its native temperature point before any cold CO_2 injected into the system.

The next step involved enabling molecular diffusion. The keyword DIFFCOIL was used to supply liquid-phase diffusion coefficients for each component because it represents the standard procedure for loading Fickian diffusion data into E300. The simulator will default to zero mass transfer between stagnant fluid parcels if this keyword is not included. The selected values (10^{-12}–10^{-9} m^2/s, increasing with temperature) originate from open-literature brine–CO_2 experiments which receive pressure corrections during simulation runtime.

The legacy EQUIL block used to determine mole fractions after salts were included so an explicit mapper was required for salinity initialization. The AMFVD tool established an equilibrated starting composition for each cell which matched core-flood data by setting NaCl at 3,2 mol/kg and $CaCl_2$ at 0,1 mol/kg. The AMFVD keyword serves this specific function while replacing the previous AMF tables during CO2STORE operation.

After establishing the fluid system, a single-component CO_2 stream was created in the SCHEDULE section. WINJGAS linked the Alpha injector to this stream so that the well maintains the correct composition regardless of future impurity blending decisions. The WINJTEMP was set to 10 °C to match the expected subsea tie-in temperature while the wellbore heat-loss sub-model can accurately simulate the fluid cooling process before reaching reservoir depth.

The E300 deck maintains the original grid layout, rock and geo-mechanical data while implementing full compositional, thermal and geochemical physics models instead of black-oil simplifications. All following predictions regarding pressure build-up, plume shape, salting-out risk, injectivity evolution are now controlled by fundamental phase behavior models instead of using empirical multipliers which produces more reliable storage performance predictions.

3.3.3 Advanced CO_2 Storage Modeling

The investigation of OCD into injectivity and plume conformance involves reconstruction of the Smeaheia case-study by removal of CO2STORE and THERMAL in CO2SOL option with the multi-segment-well formulation.

This was initiated by the CO2SOL simulator physics implementation in which the implementation automatically produces temperature and salinity dependent on carbon dioxide water solubility tables that can be directly fed to the flash algorithm. CO2SOL is used as a two phase system, but it still retains the brine-CO_2 gas dissolution effects, where the result is modification of density and viscosity and change of volume hence it can be applied in situations where chemical reactions and solid precipitation is not the major concern other than accurate composition is desired.

EOS PR was a RUNSPEC command which was taken to enable the PR EOS prior to restriction of fluid system to CO_2 and H_2O only to reduce CPU costs besides still retaining the necessary freedom in phase-behavior. While in CO2STORE it was hidden EOR, in CO2SOL user must define the model. In simulation the effect of DIFFUSE had to be added in order to continue the molecular diffusion in the large shut-in time after injection. The parameters in its phase-interaction were a binary-interaction-coefficient of 0,1896 to correct mutual-solubilities and a PARACHOR of 78 to a surface-tension calibration in capillary-rise diagnostics and a background SALINITY of 0,51% to conciliate brine-density measurements. The PVT description needed component wise diffusion coefficients (DIFFCGAS 0,2 and DIFFCOIL 0,01 cm2/s) and an ACF 0,225 – acentric factor.

The inherent representation of salts by the salinity flag allowed that the standard EQUIL block could be used in setting the initial composition rather than the AMFVD distribution of the CO2STORE run. By deploying the profile of hydrostatic pressures obtained by the system, CO2SOL adjusts automatically the absorption capacity of CO_2 distributed over the grid.

It went ahead and modeled well-bore hydraulics upon defining the fluid model. When WSEGDIMS is activated the parameter-data structure multi-segment-well and pressure, temperature and flow rate arrays first become active since it is the basic switch that makes parameter-data structures of a type segment keyword parsing.

WELSEGS command was used to divide the Alpha injector into six segments of the vertical, or true-vertical depth coordinate at the depth range of 1476 m to 1500 m in increments of 4 m. The entries specify the points of the measured-depth end point, reference grid block and inside-radius of tubing sections.

The next keyword that tied each of the well segments along with the corresponding grid cell perforations was COMPSEGS to produce transmissibility multipliers among the segment hydraulics and the reservoir flow. The six segments indicate discrete yet close cells within the single laminated sand pack due to the existence of the perforations situation in the high quality Sognefjord region.

WSEGVALV provided each segment with specific valves towards imitating the operations of an OCD. The sub-critical valve type of this segment has the need of two parameters of control, namely: the flow-coefficient C_v, and the effective fraction of the flow-area. These parameters cause an extra pressure loss which amounts to the following mathematical equation:

$$\delta P_{cons} = C_u \frac{\rho v_c^2}{2C_v^2}$$

Where δP_{cons} – construction differential pressure (Pa), C_u – unit-conversion constant (-), ρ – density (kg/m^3), v_c – fluid velocity (m/s), C_v – flow coefficient (-).

A PR compositional solver and explicit control of the solubility of CO_2 and a fully discretized model of the wellbore are used to maintain the original grid structure and rock properties of the deck. The segment-based diagnostics shows a much flatter injection-profile as compared to the single-node well and parametric sweeps on valve imply that simple OCD tuning might postpone early breakthrough into the saddle by many years. In future, the multi-segment well will be integrated to closed-loop control of the valve settings such that the settings will adjust in response to the changes in reservoir pressure and temperature in order to achieve maximum efficiency of the storage and at the same time protecting the integrity of the cap-rock.

3.4 Coupled Simulation Framework

The entire injection chain requires a single thermodynamic system from the surface network to wellbore and reservoir to analyze the integrated behavior. The physics of individual domains receive high fidelity modeling from standalone simulations where Ledaflow handles transient multiphase flow in pipe system and Eclipse that handles porous-media multiphase flow. The standalone operation of these tools prevents information exchange about the time-dependent boundary conditions which link their solutions because surface facilities mass-flow rates determine reservoir pressure buildup and reservoir back-pressure affects both choke behavior and well-bore hydraulics. The absence of these feedbacks and exchange between simulators results in either non-conservative design margins or unachievable operating envelopes in field operations.

3.4.1 Loose-Coupling Approach

In the coupled workflow distinguishes two main approaches – loose-coupling and tight coupling (Figure 3.13). In this figure the left side represents the loose-coupling approach in which each module (circle) interact only through narrow arrows (exchange files, information). In the context of this study – each circle retains its own space, illustrating Ledaflow and Eclipse. They run as independent simulations whose only connection is the exchange of pressure, temperature and flowrates through the files or external scripts.

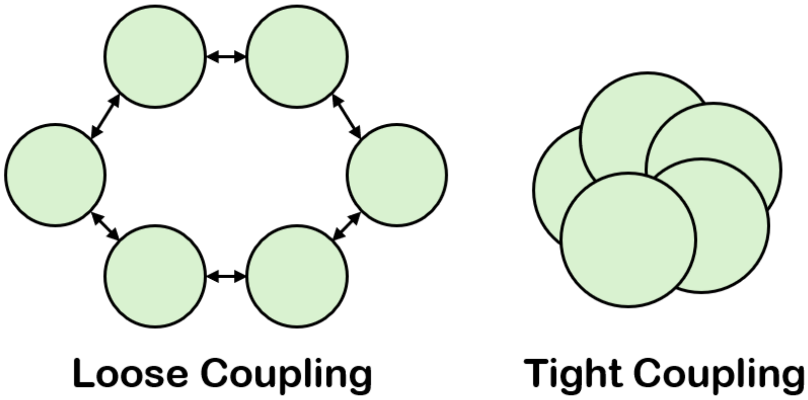

Figure 3.13 – Conceptual comparison of loose-coupled (left) and tight-coupled (right) integration architectures.

The right-hand of the figure 3.13 shows a tight-coupled approach. In this technique, the same circles are integrated together, symbolizing a single executable in which reservoir and wellbore system share memory and are being solved in one global Newton loop. Such a integrated approach would eliminate file transfers and could improve the numerical efficiency. Unfortunately, for coupling Ledaflow and Eclipse in this technique, it requires joint licensing and full model development with bug fixes, recompilation and re-verification. For industrial purposes that might be justifiable, whilst for the academic study that should be agile.

The loose-coupling approach was adopted in this work since the two simulators are independent of the internals of the other, they are independently upgradeable, swapped or debugged, and the supervisory loop can be evolved independently of the source code.

Firstly, for the coupling process, it was decided to implement 20 different steps. The scheme of these steps presented in figure 3.14. The first step represents the first month of injection with injection rate equal to 175000 m^3/day, so the first 12 steps – first year. The following 8 steps – different subsequent years, where the 20th step is the last year of injection.

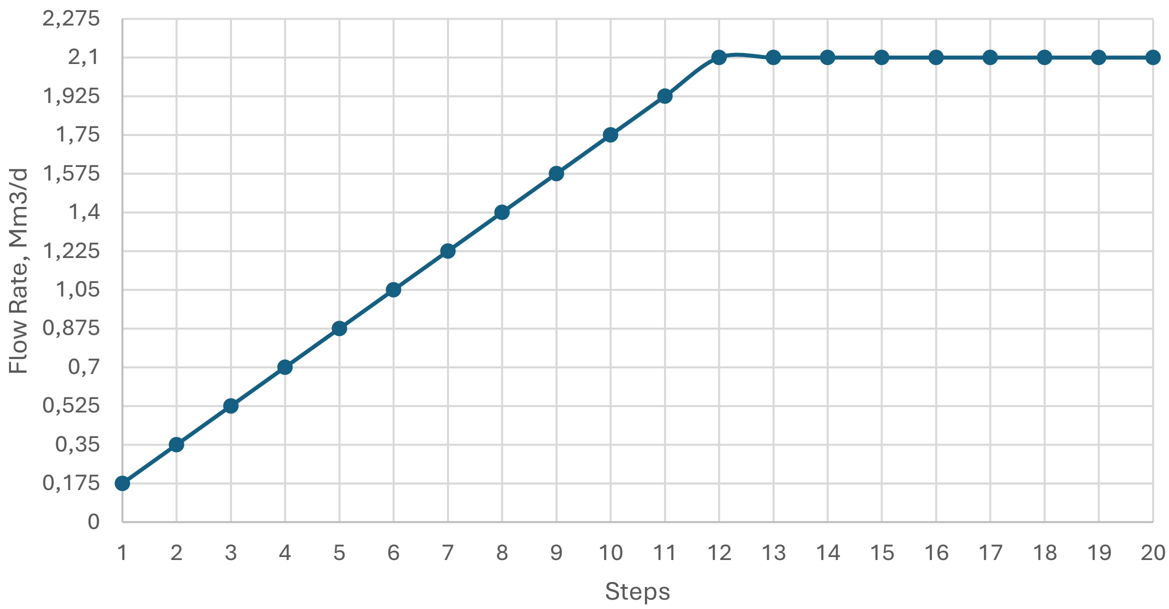

Figure 3.14 – Suggested steps for the loose-coupling.

Figure 3.15 summarizes the proposed logic for loose-coupling. It should be noted that this flowchart will be applied for each defined step. The process involves the following:

1. Set inlet pressure in the PS point and set hypothetical choke configuration (% opening and Cd).

2. Set hypothetical injection temperature on the BHP. Set the maximum injection pressure (P(wfmax)). Set Mass Flow Rate (MFR) for the well and Run Eclipse model. After calculating it can give the reservoir pressure for the step.

3. Get the reservoir pressure from the Eclipse and run Ledaflow model

4. Get MFR and compare it with the MFR that was set for Ledaflow. If they are not equal, then users need to go back and change the hypothetical choke configuration. For this purpose, is highly recommended to use Proportional-Integral-Derivative (PID) – controller that levitate the necessary process.

5. Get bottom BHP and tubing hanger pressure (THP) from both model and compare it.

6. In case, if they are not equal, the user must implement the BHT from the Ledaflow to Eclipse and run all algorithm again.

This algorithm must be repeated as many times as needed, since Ledaflow run can give the bottom hole temperature that must be implemented in the Eclipse run, and again it will be run to match the pressures, temperatures and flowrates.

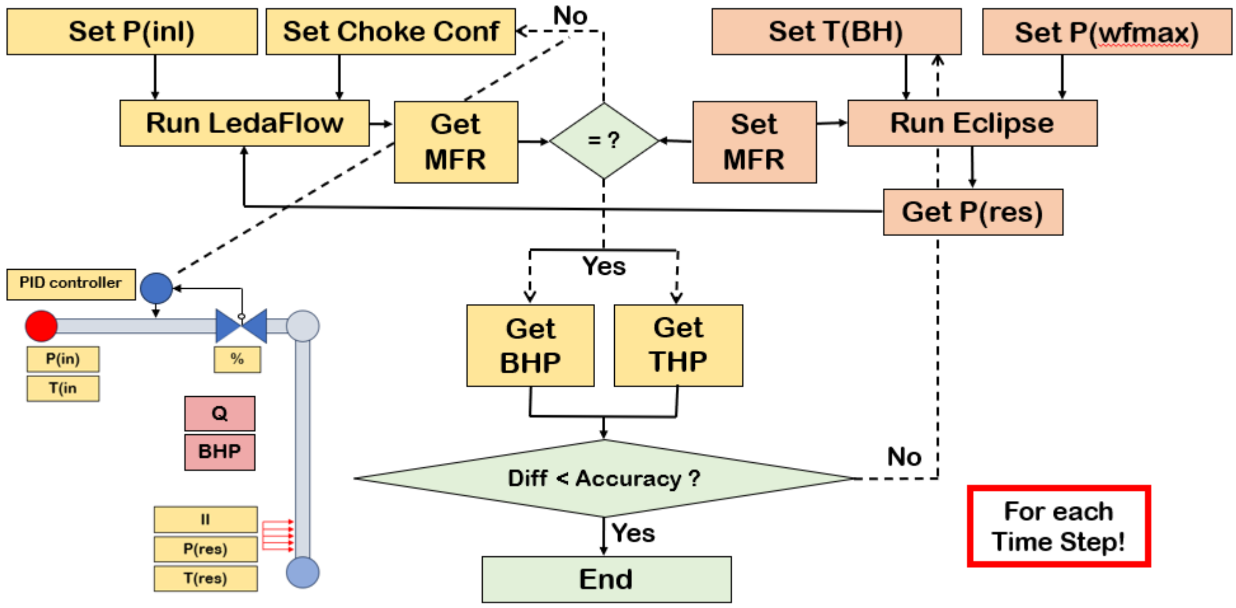

Figure 3.15 – Suggested loose-coupling approach.

Chapter 4. Results

The chapter is opened by the dynamic simulations that show CO_2 injection in Smeaheia site by Ledaflow and Pipesim. Although pressure and temperature and phase behavior plots have been compared and are found to gauge a similar near wellbore thermohydraulics, they yield slightly varying bottomhole pressure estimates when the super-critical flow state is perceived. It followed by the display of scenarios run E100 (black-oil) and E300 (thermal compositional) to present realistic compositions. Results of reservoir, well, pipeline will be given using a newly introduced coupling flowchart. An OCD which meets Smeaheia specifications is designed with the output of the CO2SOL equilibrium model.

4.1 Wellbore and Pipeline Simulations

4.1.1 Comparative Analysis: Ledaflow vs. Pipesim

Firstly, a comparative analysis was conducted to validate simulation accuracy for both software – Ledaflow and Pipesim. They were fed with the presented before case geometry, fluid properties and boundary conditions. The pressure profiles from the tanker to choke, followed by the injection in the well are shown in figure 4.1.

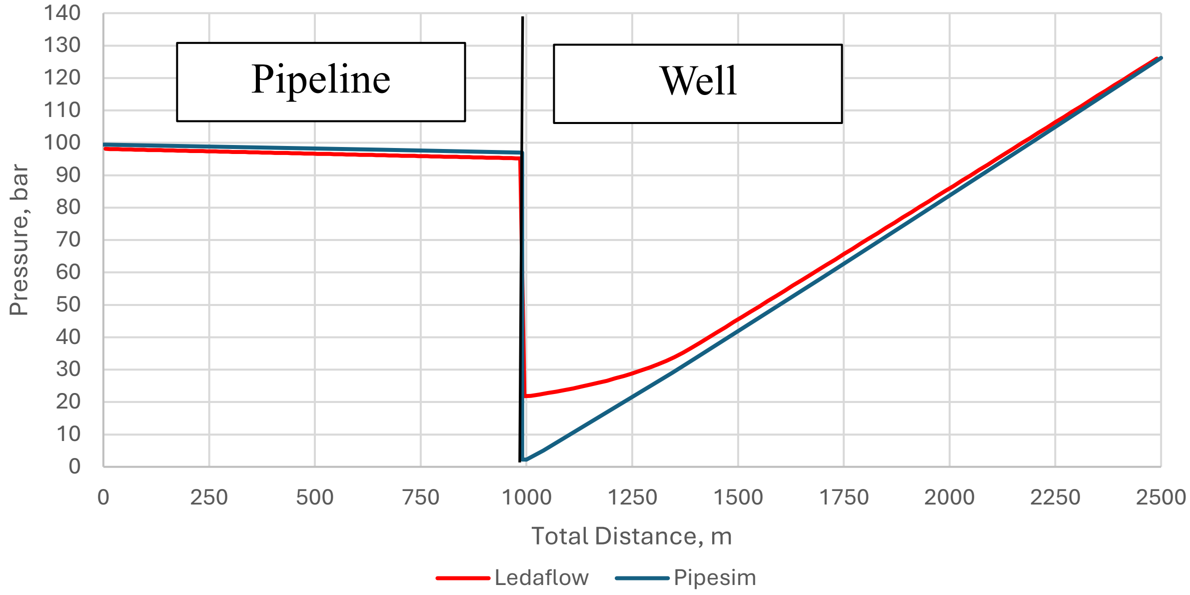

Figure 4.1 – Pressure distribution along the case.

Both simulators contain the same profile in terms of pressure, and this profile reveals a smooth decrease in pressure on the horizontal line (0-1000 m), pronounced drop in pressure on the choke and a smooth increase in pressure in the injection well (1000-2500 m) due to hydrostatic pressure. The pressure drop at the choke also has a huge implication under the influence of the chosen mode of valve between Ledaflow with Perkins model and Pipesim with Mechanistic model. The result is that the pressure drops inside the choke are not the same in Ledaflow and Pipesim as the changes are bigger in Pipesim. Then, it was followed by the increase to the bottom hole point. It should be noted that Pipesim use simple line dependent pressure, while Ledaflow present it as curve line because of condensation process. The two models show a convergence with the same value of bottomhole pressure in the wellbore section wherein the value of bottomhole pressure using the hydrostatic calculations are equal. The difference between the two tools is dominated by the PVT handling and the modeling of phase behavior that differs slightly.

The prediction of well pressure distribution in both models was accurate as they were able to give similar values of bottom hole pressure that is 126 bar. The smooth non-linear changes in the pressure of Ledaflow were caused by the fact that it represented a condensation or gas into liquid at the well top.

Then, the temperature profiles were analyzed in both software. The figure 4.2 shows the temperature evolution that were predicted by Ledaflow and Pipesim.

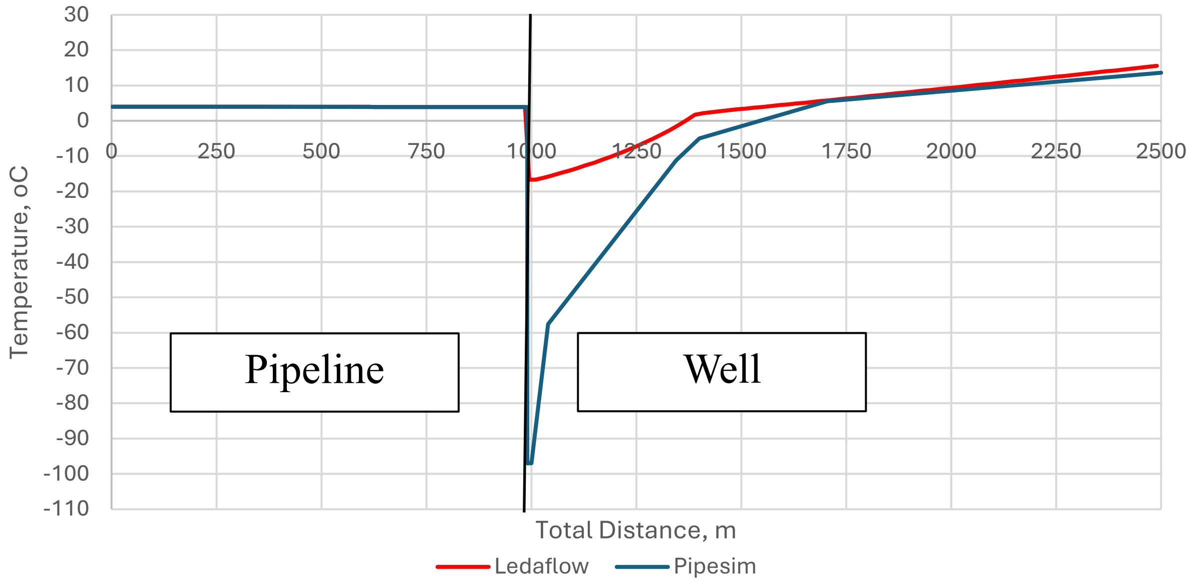

Figure 4.2 – Temperature distribution along the case.

The riser segment (0-1000 m) shows identical and stable temperatures 4°C for both software. The biggest difference occurs when carbon dioxide comes through the wellhead choke. Since, Ledaflow predict modest temperature drop to around -12°C. On the other hand, Pipesim predict the sharpest temperature drop to nearly -97°C.

The modeling of the valve produces this major difference. The Perkins model that was employed by Ledaflow incorporates real-gas effect and partial pressure recovery to produce a more realistic throttling process. While Pipesim's mechanistic model leads to excessive Joule-Thompson cooling prediction when expansion rates are quite high especially for the CO_2-rich mixtures.

After the wellhead choke, both simulators shows physical picture – heating of carbon dioxide cause by formation heat and friction. Both simulators shows gradual convergence from 1000 to 2500 m. It should be noted that Ledaflow present linear heating – there is 2 region, first one is from 1000 – 1400 m – where the condensation process occur, second one is from 1400 to 2500 m, where the heating of single phase – liquid occur. Conversely, Pipesim presents heating process as hyperbolic process. Still, after the heating process, both simulators present the same temperature at the bottom hole point (around 14-16°C).

These results demonstrates the significance of correct valve modeling for CO_2 injection simulations case, particularly when the large pressure drops are involved. The incorrect cooling predictions from Pipesim would result in incorrect hydrate/ice formation risk assessments and possibly require more conservative insulation or dehydration measures.

Next, the phase volume fraction will be compared. Figure 4.3 shows the predicted gas volume fraction (GVF) distribution across the whole chain.

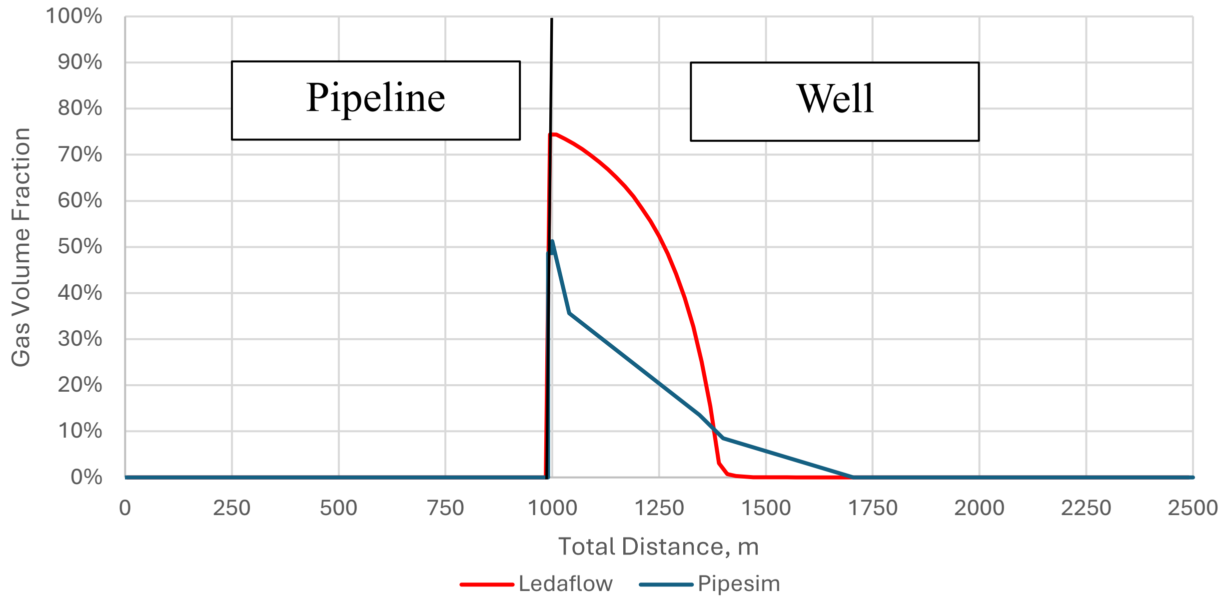

Figure 4.3 – Gas volume fraction distribution along the case (blue – Pipesim, red – Ledaflow).

The difference is as follows:

— Ledaflow predicts a peak GVF of 76% with a gradual condensation process. The full condensation occurs around 1400 m.

— Pipesim predict lower GVF of 51% and gradual condensation with the full condensation on 1700 m.

These differences can be explained in teams of thermodynamic modeling and gas-liquid separation criteria:

— Ledaflow, using the CO2PURE EOS more accurately represents real-gas behavior of CO_2 and tracks phase boundaries with finer resolution. This results in more pronounced and persistent gas formation during rapid pressure drops.

— Pipesim, with its PR EOS, tends to underpredict gas volume fraction in high-density CO_2 systems and often simplifies phase equilibrium in the near-critical region.

Additionally, the greater cooling observed in Pipesim (as previously shown) increases CO_2 density and suppresses gas formation due to condensation, artificially limiting GVF. Meanwhile, Ledaflow's more moderate cooling leads to less recompression of the vapor, allowing a larger gas fraction to persist until hydrostatic pressure and geothermal heating eventually force recondensation.

The next step is analyzing the pressure-temperature (P-T) plots comparison between Ledaflow and Pipesim. It was plotted with CO_2 dew point to analyze the alignment. This plot presented in figure 4.4. Both simulations start from identical conditions at the point "PS" – 4°C and 100 bar, yet the trajectories diverge markedly.

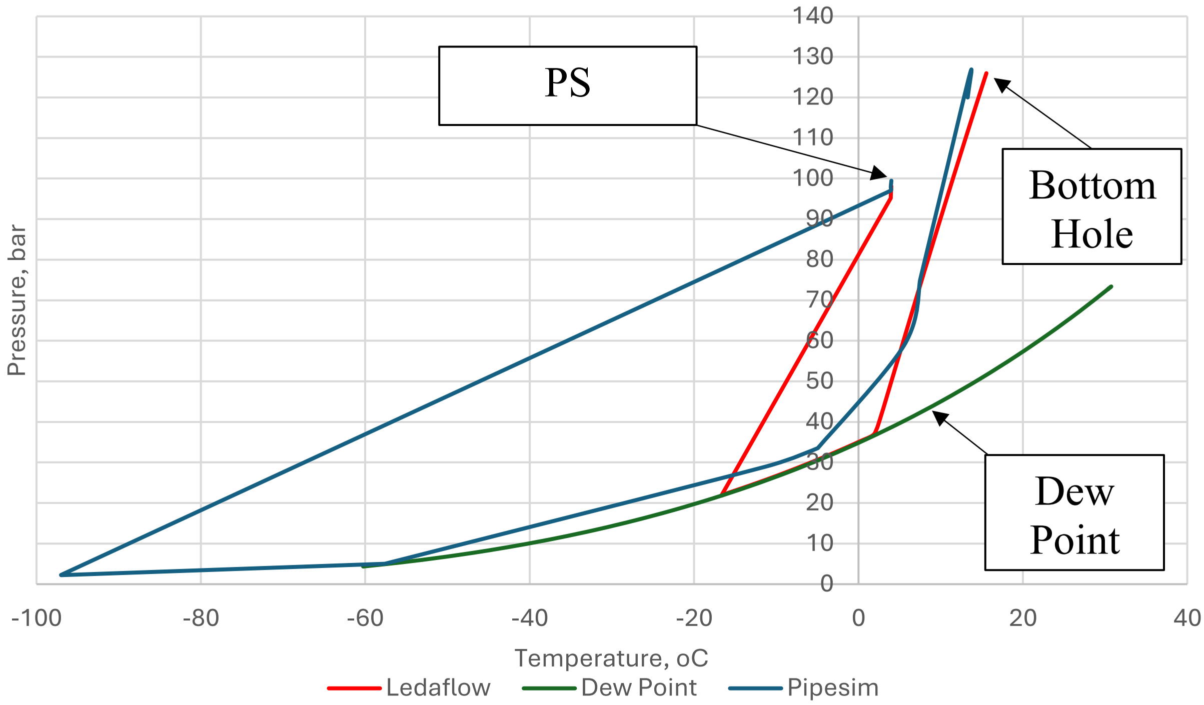

Figure 4.4 – Dew point graph comparison between Ledaflow and Pipesim.

Ledaflow only predicts a mild amount of Joule-Thomson cooling and a short crossing into the two-phase domain, but Pipesim predicts a temperature low of -95°C and stays in the two-phase range near almost all of the length of the wellbore. This difference is mostly the result of the differences in the thermodynamic models behind the Ledaflow (CO2PURE EOS) and the Pipesim (PR EOS) as well as the treatment of the choke pressure drop. PR is no longer considered reliable in Joule-Tompson cooling near critical point of CO_2, and Pipesim single-step choke model over-estimates the enthalpy decrease. The result of Pipesim will therefore be considered conservative/ non-physical within the operating envelope. To perform comparative tests in the future, a unified EOS or a calibrated property table should be suggested.

It should also be mentioned that the results of the Ledaflow demonstrates the physical picture as P-T line was situated on the Dew Point, however, the results of Pipesim oversimplifies and demonstrates only the rough alignment. The cause may be the following way: Ledaflow has about 500 meshes and time steps, which present correct results, and Pipesim has only 12 points. It ensures that there is speed in calculating things but can have an influence on the accuracy of the results.

The current analysis agrees that Ledaflow is better and physically realistic when describing the coexistence of gas and liquids, which is of the high importance with regards to assess the risk of gas slippage, erosion, and hydrate formation – at choke location, as well as in the upper wellbore. On the basis of this it was resolved to use the Ledaflow for coupling framework.

4.2 Reservoir Simulation Outcomes

This part of the thesis presents simulation results in regard to CO_2-rich injection streams at subsurface conditions to determine the way they behave in reservoirs. The outcomes were analyzed in comparison of E100 and E300 compositional models conducted to examine the effect of simulator options and management of fluid properties on the prediction of reservoir performance.

4.2.1 Comparative Analysis: E100 vs. E300

Two described in previous sections models (black-oil and thermal compositional) was run and results were in comparison. One of the main differences between them lies in their computational time requirements. The black-oil approach requires around 10 minutes to perform calculations over a 50-year period, while complex thermal compositional approach took around 12 hours for its calculations. These runs were performed on a workstation equipped with an Intel Core i7 CPU, 32 GB of RAM, running Windows 10.

Firstly, the pressure profile were compared for two different models. The comparison of BHP and reservoir (pore) pressure are presented in figures 4.5 and 4.6 consequently.

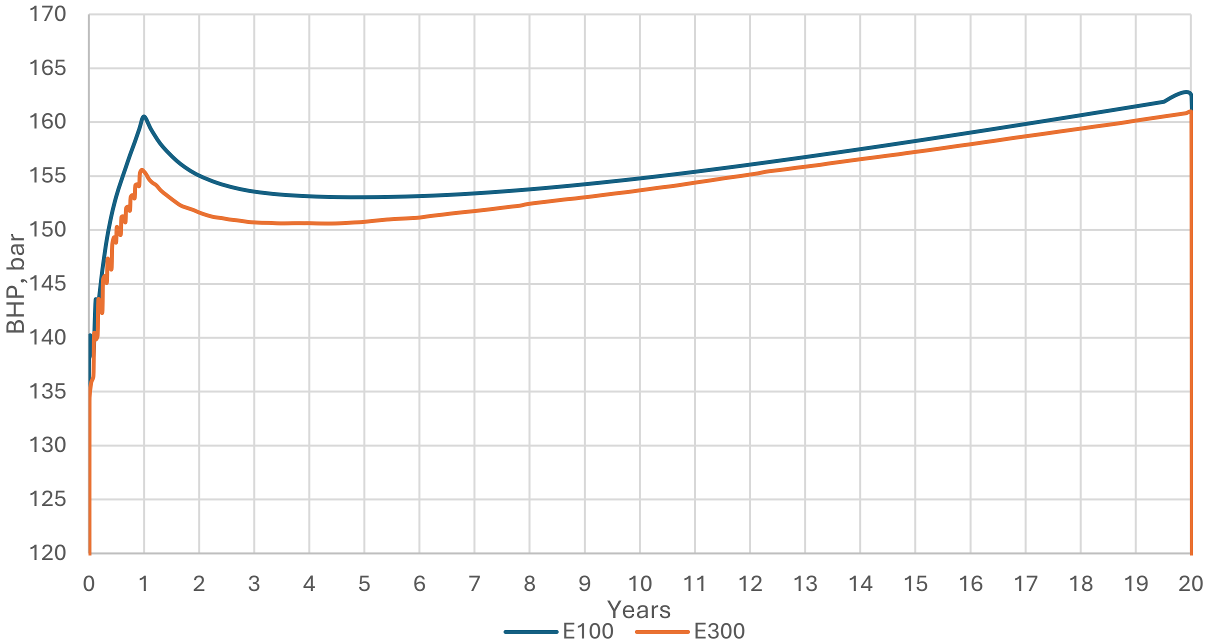

Figure 4.5 – Bottom hole pressure comparison between E100 and E300 models.

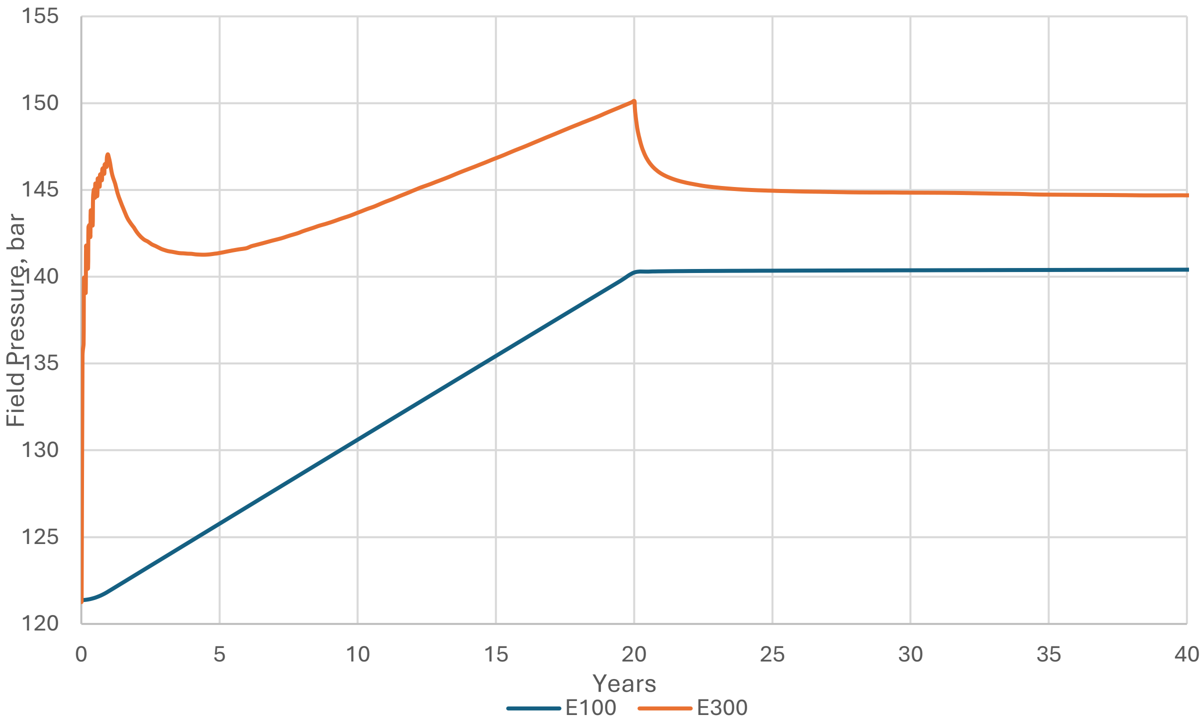

Figure 4.6 – Field (pore) pressure comparison between E100 and E300 models.

The BHP shows a steep increase during the initial months of injection. The reason of this peaky behavior is that the loading is coming gradually. By the achievement the full load (1st year), however, E100 generates higher pressures than E300 by 5 bar at the peak and continuous with the 4-6 bar higher pressure during the 20 years injection period. The reasons for this are:

- Both simulators are different in the sense of calculation of densities. While black-oil approaches assumes density is only pressure-dependent and gets it from the PVT tables, the compositional approach calculates it through the EOS. The analysis of results approved it because E100 showed average density close to 700 kg/m^3, while E300 presents higher values – 900 kg/m^3. Both models receive equal mass flowrates, so CO_2 occupies different reservoir volumes. The BHP in E100 exceeds the BHP in E300 because of these differences.

- The black-oil approach treat CO_2 as gas with lower solubility and viscosity compared to compositional model which leads to reduced pressure requirements for achieving the same surface flow rates.

The difference between these two models are greater in the development of field pressure responses and they display transient behaviors, which are unique to the compositional model. Both E100 and E300 exhibit dominant linear behaviors but E300 exhibits unpredictable behavior patterns. The E100 model works in isothermal conditions thus it does not cause any pressure disturbances. The E300 model contains the temperature effects due to the 16°C injection which creates the pressure pulse that brings the field pressure to 147 bar in the initial month. With the increasing rock temperature following the CO_2 dissolution, pressure decreases up to 141 bar despite the injection persisting. The dissolution of CO_2 occurs as the gas reaches a free phase that subsequently leads to an increment in pressure linearly with increase in pressure to 150 bar.

The CO_2 migration path analysis included two different vertical intersections that are shown in figure 4.7.

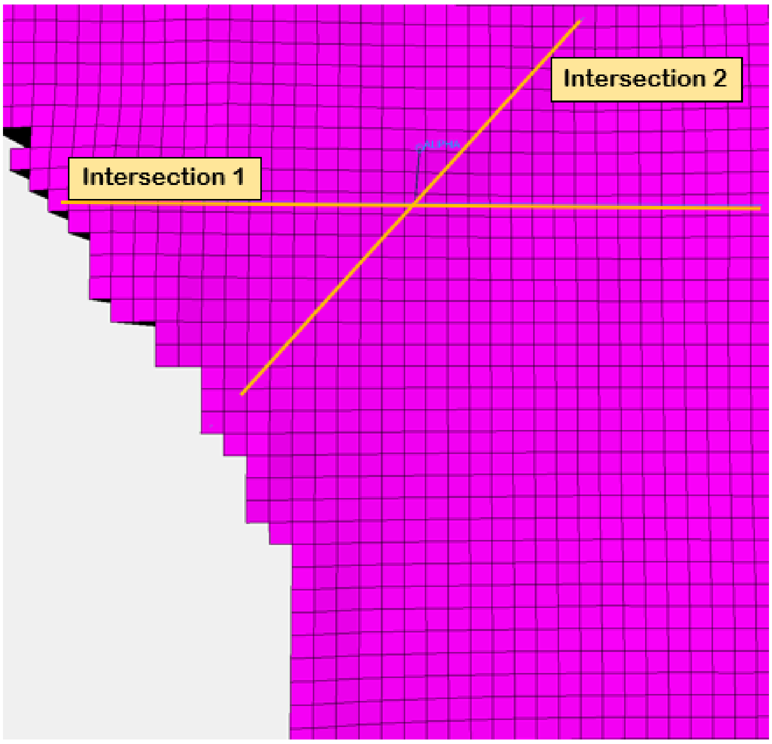

Figure 4.7 – Intersection for flow distribution (top view).

As shown by the CO_2 Plume images given in figures 4.8 and 4.9, the free CO_2 shows a wider lateral movement in the case of the E100 model, whereas, in the case of the E300 model, the plume remains closer to the area of injection. This difference occurs as a result of differences in treatment of phase behavior and the mechanism behind dissolution and trapping in brine aquifer system between the simulators.

Since E100 treats CO_2 as gas, surely it has lower viscosity and density. It leads that CO_2 having larger buoyancy effects, and as the upper layer in Smeaheia site has high permeable facies, CO_2 span vast areas. In E300 CO_2 is treated as liquid in the reservoir condition.

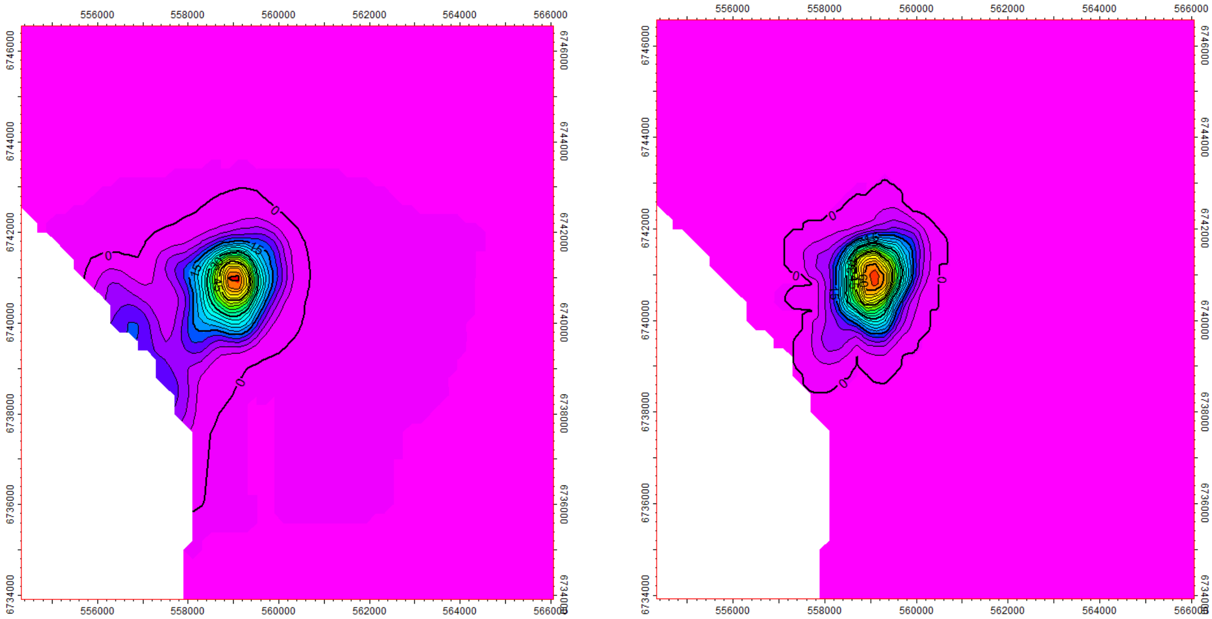

Figure 4.8 – CO_2 saturation comparison for E100 and E300 (top view) (E100 – left, E300 – right).

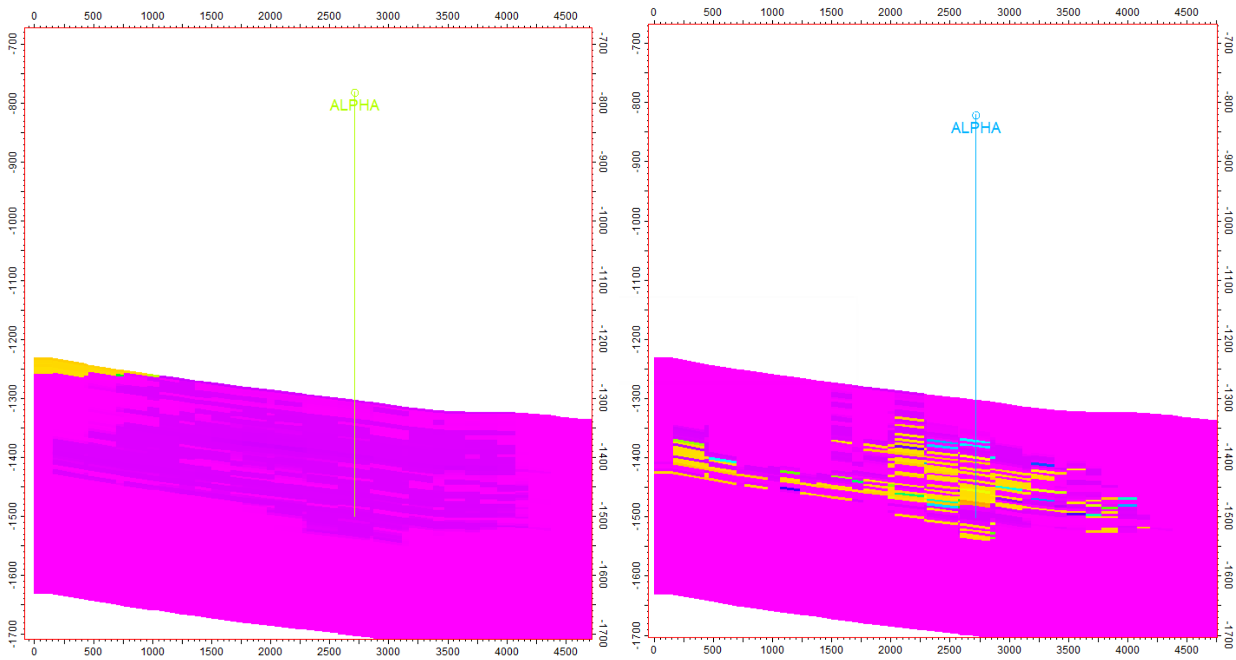

Figure 4.9 – CO_2 saturation comparison for E100 and E300 (intersection 1 view) after 200 years of injection (E100 – left, E300 – right).

The main reasons for these features are presented in table 3.

Table 3 –Explanation of the difference in CO_2 migration flow

Physical mechanisms	Representation in E100	Representation in E300	Impact on plume geometry
CO_2 dissolution	Approximated by a fixed solution-gas/water ratio; solubility is capped and pressure-independent.	Calculated explicitly as a function of P-T via an EOS; significant mass partitions into the aqueous phase.	Less dissolved CO_2 in E100 leaves a larger mobile free-gas volume, enlarging the plume.
Density & viscosity of free CO_2	Single pseudo-component (gas) with constant PVT tables; density under-estimated and viscosity under-estimated once CO_2 mixes with brine.	Density and viscosity updated continuously from EOS; heavier, slightly more viscous free phase.	E100's lower viscosity and higher buoyancy accelerate up-dip and lateral fingering.
Capillary pressure & residual trapping	One static Pc-Kr set, no hysteresis; residual trapping is underestimated.	Separate Pc-Kr functions for brine and CO_2 with hysteresis; residual gas saturation rises behind the front.	Higher residual trapping in E300 immobilises part of the plume, limiting outward spread.
Brine compressibility	Fixed value: pore-pressure support is weaker.	Increases with dissolved CO_2; pressure propagates faster, reducing the local driving force for lateral flow.	E300 dissipates injection pressure more uniformly, curbing radial migration.

The entire findings of the study consist of:

- At E100 the low viscosity CO_2 has not dissolved well and gives rise to greater pathways and is more dispersionally far going up-dip leading to a wider halo as observed on the left map.
- E300 exhibits constant dissolution and high residual trapping high and genuine PVT features reducing the mobile free phase to a small zone as in the right map.

4.3 Coupled Wellbore-Reservoir Performance

The findings made regarding the integration of the Ledaflow with the Eclipse have been illustrated in twenty consecutive steps in the section. The surface wellbore hydraulic response was compared and analyzed to the Eclipse reservoir pressure responses against a particular injection system. Monitoring the performance follows two key indicators that are BHP and THP at every processing point. The numerical results of the first and second iteration of coupling are discussed independently of the determined order where it started with the definition of inlet pressure and choke opening as well as injection temperature and then running Eclipse before updating Ledaflow and proceeding through iterations until convergence is attained.

During the initial iteration of the workflow that was coupled, Eclipse was run with default temperature profiles whereas Ledaflow was run with a fixed temperature value in the simulation.

The initial coupling instalment had been supplied with a fixed injection temperature by Ledaflow and Eclipse applied its auto-generated temperature profile. The original mass flow rate was determined in Ledaflow and Eclipse produced the reservoir pressure data which was fed back into Ledaflow through an iterative process until the process finally terminated.

— The 20-step coupling process produced simulated BHP values from both Ledaflow and Eclipse that ranged from 130 to 160 bar. The BHP profiles from both simulators appear in Figure 4.10.

- This first iteration got perfect results as Eclipse and Ledaflow demonstrated a 0,28% Mean Absolute Percentage Error (MAPE) in their BHP calculations.

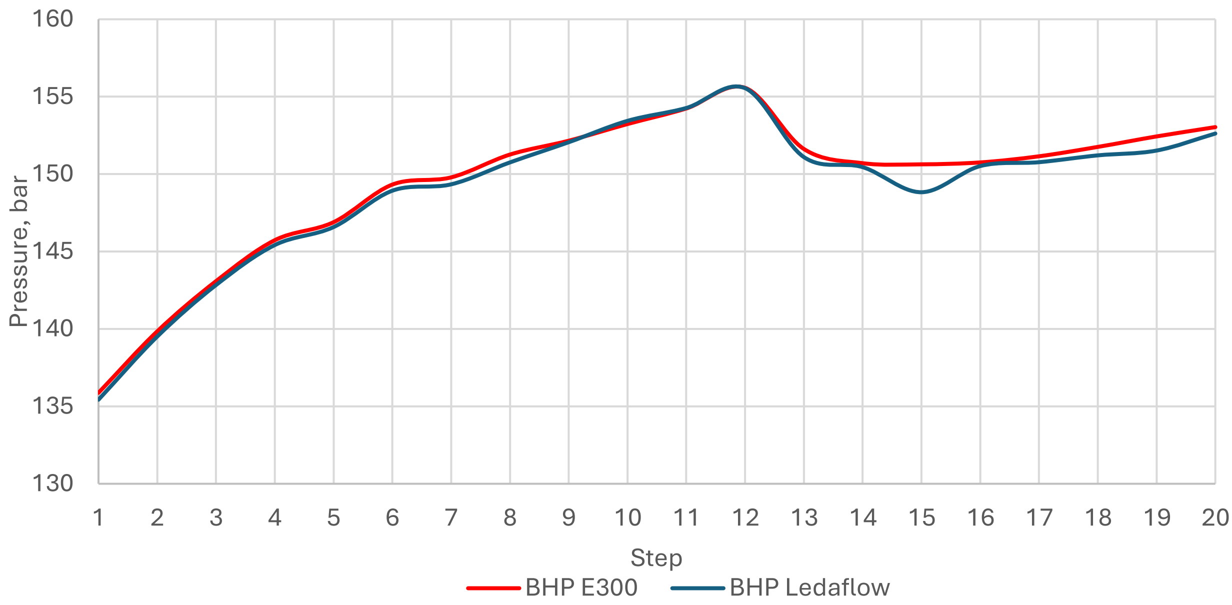

Figure 4.10 – Bottom hole pressure comparison between E300 and Ledaflow.

— The THP values at the wellhead showed a range from 30 bar to 50 bar for both models as shown in Figure 4.11.

- The first simulation produced a 1,44% THP MAPE which showed greater discrepancies between models at the surface pressure compared to downhole pressures.

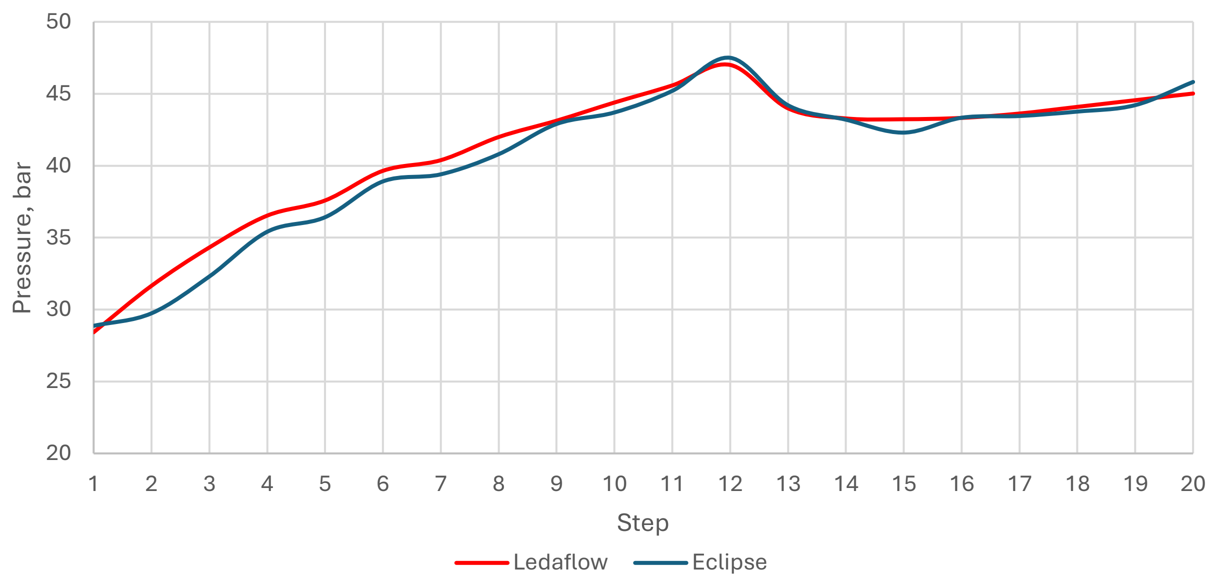

Figure 4.11 – Tubing head pressure comparison between E300 and Ledaflow.

The core reason of such errors was revealed since Eclipse required specific profile of BHT of Ledaflow to compute rightful properties of PVT which were presumed by Ledaflow to be two-phase fluid properties. Difference in temperature was small; hence there were slightly larger relative errors at the tubing hanger with the similar values in pressure.

The second iteration coincided with Ledaflow calculated injection temperature provided to Eclipse at every coupling step. In the second run Ledaflow used the same fixed injection temperature as in the previous run whereas Eclipse used the bottom hole temperature that had been calculated by Ledaflow as an input condition. There were no further iterations done after this, since:

- The bottom hole pressure comparison showed better accuracy. The matching of thermal boundaries across Eclipse and Ledaflow gave considerable improvement in the downhole pressure match between both the models. The BHP comparison MAPE reduced from 0,28% to 0,11% when the bottom-hole temperature was dispensable to the two models by Ledaflow.
- As well as it appears with the THP. The BHT update has little effect of THP values at surface but has significant effect on PVT behavior at downhole conditions. The Ledaflow-Eclipse THP comparison reduced beyond the second iteration but it was still above the BHP discrepancy level. The second iteration generated a THP MAPE measurement equal to 1,05% that fell relative to 1,44% that was generated in the first iteration.

These two iterations confirms that:

1. The PVT tables provided by Eclipse do not match the wellbore fluid conditions during the simulation in which Ledaflow-calculated bottom-hole temperatures are not exchanged which results in a bottom hole pressure deviation of 0,28 % during the simulation. The alignment of BHP increases to 0,11% upon the introduction of BHT.
2. THP is more sensitive to temperature change. The THP change between both software still exceed the BHP error after thermal coupling is applied. THP calculations depend on downhole pressure as well as on downhole PVT properties matching
3. The process took only one iteration, since accuracy between both software lower than 0,5% for BHP and around 1% for THP. The BHT matching led to a significant reduction in difference.

The coupled workflow, that have been suggested in this thesis, between Ledaflow's wellbore hydraulics and temperature calculations and Eclipse's reservoir pressure simulation produces quite convergent BHP and THP values that converges within a few percent error. This demonstrates that proposed framework for coupling works effectively to simulate transient CO_2 injection behavior during 20 defined steps.

Figure 4.12 presents calculated BHT for all 20 steps.

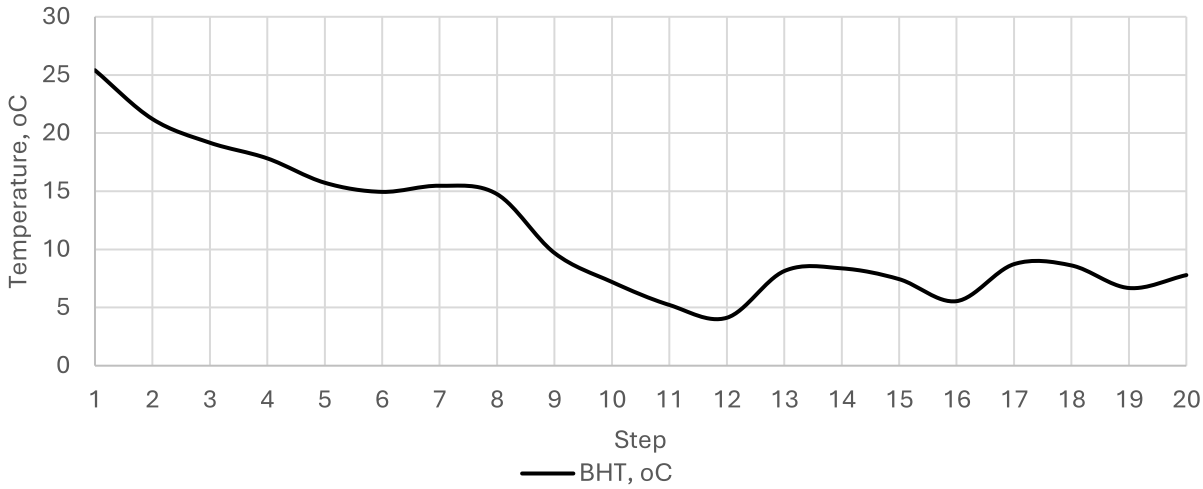

Figure 4.12 – BHT for each step (first iteration).

Figure 4.13 visualizes how the thermal footprint of the injected CO_2 develops within the aquifer as injection proceeds. Each panel shows a depth-versus-distance slice through the reservoir, colored by the temperature.

After the first month of injection, a small lens-shaped area around the completion cooled to 30°C, while the reservoir temperature remains on the same level – 45°C. The patchy outline indicates that conductive heat transfer dominates at this stage: cold fluid in the near-well cells extracts heat from the matrix, but there has been little time for advective spreading along higher-permeability layers. Outside a radius of perhaps 15-20 m, the temperature field remains virtually undisturbed, so the plume is thermally and hydraulically – confined.

By the time to the full injection rates, the cold anomaly has expand dramatically. Now, the area close to the well cooled to 15°C, while cooled zone (30°C) expands laterally 50-70m from the well. This broader, smoother effect reveals a transition to advection-dominated heat transport: buoyant CO_2 threads preferential flow paths, displacing brine and exporting low-enthalpy fluid outward.

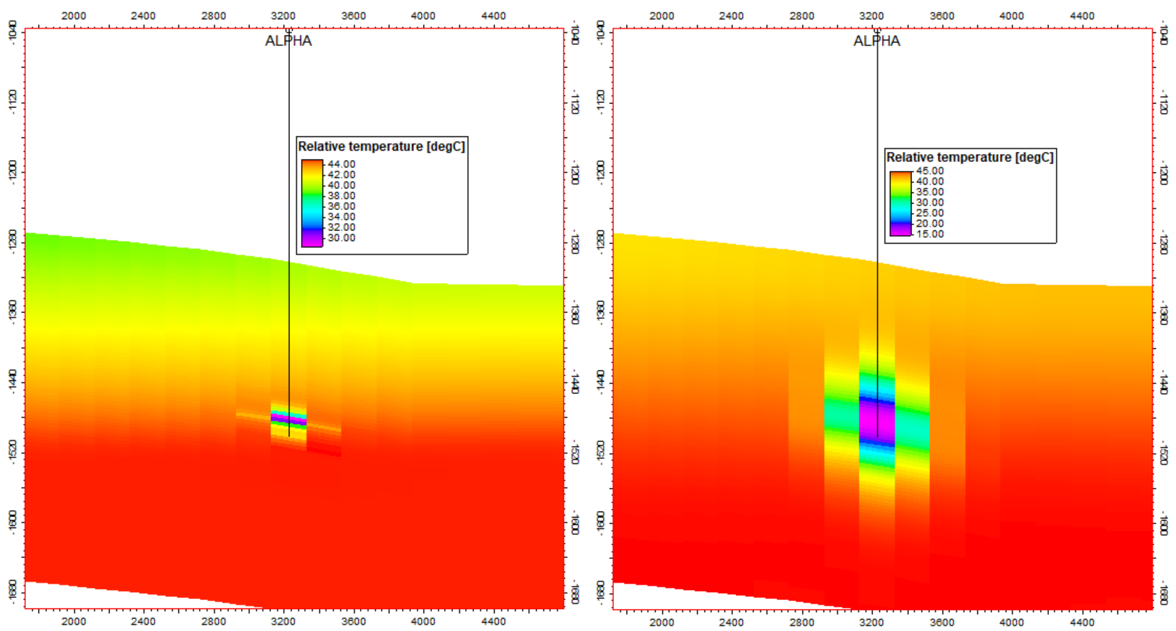

Figure 4.13 – Temperature distribution across the aquifer cross-section: Step 1 (left) and Step 20 (right) injection stages.

The twenty coupling steps that were followed Ledaflow and Eclipse workflow produced a wellhead choke opening schedule that resembles the common injection control strategy. In the simulation two main periods of operations are shown:

1. The steps 1-12 presents gradual loading mode of operation. Figure 4.14 shows choke opening measurements of the simulation results. The choke opening increases gradually during the initial twelve months of operation corresponding with steps 1- 12 by about 2 % to about 23 % of opening. The deliberate opening pattern of valves shows that there is need to increase the flow rates of mass steadily. The operator regulates the pressure in the reservoirs by advancing the valve position by approximately 2 % every month. This behavior is automatic when using the coupling algorithm that adjusts its initial guess of the mass flow rate step-by-step with the actual reservoir pressure that Eclipse provided. When injectivity in reservoirs starts, the coupling loop establishes the fact that it is possible to open the choke to a much greater extent due to the ability of the reservoir to sustain high pressure and at the same time keep bottom-hole pressure constrains under control. The system works by gradually raising the choke setting, until the level of injectivity falls to inadequate levels.
2. Small adjustments (steps 13-20) at the full load. At step 12 the choke is 23% open, but the injectivity reduces substantially after that. The injectivity index declines since the CO_2-brine saturation grows but at the same time the reservoir pressure elevates resulting in a decline in the formation ability to consume more volume. Because of these desired outcomes, which are to maintain both the target mass flow rate and the bottom-hole pressure limit even under the conditions of the coupling loop, tiny increments of 0,1-0,5% choke opening are maintained through steps 13-20. There is a small increment in the choke position which stands at 23 to 23,5 percent during the procedural steps 13-20. The trend of the increased choke opening is also in agreement with the declining trend of the injectivity index (see figure 4.15) between step 12 and step 20 where the index decreases to 4,8 kg/s/bar with a drop in the index as against the index of 5,6 kg/s/bar. With the same injection target the system only requires minute changes in throttle areas at this time.

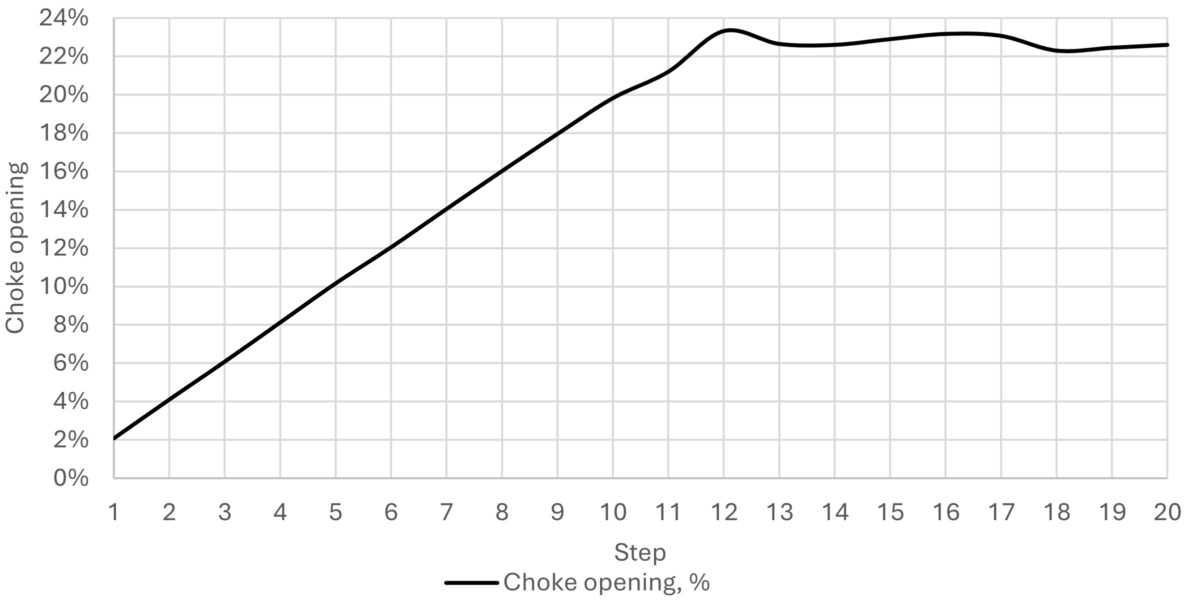

Figure 4.14 – Choke opening for each simulation step.

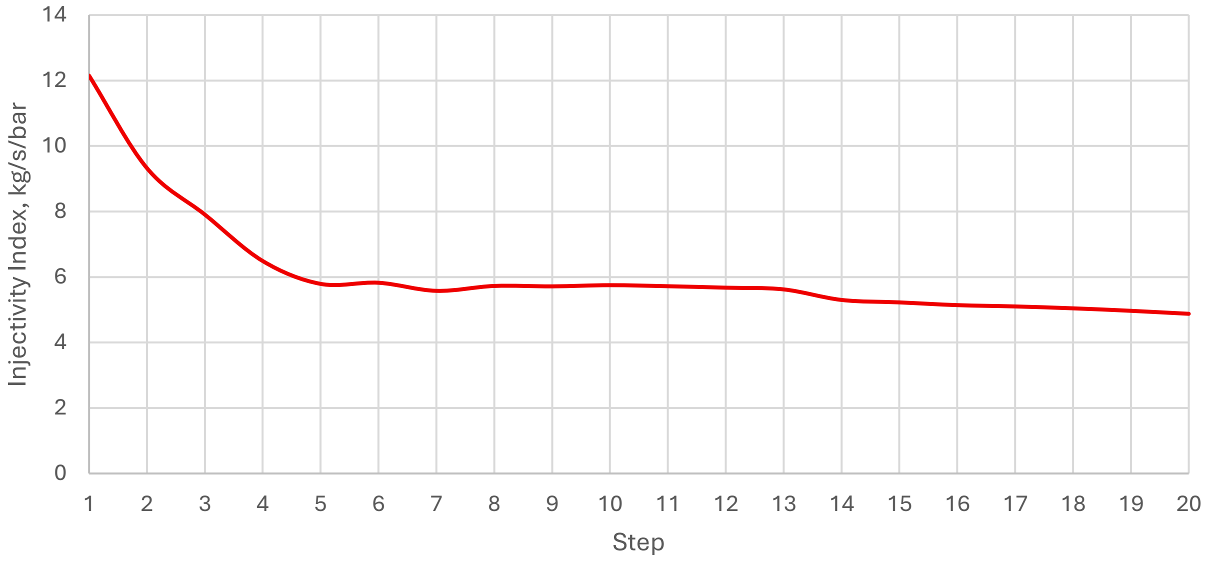

Figure 4.15 – Total injectivity index for each simulation step.

Figure 4.16 illustrates how the gas-liquid flow pattern evolves along the 1500 m wellbore for the 1st and 20th step.

During the first month (step), the CO_2 flows firmly in churn flow (regime 5). The low injection rates and high gas content means that gas occupies a large volume of the pipe and expands under the low hydrostatic pressure. This phenomenon creates erratic, coalescing and unstable pockets of gas. As pressure increase with the measured depth, the mixture stabilizes more and the flow regime shifts to annular flow (regime 2), where a coherent stable fluid moves with heavy droplets of gas in a central core. Deeper levels shows that the flow regimes shifts to bubbly flow. It means that the gas is compressed enough to fragment to be dispersed small bubbles in a continuous liquid phase. In this stage CO_2 is mostly presented in the supercritical state.

Conversely, the 20th step (full load) begins with the bubbly flow from the wellhead. The higher CO_2 rates and lower gas volume fraction uniform dispersed gas in the continuous liquid, suppressing the chaotic churn flow regime. Then, pattern copies from the 1st step.

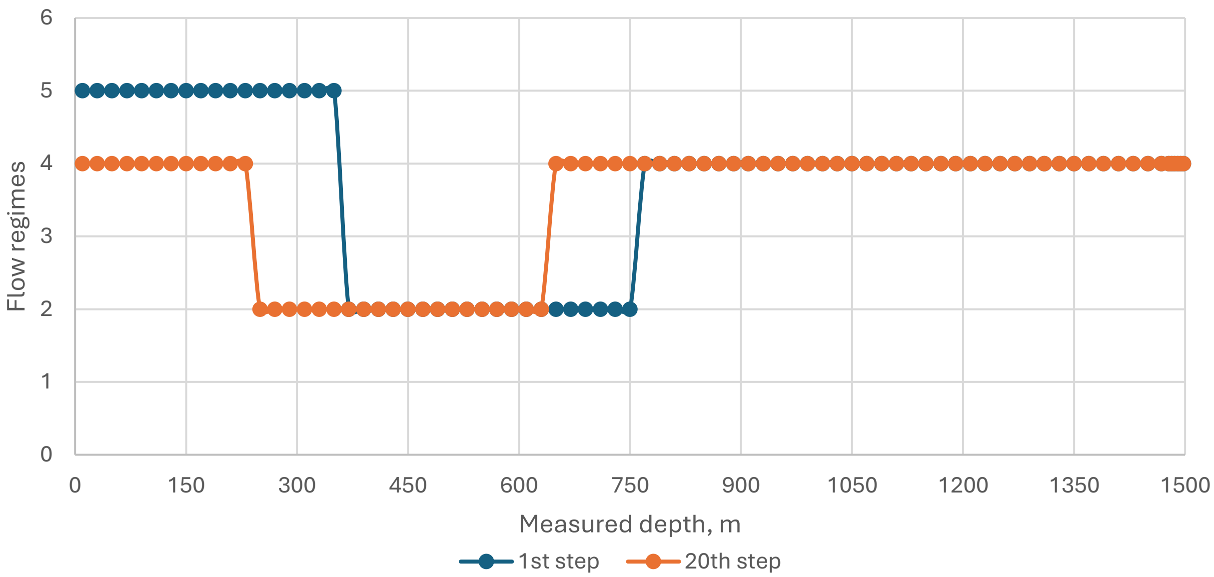

Figure 4.16 – Phase regimes during injection for the first step for the well section (2 – annular flow, 4 – bubbly flow, 5 – churn flow).

Next analyzed parameters were the phase volume distribution across the well, the interesting part here is how the gas volume fraction evolves with the increasing loading. The very low injection rate at the beginning (2 kg/s) (see figure 4.17) leads to a minimal pressure reduction of the CO_2 stream at the wellhead choke. The Joule-Thompson effect cools CO_2 not so strong as in the full loading. It leads that on the wellhead remains huge amount of gas – 95%. This vapor condenses since the fluid flows downwards and the formation warms and causes the fluid to increase hydrostatic pressure. At 150 m MD, liquid droplets begin to form when the pressure has increased to such a point where it is equal to the mixture dew point. The full condensation occurs at 300 m MD.

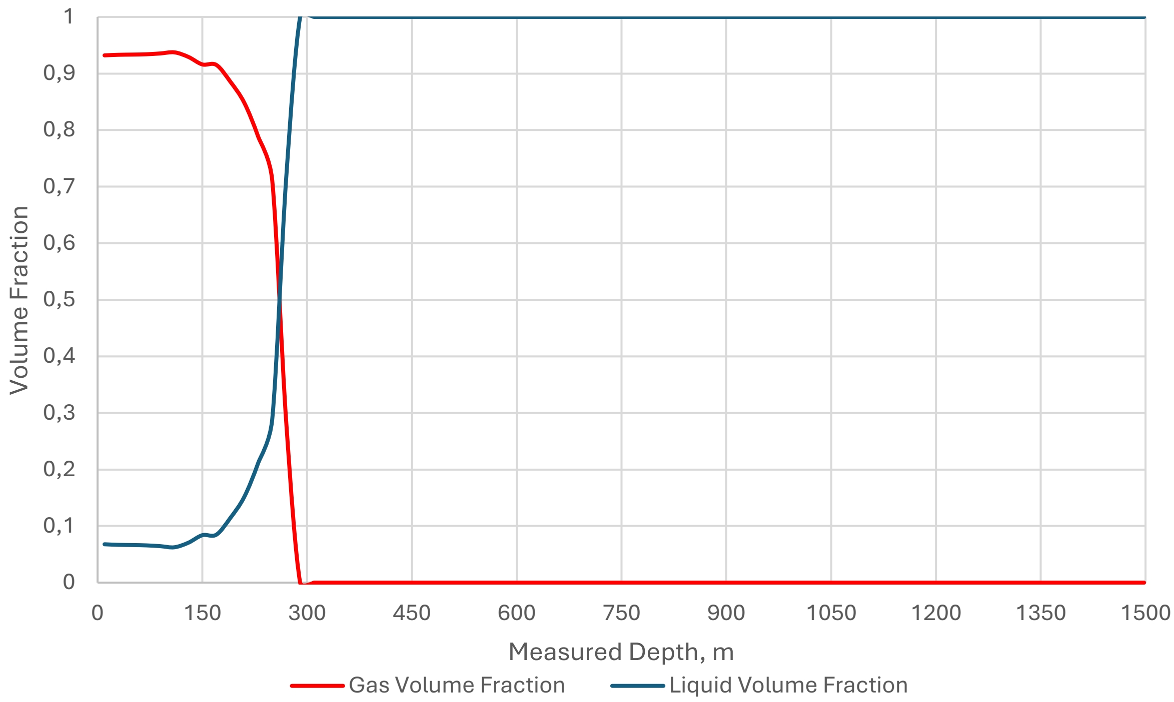

Figure 4.17 – Volume fraction profiles of gas (red) and liquid (blue) phases in the wellbore at a mass flow rate of 2 kg/s.

Field implications:

— The combination of 5% liquid mass around the choke would pose a high probability of unstable flow patterns like slug flow in the upper side of the tubing due to the fact that the mixture of liquids and gases flows fast. It has been proved before with the churn flow mode during the first month.

— Although a condensation zone, beginning at 150 m depth may result into thermal stress issues that necessitate use of insulation packages to avoid hydrate formation in cold rocks structures.

— The operations should ensure that wellbore design should have wellbore features that can accommodate intermittent liquid slugs using gas-lift packages or wellbore deflection tools to avoid hydraulic shock.

— The equipment also needs safe isolation so that gaseous CO_2 could not escape due to the fact that carbon dioxide has no identification features like color or smell.

In the flow rate of 8 kg/s the injection rate is higher which makes the pressure loss across choke to grow and Joule Thomson cooling effect to be more explicit (figure 4.18). The immediate sphere just beyond the choke has 70% gas and 30% liquid. This raised liquid proportion is produced by the increased back-pressure and its more pronounced lowering of temperature. Hydrostatic pressure, which increases as the mixture flows down together with heat transfer with the formation, increases temperature until condensation stops. A two-phase mix in this case stretches in between 200- and 300-meters MD but with a shallower depth and a narrow zone and higher liquid content with increase in proximity to the surface.

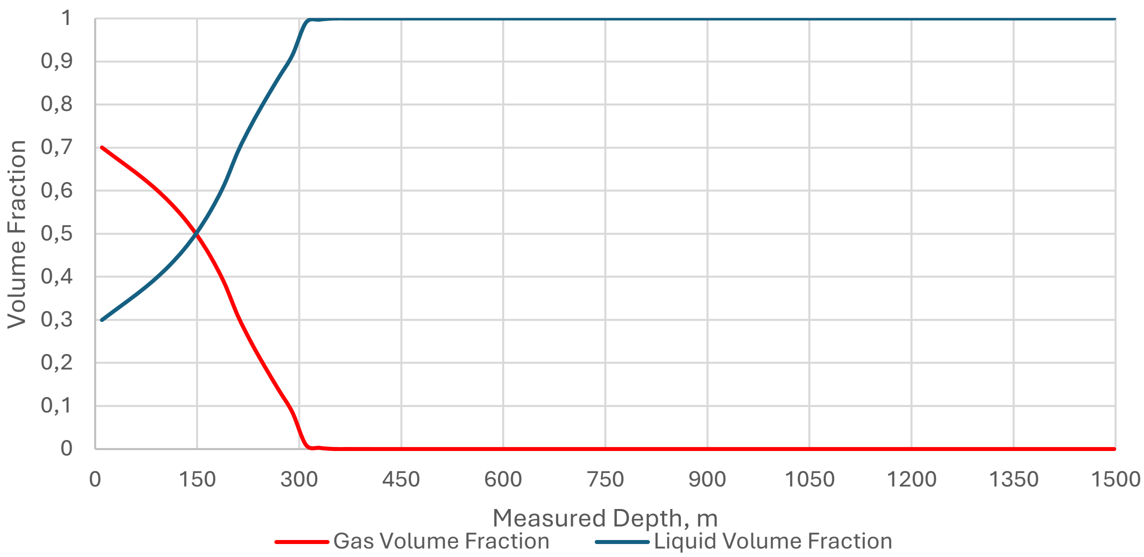

Figure 4.18 – Volume fraction profiles of gas (red) and liquid (blue) phases in the wellbore at a mass flow rate of 8 kg/s.

Step 12 is the process in which the well is at its peak injection capacity of 48 kg/s. Due to the 23% openness of the choke, there is pressure drop and Joule-Thomson cooling and the result produces a 62% GVF and 38% liquid content beneath it. The region of the two phases is short and spans between the surface and 120 m MD up to liquid formation. It reported in figure 4.19.

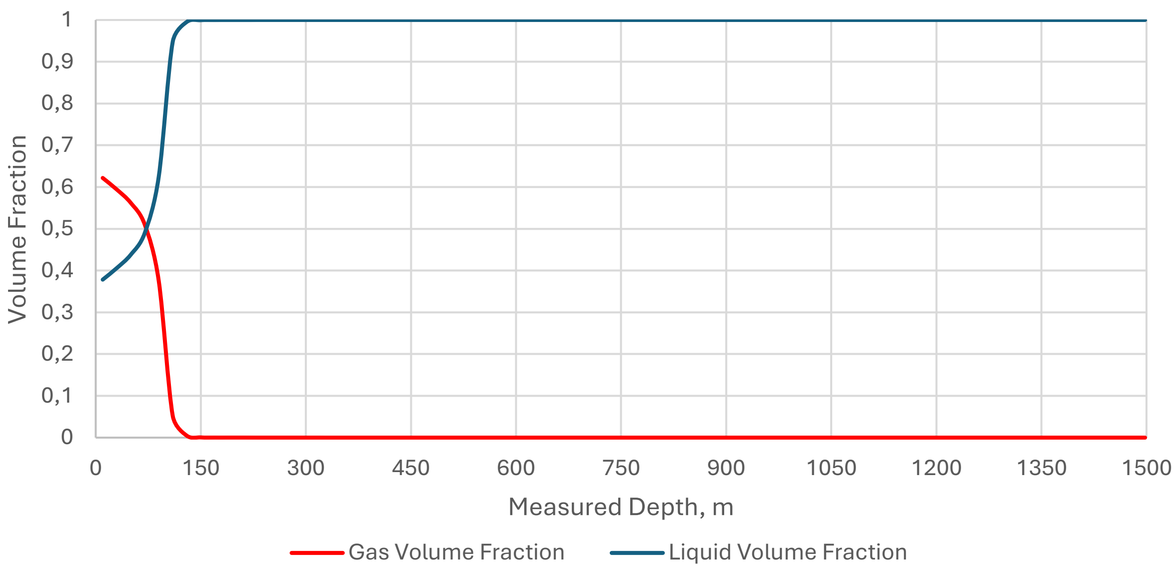

Figure 4.19 – Volume fraction profiles of gas (red) and liquid (blue) phases in the wellbore at a mass flow rate of 48 kg/s.

Key Takeaways:

— Operators should realize that the very same choke setting will produce totally different results in phase separation when the mass flow rates change. The choke setting providing 95 % GVF at a 2 kg/s flow rate provides a mere 58 % GVF at 48 kg/s flow rate.

— A practical downhole operator able to decide on the point of emergence of the two-phase front can implement downhole heaters or chemical inhibitors (e.g. injection of methanol) carefully to ensure that conditioning liquid CO_2 is not present to form hydrates or reduce heat losses so high that they affect critical components of the downhole assembly.

— The increase in hydrostatic pressure below the choke with high liquid fractions can cause the bottom-hole pressure to approach the cap-rock fracture limit. The use of downhole pressure and temperature monitoring together with careful choke management prevents unexpected fractures.

The CCS operator can use phase-behaviour knowledge to develop better choke management plans while designing downhole fluid management systems and heating infrastructure to ensure continuous and safe and efficient injection operations during the entire project lifecycle.

4.4 Advanced CO_2 Storage Scenarios

In this chapter the results of injection simulations in Eclipse with the CO2SOL module and results of implementation of OCD for CO_2 storage will be presented.

4.4.1 Advanced CO_2 solution model (CO2SOL)

The simulation results are shown in figure 4.20 and figure 4.21, it demonstrate the time-dependent changes in field (pore) pressure and BHP.

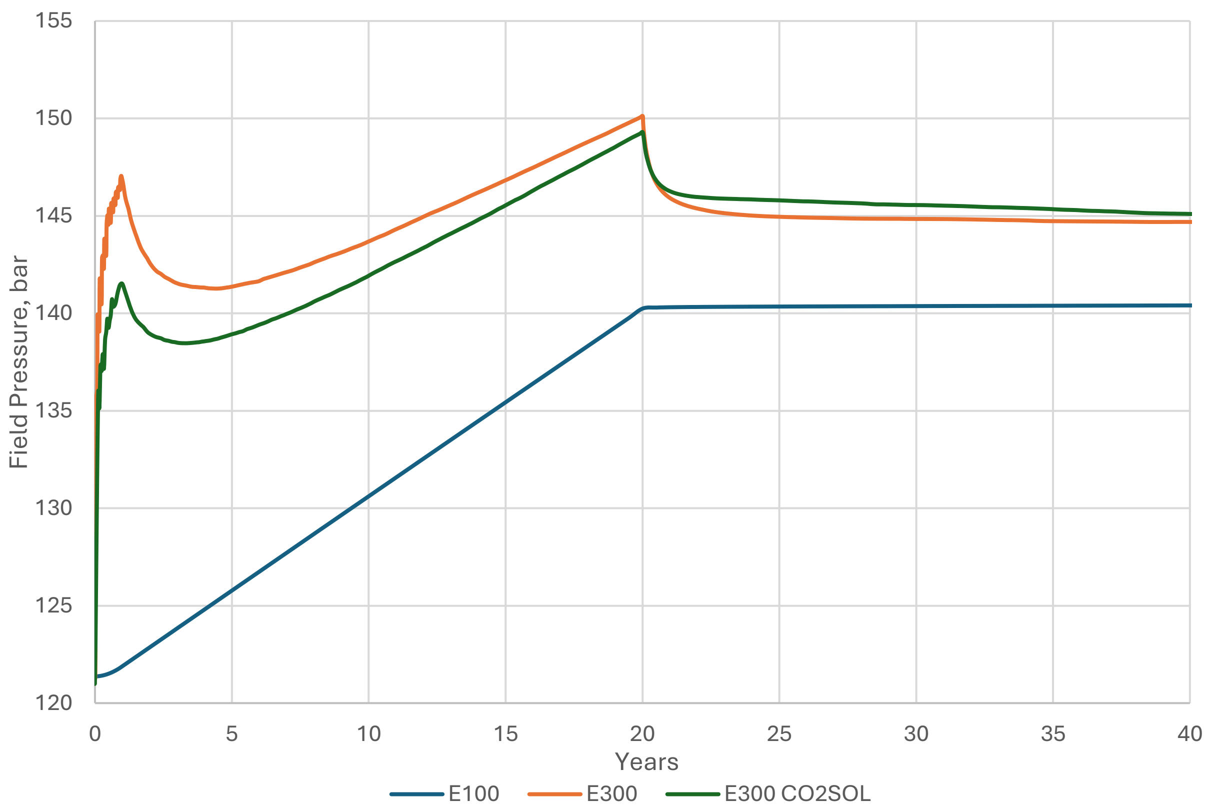

Figure 4.20 – Average field pressure comparison among E100, E300 and E300 CO2SOL results.

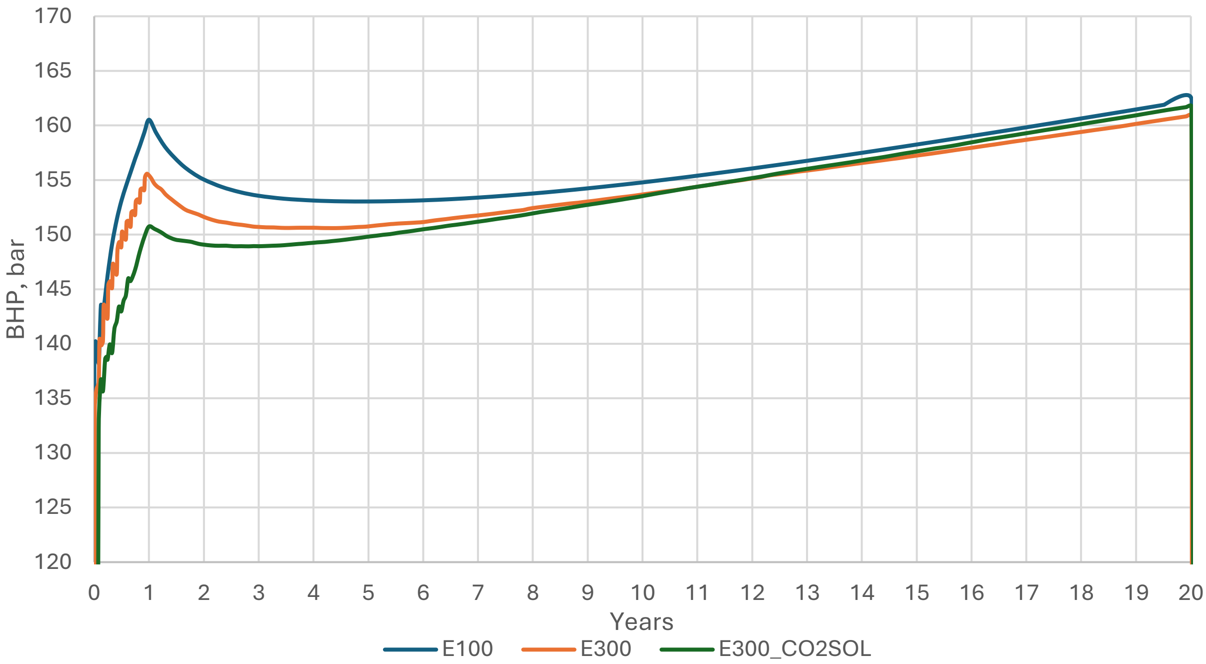

Figure 4.21 – BHP comparison among E100, E300 and E300 CO2SOL results.

Even though the three models possess the same reservoir geometry and porosity/permeability maps and injection schemes the pressure responses are highly different due to the PVT representations:

— E100:

- Failure to have any explicit model of CO_2 dissolution in the brine leads to all the CO_2 molecules remaining in free gas phase.

- The injection will lead to the development of pressure to 140 bar after 20 years of injection, followed by stabilization of BHP and field pressure.

— E300 with CO2STORE:

- In the compositional thermal model, CO_2, H_2O and NaCl and $CaCl_2$ are combined separately in mathematical equations under the PR EOS system.

- The PVT model that is used at CO2STORE, does not stipulate rigorous calculations of CO_2 dissolution in brine and hence a pseudo-aqueous component captures CO_2 portions based on pre-determined k-values, but the overall impact is still less than that of a solubility model.

- There is rapid buildup of field pressure to 147 bar after the first year of injection but builds slightly downwards due to change in saturation distribution, as a line input gravity override and thermal effects also occur.

— E300 CO2SOL:

- This CO2SOL module works using the same EOS system but narrows down the component list to CO_2 and H_2O to obtain dynamic CO_2 solubility in formation water versus temperature, salinity and pressure.
- Disintegration of a high level of CO_2 in the liquid component will reduce the compressibility of free-gas but it aids in the lessening of the pressure climb.

- The initial pore pressure surge reaches only ~141 bar (versus ~147 bar in CO2STORE) because more CO_2 mass partitions into solution. The brief thermal and capillary dip results in pressure increase to ~147–148 bar during the late injection years.

There is a quantitative variation between the two E300 versions on the total injection and post-injection as shown:

- Mean average percentage error of field pressure change between E300 with CO2STORE and E300 with CO2SOL equals 1,093%.
- Mean average percentage error of bottom hole pressure change between E300 with CO2STORE and E300 with CO2SOL equals 0,833%.

CO2SOL specifically dissolves more CO_2 in the brine inducing a low value of free-gas compressibility and decrease in pressure even though the profiles of pressure do not differ much by volume size as less than 3%. The simplified tables of CO2STORE yield identical behavior of pressure distribution across a large brine aquifer despite the fact that CO2SOL solution yields more accurate computation of solubility and densities at each grid cell.

The first intersection CO_2 saturation level through both E300 modules is presented in figure 4.22.

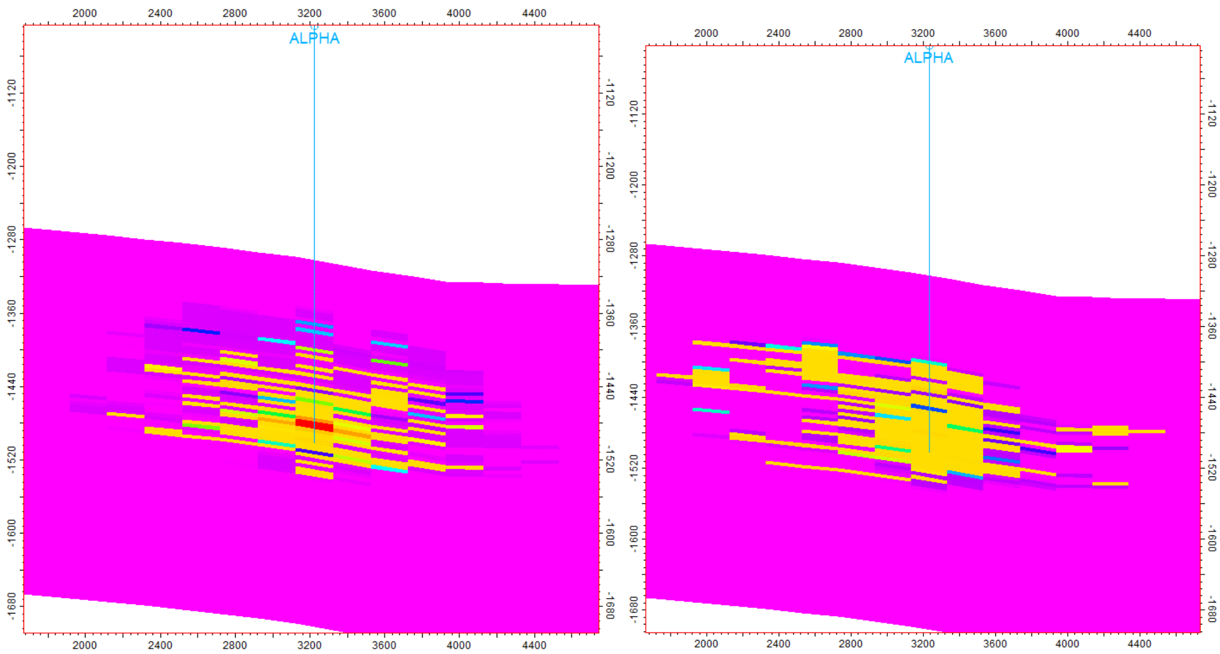

Figure 4.22 – CO_2 saturation along intersection 1 (left – CO2STORE, right – CO2SOL).

It is clearly seen that in the CO2SOL module there is less free-gas as most of them dissolved in this advanced CO_2 dissolution model.

4.4.2 Impact of OCD on Injection Efficiency

Vertical heterogeneity in terms of permeability of Smeaheia reservoir poses significant challenges to even injected CO_2 distribution due to the generation of primary fluid flow patterns in high-permeability layers that essentially cause channelization to occur prematurely. The permeability intersection between 1300m and 1700m is shown in figure 4.23. The value of permeability was found to be higher than 5000 mD in upper sands but lower than 0.5 mD in lower fine-grained formations. Continuous perforation between 1476 and 1500 m would allow majority of injected volume to pass through the high-permeability areas leaving the low-permeability levels undisturbed. Not only does such preferential flow reduce the overall sweep efficiency but it also causes BHP to approach its operational limit which limits the total injection capacity that can be used without further surface compression.

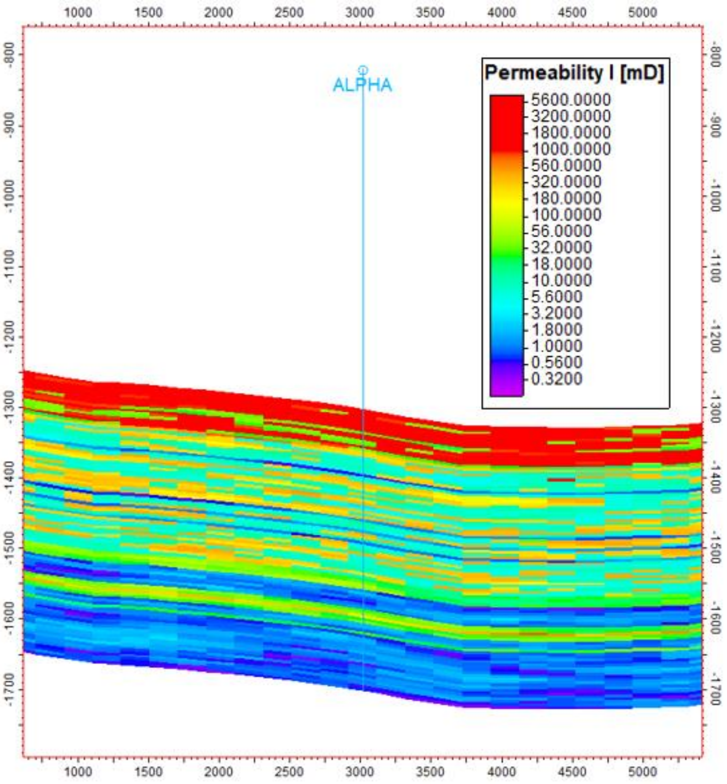

Figure 4.23 – Permeabilities along intersection close to “Alpha” well.

It was observed by steady-state tests that the injectivity indices of six four-meter segments between 1476 and 1500 m (figure 4.24) were obtained to quantify the imbalance of flow:

- 1476–1480 m: II = 110 t/d/bar
- 1480–1484 m: II = 87.1 t/d/bar
- 1484–1500 m: II < 1 t/d/bar

Total injectivity of the interval is mostly located at the 1476-1484 m segment as this segment contains 98 % of all the injectivity whereas 1484-1500 m segment does not provide much at all to the whole capacity. Perforations spanning the total of 24 m would cause severe most CO_2 to trap in the layers characterized by high permeability and those that are on top. BHP must be at or below 230 bar due to the fact that this is the maximum pressure that could be produced with 100 percent of choke opening with no surface compression equipment. The BHP threshold shows its peak at 230 bar, where throttling or suspensions of the injection services to low-permeability strata is applied so as to get enough injection.

To resolve the imbalance situation, it is proposed that the OCDs be implemented to be staged deployment along the perforated intervals. The pressure-based flow resistance created by OCD enables it to avoid entering CO_2 in the high-Injectivity Index portion (1476-1484 m) and send more CO_2 into low-permeability portion (1484-1500 m). The configuration deployed leads to a standardized injectivity pattern that prolongs the time to achieve 230 bar BHP limitation, engulfs more sweep efficiency with CO_2 flow to invade less trenches. To that extent therefore, 90 percent of the flow is carried away by the top perforation and only 10 percent by the lower levels.

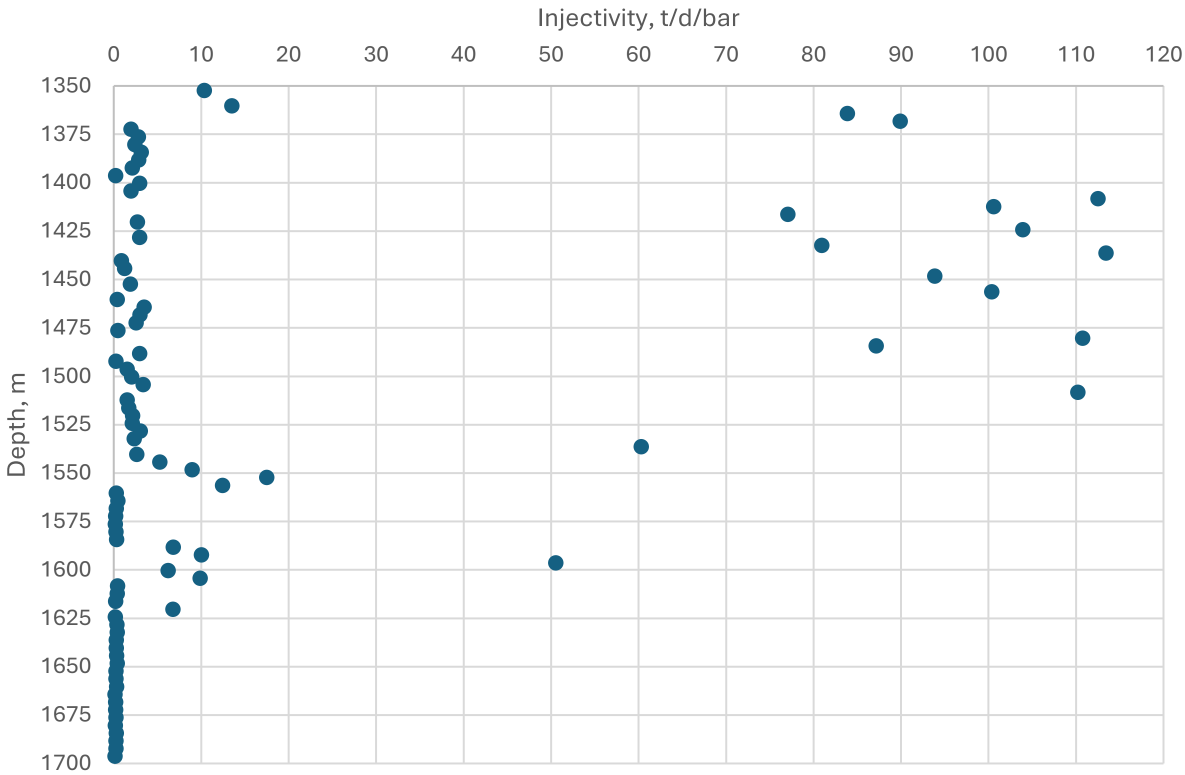

Figure 4.24 – Injectivity analysis along the “Alpha” wellbore.

Based on the simulation results, we have the following flowrate through each level:

— 1476 – 1480: 13,21 m^3/s

— 1480 – 1484: 8,98 m^3/s

— 1484 – 1488: 0,06 m^3/s

— 1488 – 1492: 0,021 m^3/s

— 1492 – 1496: 0,47 m^3/s

— 1496 – 1500: 1,56 m^3/s

So, around 90% of flow goes through the top perforation, while 10% is only through the lower levels.

The post-20-year distributions of saturated gas are shown in figure 4.25 and 4.26. The figure on the left side indicate saturation of the gas is confined in the upper high permeability sections when there are no OCDs providing focused flow channels, even so, the deep low permeability zones remain largely untapped. The right panels indicate that OCDs serve as the device of controlling the outflow that minimize the high-permeability streak flow and instead channel CO_2 to lower-permeability layers. Saturation by gas in OCD case extends throughout the entire injection interval vertically, decreasing the number of isolated high-saturation fingers, and increasing the utilization of under-injected strata.

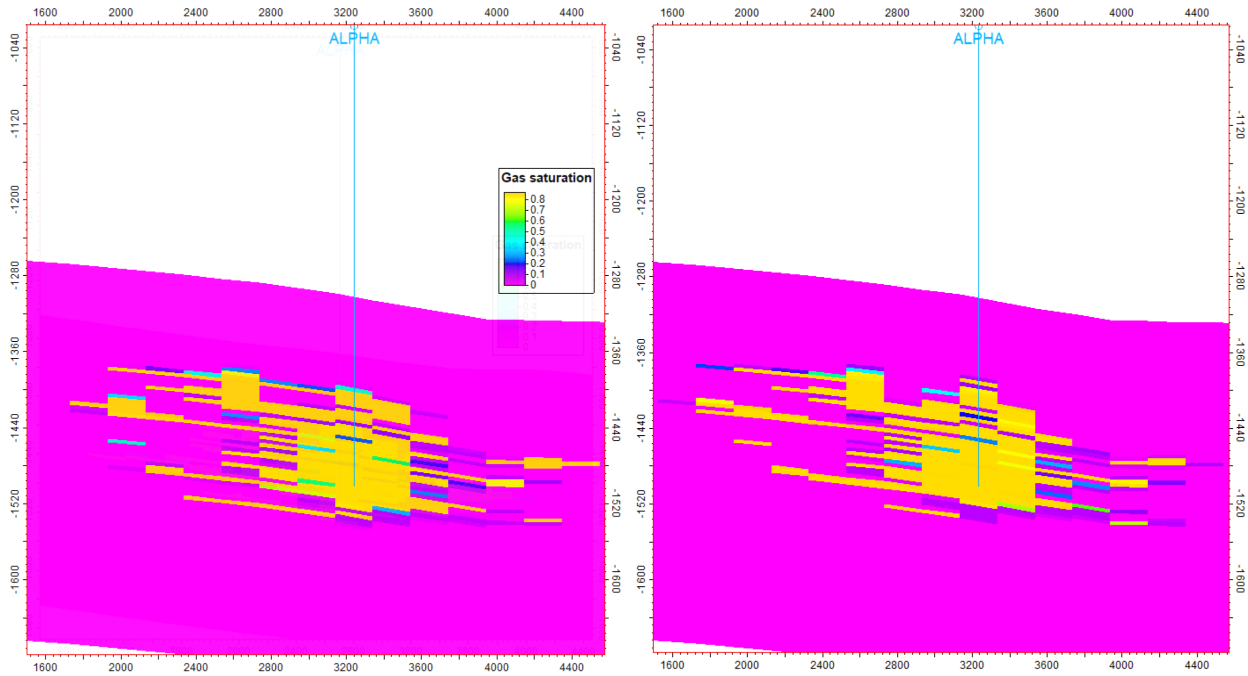

Figure 4.25 – CO_2 saturation along intersection 1 (left – without OCD, right – with OCD).

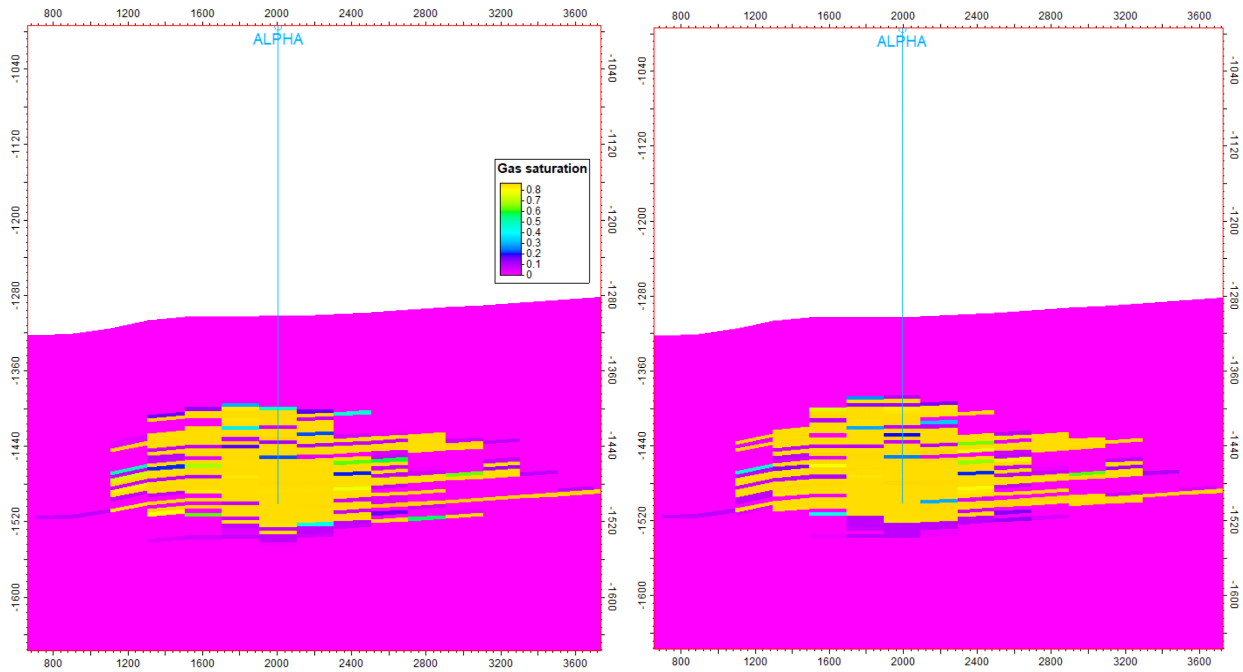

Figure 4.26 – CO_2 saturation along intersection 2 (left – without OCD, right – with OCD).

Figure 4.27 denotes the locale improvement of the CO_2 saturation after the intervention of OCD (at the end of injection and migration duration). It is to note that within a single grid block of the well, the OCD enhanced the low-permeable intervals. Further than 2-3 blocks (lateral proximity) depths jump back to 1484-1488 m and this proves that buoyant CO_2 does move upwards. The gain is essentially vertical along with comparable gains lateral cells of the same radius, the OCD equalizes flow along the completion extending no special reach horizontally. When wider conformance control is needed, the extra OCDs or zonal isolation at greater distances beyond the well could be needed to overcome CO_2 buoyancy field level.

Figure 4.27 represents the locale improvement in CO_2 saturation after the implementation of OCD (after end of injection and migration period). It should be noted that withing one grid block around the well, the OCD improved the low-permeable intervals. Beyond 2-3 blocks laterally, depths rebounds to 1484-1488 m, confirming that buoyant CO_2 moves upward. The depth gain is primarily vertical, while lateral cells at the same radius show similar improvements, indicating the OCD equalizes flow along the completion but does not extend its reach far horizontally. If broader conformance control is required, additional OCDs or zonal isolation farther from the well may be necessary to counteract CO_2 buoyancy on the field scale.

	23	24	25	26	27	28	29	30	31
138					1488				
139	1488				1484				
140	1488	1488	1488	1488	1484	1484	1488		
141			1492		1484		1492		
142	1488	1488			well		1492	1492	
143		1492	1492	1500	1492	1488			1484
144				1500		1488			
145				1500	1492		1484		
146			1496	1496	1492		1484		

Figure 4.27 – Localized positive impact of OCD on CO_2 saturation (top view on the grid).

Figures 4.28, 4.29 and 4.30 show that the gas saturation development is assessed in three 4 m-thick blocks in the low-permeability zone (1476-1500 m). The blue curve displays the character of no OCD condition with open completion scenario and orange curve represents the implementation of an OCD to this particular case.

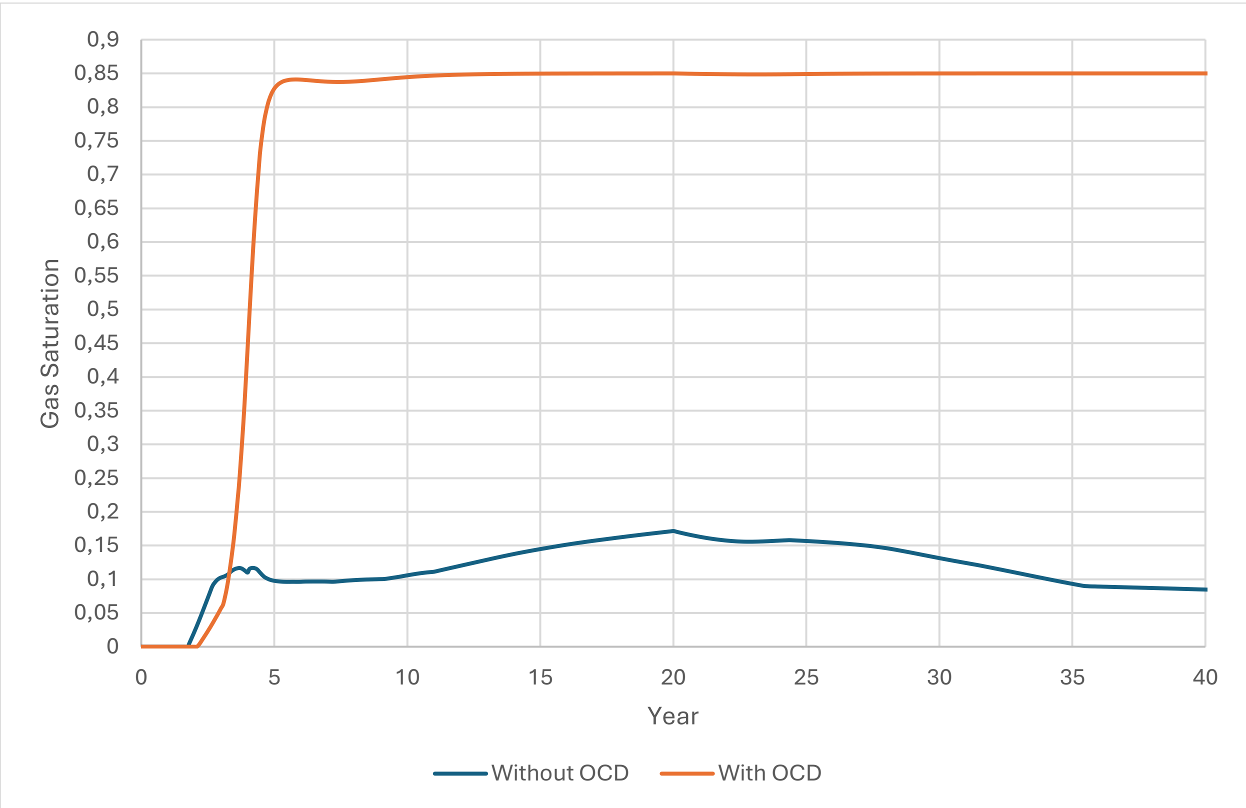

Figure 4.28 – CO_2 Saturation for the Block (26;143;1500).

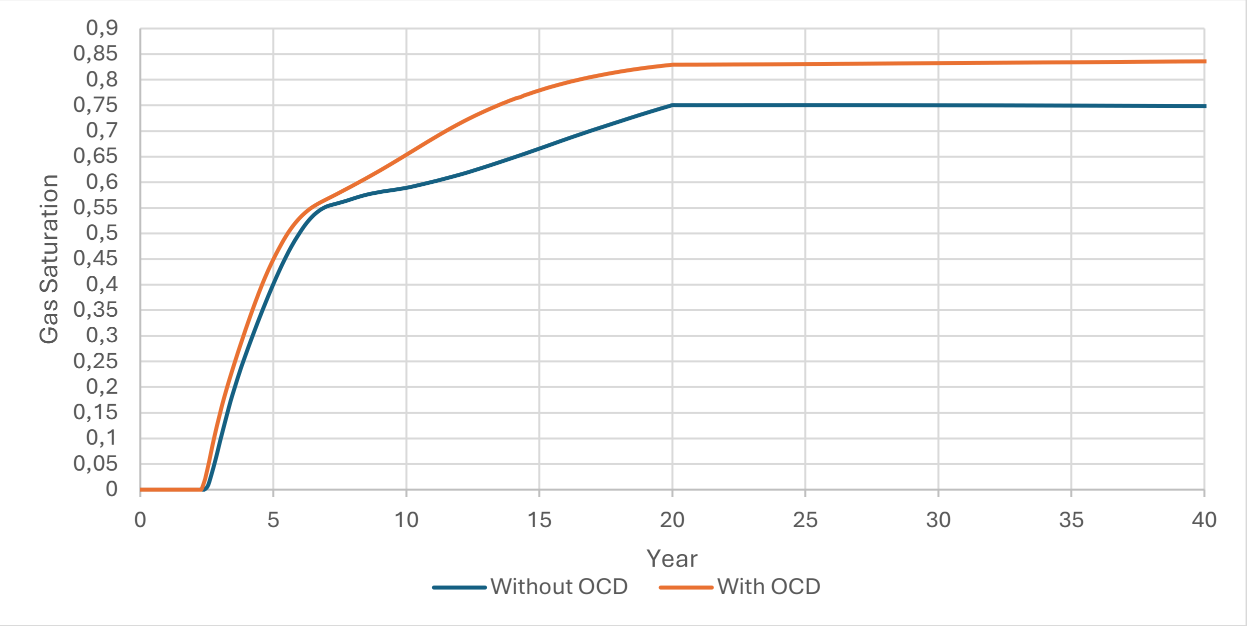

Figure 4.29 – CO_2 Saturation for the Block (27;143;1492).

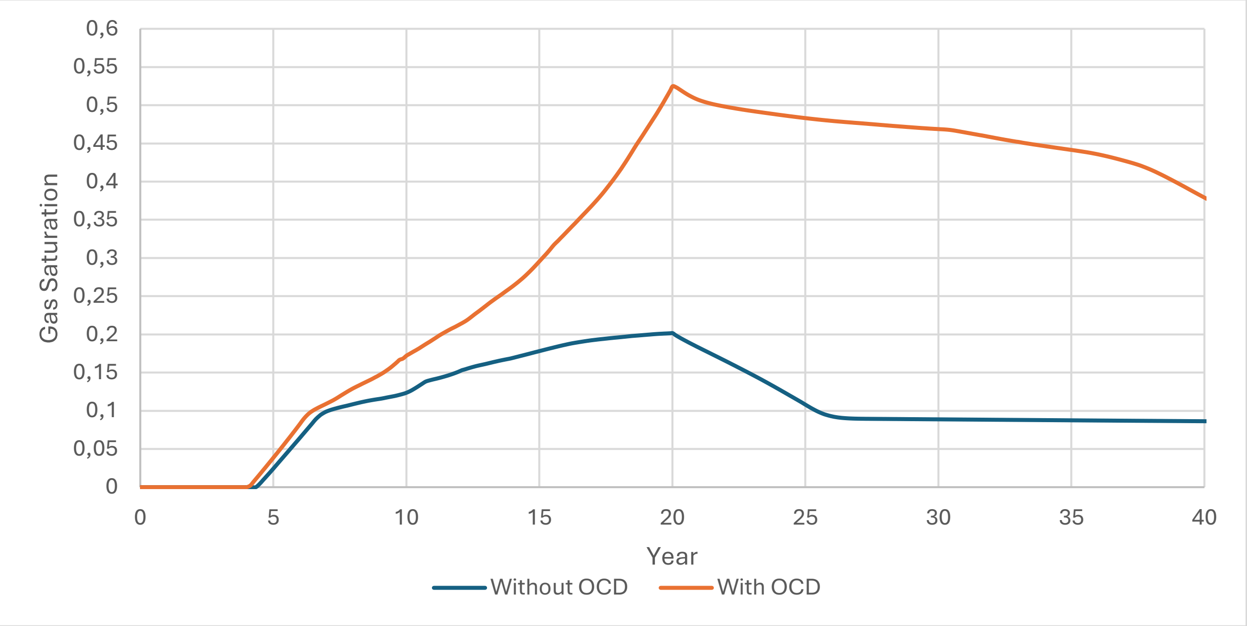

Figure 4.30 – CO_2 Saturation for the Block (28;143;1488).

With OCD implementation, it is noticeable that the levels of gas saturation are increased by many orders of magnitude in the intermediate and low-permeability column located between 1488 and 1500 meters in all the three blocks. OCD installation results in a reduction in injection amount that goes through the slices of maximum permeability. The homogeneity of CO_2 occupancy is increased since OCDs eliminate vertical heterogeneity by redistributing injectivity more homogenous within the 1476-1500 m interval.

The percentage of injected CO_2 that went into the upper perforation was rather small at 82% after OCD was placed as compared to the original 90%. The existing OCD design has little potential to prevent high-permeability channeling, suggesting that there is a need to have additional techno-economic evaluation criterion to check the possibility of cost effective improvement by device position change or OCD device change or addition of completion modification.

Chapter 5. Conclusion and Future Works

In this section will be presented main conclusions of the study along with practical advice for CCS and limitations with recommendations for future directions of studies.

5.1 Summary of Key Findings

The presented thesis established a new mathematical workflow which connected surface facility to wellbore and reservoir simulation tools for operational responses for CO_2 injection within the Smeaheia site. The research produced the following fundamental results:

1. Accuracy and consistency of wellbore and pipeline simulations could be different. The analysis of results between Ledaflow and Pipesim has proven it. These simulators under similar case settings, boundary conditions and fluid properties produce different results. Through they present matching inlet and bottom hole pressure and temperature, they still calculate pressure and temperature profile differently. This assumption can be explained as Pipesim has different choke simulation model and thermodynamical model apart from Ledaflow.

    - Pressure drop and thermal effects are various. On the one hand, Ledaflow (that is employing CO2PURE EOS) simulates moderate Joule-Thompson cooling effect, since temperature shifted only from 4 °C to around -12°C across the choke. On the other hand, Pipesim (that is working with PR EOS) predicted extreme temperature drop, it turned from 4°C to -97°C that looks not so physically.
    - Despite the difference in calculation of Joule-Thompson effect in Pipesim, generally, the pressure and temperature profiles seems to be similar to Ledaflow.
    - The results from Ledaflow predicted that the highest gas volume fraction is 76% after the wellhead choke and full condensation has appeared to be at 400 m MD. However, Pipesim generated lower peak gas volume fraction – around 50% through its severe temperature drop while it achieved one single-phase flow at 700 m MD.
    - Above presented results confirms that it is essentially important to use advanced and modern thermodynamical models (e.g. CO2PURE, GERG-2008 or CSMA) and proven choke models. The suggested temperature drop in Pipesim may produce wrong hydrate risk assessment.
    - Calculation set-ups are different. Another cornerstone between these software can be number of meshes, since Ledaflow employ around 400 meshes around whole scheme. However, Pipesim uses only 6 meshes that might have an impact on the quality of output. It leads to Pipesim taking around few seconds to calculate pressure and temperature profiles, while Ledaflow need 10 minutes to calculate.

2. Reservoir simulations outcomes (E100 and E300) are also different. Eclipse was used to create a few reservoir models to simulate realistic CO_2 behavior through different simulation approaches:

    - Black-oil models (E100) appears to be quite useful for sensitivity analyses and risk assessments. The model is quite simple, since it exploits 3 pseudocomponents – gas, oil and water. The main thermodynamical properties in this case is asserted through special PVT tables. In the model CO_2 is presented as gas, while brine is oil. This approach alleviates the calculation and grants that calculation time will not exceed 30-40 minutes for medium size models. However, since CO_2 is treated to be gas, it can lead to overestimated viscosity, buoyancy and mobility ratio – CO_2 occupies vast areas that are close to caprock. In sense of technical results – black-oil approach predicted pore pressure to increase linearly from 121 bar to 140 bar during the first two decades before reaching stability at 140 bar. Bottom hole pressure is predicted to be like E300 with difference that does not exceed 2,5%.

- Thermal compositional model (E300) with CO2STORE utilizes a compositional framework that counts main properties through EOS. CO2STORE is a special module that facilitate modelling of CO_2 storage, since it used predefined K-values to CO_2 and brine. In spite of accuracy, it may lead to long calculation period. In this study the black-oil model took only 20 minutes to calculate, while thermal compositional models took around 12 hours. In sense of technical results – the model produced fast pore pressure increase from 121 bar to 147 bar during the first injection year. It can be explained as thermal and dissolution effects. Unlike E100 model, E300 presents non-isothermal and advance approach.

- Thermal compositional model (E300) with CO2SOL incorporates advanced equilibrium solver for CO_2-brine reactions. This approach enables CO2 dissolution to depend on pressure, temperature and salinity level. The aqueous phase absorbed a significant amount of injected CO_2 which helped regulate pressure increase. The pressure within the field increased gradually until it reached approximately 145 bar during the injection process because of solubility trapping and reduced gas compressibility.

In general, the black-oil models provide fast computational performance, while omitting essential thermal and solubility phenomena. On the other hand, compositional models generate more accurate pressure dynamics and trapping outcomes while facing long computational time.

3. Coupled wellbore-reservoir framework through loose-coupling scheme can be quite useful to analyze and monitor main technical parameters in time. Ledaflow as surface network and wellbore simulator and Eclipse as reservoir simulator operates as separated “black boxes” which exchanged boundary conditions at predefined time steps through a sequential loose-coupling process. The thesis provide flowchart for making it much easier to redo in any reservoir/wellbore simulators. The proposed approach demonstrated effective capture of transient relationships between surface cooling effects and subsurface fluid behavior changes. It proves integrated modeling becomes more essential for preventing undesirable events during the start and operation of injection.

4. Implementation of OCD were analyzed. For making it two advanced models were developed:

    - CO_2 solunility module (CO2SOL), as noted above, moderated reservoir pressure trajectories by converting a portion of free-phase CO_2 into dissolved form in the brine. This model was used since it is compatible with WELLDIMS, module that allows to create OCD instead of usual perforations for the injection well

    - Multisegmented well module (WELLDIMS), this module allows user to divide well to separated segments to calculate, it leads that user to define OCD on the toe.

Introduced OCD changed CO_2 distribution pathway slightly, since there 2 main layers – highly permeable (1476-1488 m) and low permeable (1488-1500 m). So, 90% of all outflows goes through the highest layer. After implementation of OCD, it could decrease the value only to 82% of the total flow. At the same time, low-permeability sands experienced higher saturations and more uniform sweep. In spite of this improvement, the modest 8% change suggests that further optimization is needed. However, even this limited small redistribution of CO_2 underscores the potential of this technology to mitigate vertical heterogeneity and ensure CCS integrity.

To sum up, these findings demonstrate that:

— Accurate thermodynamic modelling for the surface and wellbore level is critical to accurately predict flow behavior, phase distribution and thermal effects caused by choke. Ledaflow presented more physical picture in comparison with Pipesim.

— Thermal compositional modeling with specific modules (CO2STORE, CO2SOL) yields more realistic pressure forecasts and quantification of dissolved CO_2 in comparison to traditional black-oil approaches. However, the difference in computational sources for compositional modeling is still sufficient.

— A loose-coupling, proposed in this thesis, captures three main characteristics – pressure, temperature and flow between two independent simulators. It ensure that injection strategies remain feasible in practice.

— Advanced strategy with application of OCD showed that it can improve sustainability by enhancing long-term storage security and sweep efficiency.

5.2 Practical Implications for CO_2 Storage

This section applies the research result to provide industry workers, regulators and researchers working on carbon sequestration with practical guidance.

1. Selection of thermodynamic and flow-simulation tools is essential for integrity and full capture of flow behavior. The presented results from Ledaflow and Pipesim simulations regarding choke-induced pressure drop and sequential cooling shows that accurate EOS must be used for high-pressure CO_2 modeling. The incorrect estimation of Joule-Thomspon cooling effect results in incorrect assessment of hydrate formation risk. As a result industries should take the following steps:

   - Choose high-fidelity thermodynamical models for CO_2 when performing CO_2 modeling. It can be – CO2PURE, GERG-2008 and CSMA. PR oversimplifies the behavior of CO_2.

   - The wellbore simulator comparison should be made through sensitivity analysis to detect temperature and phase change hotspots that located near to wellhead choke. It might need additional protection against leakage or hydrate formation.

   - Simulation output should have been verified through laboratory of PVT properties as well as field measurements validation to ensure predicted temperature drops match observed modeled value.

2. The results from black-oil (E100) and thermal compositional (E300) simulations show that ignoring accurate thermodynamical properties of CO_2 and CO_2 solubility in brine may lead to migration overestimation and higher predicted pressure in the reservoir. In field practice:

    - Project teams should select compositional approaches with advanced modules to build high-fidelity models for their projects. Using this approach leads to have less wellhead pressure limits that allow increased injection volumes without risk of compromising caprock integrity.

    - The compositional and thermal model enable optimal development of operational strategies through its ability to accurately capture trapping effects that allows the optimization of injection schedules.

    - Monitoring and verification tests need to include formation brine sampling test to verify the dissolved amount of CO_2. Then, it should be compared to modeled value.

    - Black-oil models can be used for express evaluation of pressure in the reservoir since it does not require as much computational sources as compositional models.

3. The loose-coupling flowchart between two independent software demonstrates that thermal feedback from cooling created two-way interactions that have an effect on injectivity and pressure. In practice:

    - A coupled approach enables real-time reservoir pressure adjustment through choke opening/shutting without relying on fixed setpoints and empirical approaches.

    - Drilling and completion engineers needs to design the injection wells by evaluating their thermal profile so the material and seals retain their strength and deformability at the lowest expected temperatures. In this study it was -12 °C as seen in Ledaflow.

4. OCDs create limited but detectable improvements for vertical distribution of CO_2. From the practical standpoint:

    - For future projects well completion designs need to include simple OCDs to multi-layered reservoirs that shows high heterogeneity. The 8% simulated change appears to be minor, but its effects multiply across several wells to produce additional storage capabilities. As a result, it will increase storage efficiency.

    - The operational performance of OCD can be verified through special periodic tests such as distributed temperature sensing or distributed acoustic sensing systems to detect flow patterns through different layers to assess the effectiveness of implemented devices.

5. The practical implications span operational metrics to embrace both storage efficiency over long-term and economic aspects of the project:

    - The thesis demonstrated that solubility counting in compositional models effectively reduce pressure.

    - Accurate reservoir simulations enable operators to optimize injection schedules and well spacing which could and have an effect on economics.

    - The development of real-time data in coupled models allows operators to adopt adaptive management practices. The adaptive strategy allows them to change injection strategies based on the reservoir feedback. It helps operators to decrease the risks of overdesign of project.

The practical implications presented above strengthen the case that complete integrated modeling serves as a fundamental requirement for operational safety and economically viable CO_2 injection projects. Team projects can better control risks and act accordingly to regulatory needs while improving long-term storage safety. The implementation of these findings in field operations remains vital for CCS expansion because it will help to mitigate climate change in the future.

5.3 Limitations and Recommendations for Future Research

The modeling framework that was presented in this study delivers sufficient knowledge about CO_2 injection into saline aquifers. The expansion of coupled simulations requires existing constraints while increasing their usability across operational and field-based conditions.

Future research needs to expand the study to implementation of impurities (such as CO, CH_4, N_2, N_2O, NO, H_2O), since it is impossible to have only 100% mixtures of CO_2 that are presented in this thesis. Multiple impurities, such as presented before, modifies phase behavior and hydrate formation potential and corrosion risk within injection networks. In other words, the current framework lacks of specific inclusion of these impurities which may lead to underestimation of temperature drops along with phase envelopes.

Future research also should be expanded by adding water vapour for zone formation. The generation of accurate thermodynamic models relies on using laboratory PVT experiments or high-fidelity EOS. The best for such impurities and hydrate formation modeling – CSMA. The extended multicomponent mixture must be modeled in both wellbore and reservoir simulations to analyze their effects on pressure, temperature and phase distribution.

The loose-coupling method used in this research transferred CO_2 pressure, temperature and mass flowrates between surface and subsurface models. Using this loose-coupling method for imputiry-rich injection requires defining each component and its properties to provide the reservoir model with complete capturing of pressure, temperature and compositional details. The implementation of these improvements will lead to more accurate and real-world coupled predictions. It is quite useful framework for better operational decision-making processes during multi-component stream operations.

This thesis conducted work in wellbore and reservoir simulators – Ledaflow, Pipesim and Eclipse. CO_2 storage projects worldwide now tends to use several specialized tools including tNavigator, CMG, Intersect, TOUGH and others for validation of results (Tavagh Mohammadi et al, 2025). Each of these software possesses individual numerical methods together with meshing methods and physical capabilities.

A systematic cross-software comparison should be undertaken to:

- Different numerical solvers should be compared for their performance in modeling CO_2 behavior in different conditions. It should be tested how they handle non-isothermal multi-component flow.
- It would be useful to analyze how process the geomechanical feedback and geomechanical interactions from particular software, such as TOUGH-FLAG or TOUGHREACT model trapping of CO_2.

This study applies only deterministic approaches to model CO_2 injection. So, it assumes that the reservoir properties remains constant without any risks, while the actual reservoir properties consist of spatial variations together with operational uncertainties. The omission of these uncertainties results in overconfident predictions about injectivity and plume migration.

So, it leads to the idea that stochastic or probabilistic models should be used in future research to evaluate parameters uncertainty. It can be done through:

— The Monte Carlo simulation method should be used to draw samples from permeability, porosity, skin factor and other parameters. It can draw curved distribution that are based geostatistically.

— The sensitivity analysis should be performed to understand which variables most affect performance indicators including injection rate, storage efficiency and integrity.

— Discrete parameters uncertainty analysis implementation will improve risk management strategies and allow regulators to obtain probabilistic predictions about leakage scenarios.

The thesis used generic standard OCD which achieved minor CO_2 distribution changes in heterogeneous formation. However, it is possible to apply more advanced devices, such as autonomous outflow control devices as well as OCD with remote control, which allow users to manage openings remotely.

The future research agenda should focus on optimizing the OCD design and configuration for individual case, or might be develop specific methodology for C_v and opening calculations. In this study it is possible to extend OCD research by:

— A parametric design of OCD main parameters (C_v, opening percent or pressure losses) to evaluate their performance in different heterogeneous rock formations.

— The implementation of optimization algorithms including genetic algorithms or Bayesian optimization will find the best parameters for enhancing storage efficiency.

References

Aakre, H., et al. (2018) "Performance of CO2 Flooding in a Heterogeneous Oil Reservoir Using Autonomous Inflow Control." *Journal of Petroleum Science and Engineering*, vol. 167, 5 Apr. 2018, pp. 654–663.

Acevedo, Luis, and Ajay Chopra. (2017) "Influence of Phase Behaviour in the Well Design of CO2 Injectors." *Energy Procedia*, vol. 114, July 2017, pp. 5083–5099.

Ajayi, Temitope, et al. (2019) "A Review of CO2 Storage in Geological Formations Emphasizing Modeling, Monitoring and Capacity Estimation Approaches." *Petroleum Science*, vol. 16, no. 5, 8 July 2019, pp. 1028–1063.

Al-Jeboore, Ivan, et al. (2023) "Evaluation of Immiscible CO2 Injection in High Water Production Reservoir in the Pannonian Basin." *Podzemni Radovi*, no. 42, 2023, pp. 1–18

Al Hameli, Fatima, et al. (2022) "CO2 Sequestration Overview in Geological Formations: Trapping Mechanisms Matrix Assessment." *Energies*, vol. 15, no. 20, 21 Oct. 2022, p. 7805.

Alcalde, Juan, et al. (2018) "Estimating Geological CO2 Storage Security to Deliver on Climate Mitigation." *Nature Communications*, vol. 9, no. 1, 12 June 2018.

Aminu, Mohammed Dahiru, and Vasilije Manovic. (2020) "A Modelling Study to Evaluate the Effect of Impure CO2 on Reservoir Performance in a Sandstone Saline Aquifer." *Heliyon*, vol. 6, no. 8, Aug. 2020.

Anwar, Sara and John J Carroll. (2016) "Carbon Dioxide Thermodynamic Properties Handbook: Covering Temperatures from -20° to 250°c and Pressures up to 1000 Bar: Second Edition." 4 Apr. 2016, pp. 594.

Audigane, P., et al. (2007) "Two-Dimensional Reactive Transport Modeling of CO2 Injection in a Saline Aquifer at the Sleipner Site, North Sea." *American Journal of Science*, vol. 307, no. 7, 1 Sept. 2007, pp. 974–1008.

Aursand, P., et al. (2013) "Pipeline Transport of CO2 Mixtures: Models for Transient Simulation." *International Journal of Greenhouse Gas Control*, vol. 15, July 2013, pp. 174–185.

Bachu, S. (2008) "CO2 Storage in Geological Media: Role, Means, Status and Barriers to Deployment." *Progress in Energy and Combustion Science*, vol. 34, no. 2, Apr. 2008, pp. 254–273.

Bentham, Michelle, and G. Kirby. (2005) "CO2 Storage in Saline Aquifers." *Semantic Scholar*, 2005.

Bjørnstad, Anders. (2022) "Fault Gouge Characterization in the Øygarden Complex in SW Norway - Relevance for Offshore CO2 Storage." Bora.uib.no, 17 June 2022.

Burachok, O., et al. (2022) "Functional Comparison of Wellbore-Reservoir Coupling Solutions for CO2 Storage Simulations." *83rd EAGE Annual Conference & Exhibition*, 2022, pp. 1–5.

Celia, M. A., et al. (2015) "Status of CO2storage in Deep Saline Aquifers with Emphasis on Modeling Approaches and Practical Simulations." *Water Resources Research*, vol. 51, no. 9, Sept. 2015, pp. 6846–6892.

Chen, Xiaolong, et al. (2021) "Effect of Gravity Segregation on CO2 Flooding under Various Pressure Conditions: Application to CO2 Sequestration and Oil Production." *Energy (Oxford)*, vol. 226, 1 July 2021.

Darcy, H. (1857). "Recherches expérimentales relatives au mouvement de l'eau dans les tuyaux." Mallet-Bachelier, Paris. 268 pages and atlas (in French).

Das, Ayon Kumar, et al. (2021) "A Semi-Analytical Solution to Evaluate the Spatiotemporal Behavior of Diffusive Pressure Plume and Leakage from Geological Storage Sites." *Water Resources Research*, vol. 57, no. 7, July 2021

Doughty, Christine, and Karsten Pruess. (2004) "Modeling Supercritical Carbon Dioxide Injection in Heterogeneous Porous Media." *Vadose Zone Journal*, vol. 3, no. 3, 1 Aug. 2004, pp. 837–847.

Ellis, Brian R., et al. (2010) "Limitations for Brine Acidification due to SO2 Co-Injection in Geologic Carbon Sequestration." *International Journal of Greenhouse Gas Control*, vol. 4, no. 3, May 2010, pp. 575–582.

Ellis, T, et al. (2009) "Inflow Control Devices - Raising Profiles." Vol. 21, no. 4, 1 Dec. 2009, pp. 30–37.

Equinor. (2024) "CO2 Highway Europe." Equinor.com, 2024, www.equinor.com/energy/co2highwayeurope. Accessed 14 May 2025.

Farshad Mostakhdeminhosseini, and Yousef Rafiei. (2024) "An Integration of the Numerical and Soft Computing Approaches for Determining Inflow Control Device Flow Area in Water Injection Wells." *Journal of Petroleum Exploration and Production Technology*, vol. 14, no. 7, 16 Apr. 2024, pp. 1979–1994.

Furre, Anne-Kari, et al. (2017) "20 Years of Monitoring CO2-Injection at Sleipner." *Energy Procedia*, vol. 114, July 2017, pp. 3916–3926.

Gao, Ming, et al. (2021) "Joule–Thomson Effect on a CCS-Relevant (CO2 + N2) System." *ACS Omega*, vol. 6, no. 14, 31 Mar. 2021, pp. 9857–9867.

Global Carbon Budget (2023). "Fossil CO2 Emissions at Record High in 2023." *Global Carbon Budget*, 4 Dec. 2023.

Goodman, A.L. (2002) "Abstract: Carbon Dioxide Sequestration With Brines." *2002 Denver Annual Meeting* (October 27-30, 2002).

Greskovich, E J. et al (1972) "Slug Frequency in Horizontal Gas-Liquid Slug Flow." *Industrial & Engineering Chemistry Process Design and Development*, vol. 11, no. 2, 1 Apr. 1972, pp. 317–318

Gupta, R. (2023) "Supercritical Fluid – Examples, Properties, and Phase Diagrams." *Chemistry Learner*, 28 Feb. 2023, www.chemistrylearner.com/supercritical-fluid.html.

Havercroft, Ian (2024) "Overview of Global CCS and CO2 Cross-Border Transport Projects." *Workshop On CO2 Cross-Border Transport and Storage (CCS) In Asia and the Pacific*, 8 February 2024.

Hammer, Morten, et al. (2021) "Upward and Downward Two-Phase Flow of CO2 in a Pipe: Comparison between Experimental Data and Model Predictions." *International Journal of Multiphase Flow*, vol. 138, May 2021.

Hepple, R. P., and S. M. Benson. (2004) “Geologic Storage of Carbon Dioxide as a Climate Change Mitigation Strategy: Performance Requirements and the Implications of Surface Seepage.” *Environmental Geology*, vol. 47, no. 4, 16 Nov. 2004, pp. 576–585.

Hoteit, Hussein, et al. (2019) “Assessment of CO2 Injectivity during Sequestration in Depleted Gas Reservoirs.” *Geosciences*, vol. 9, no. 5, 5 May 2019, p. 199.

IEAGHG (2024) “Managing the transition of depleted oil and gas fields to CO_2 storage”, 2024-05, August 2024.

IPCC (2005) “Carbon Dioxide Capture and Storage” *Intergovernmental Panel on Climate Change Carbon Dioxide Capture and Storage*. 2005.

IPCC (2023) “Climate Change 2023 Synthesis Report.” 2023.

Jinju, Han, et al. (2016) “Effect of Gravity Segregation on CO2 Sequestration and Oil Production during CO2 Flooding.” *Applied Energy*, vol. 161, 1 Jan. 2016, pp. 85–91.

Kais, R, et al. (2016) “Design a Multiport Completion with Inflow Control Devices: Hydraulic Modeling to Meet Financial Function Optimization in a High Water Cut and CO2 Environment.” 7 Nov. 2016.

Kampman, N., et al. (2014) “Fluid Flow and CO2–Fluid–Mineral Interactions during CO2-Storage in Sedimentary Basins.” *Chemical Geology*, vol. 369, Mar. 2014, pp. 22–50.

Karvounis, Panagiotis, and Martin J. Blunt. (2021) “Assessment of CO2 Geological Storage Capacity of Saline Aquifers under the North Sea.” *International Journal of Greenhouse Gas Control*, vol. 111, Oct. 2021.

Kaszuba, John P, and David R Janecky. (2009) “Geochemical Impacts of Sequestering Carbon Dioxide in Brine Formations.” *Geophysical Monograph*, 1 Jan. 2009, pp. 239–247.

Kaszuba, John P., et al. (2005) “Experimental Evaluation of Mixed Fluid Reactions between Supercritical Carbon Dioxide and NaCl Brine: Relevance to the Integrity of a Geologic Carbon Repository.” *Chemical Geology*, vol. 217, no. 3-4, Apr. 2005, pp. 277–293.

Kaszuba, John P., et al. (2006) “Immiscible CO2-H2O Fluids in the Shallow Crust.” *Geochemistry, Geophysics, Geosystems*, vol. 7, no. 10, Oct. 2006.

Kirchin, A. (2019) “The Pros & Cons of Depleted vs Saline Reservoirs in CCS | RPS.” *RPS*, pp. 1-6, 2019.

Laurent André, et al. (2009) “Numerical Simulations of the Thermal Impact of Supercritical CO2 Injection on Chemical Reactivity in a Carbonate Saline Reservoir.” *Transport in Porous Media*, vol. 82, no. 1, 29 Sept. 2009, pp. 247–274.

Lindeberg E, et al (2002) “The Long-Term Fate of CO2 Injected into an Aquifer.” *Greenhouse Gas Control Technologies - 6th International Conference*, vol. 1, 1 – 4 October 2002, pp. 489–494.

Linga, Gaute, and Halvor Lund. (2016) “A Two-Fluid Model for Vertical Flow Applied to CO2 Injection Wells.” *International Journal of Greenhouse Gas Control*, vol. 51, 31 May 2016, pp. 71–80.

Lu, Hongfang, et al. (2020) “Carbon Dioxide Transport via Pipelines: A Systematic Review.” *Journal of Cleaner Production*, vol. 266, Sept. 2020, p.

Machado, Marcos Vitor Barbosa, et al. (2023) "Potential Benefits of Horizontal Wells for CO2 Injection to Enhance Storage Security and Reduce Leakage Risks." *Applied Sciences*, vol. 13, no. 23, 29 Nov. 2023, p. 12830

Moiseev, B., et al. (2016) "Thermal Calculations of Underground Oil Pipelines." 2016.

Ministry of Petroleum and Energy. Ministry of Petroleum and Energy Feasibility Study for Full-Scale CCS in Norway Contents.

Muhammad Hammad Rasool, et al. (2023) "Selecting Geological Formations for CO2 Storage: A Comparative Rating System." *Sustainability* Vol. 15, no. 8, 13 Apr. 2023, pp. 6599–6599.

Mulrooney, Mark Joseph (2020). "Derisking the Smeaheia Fault Block: Geological Controls on CO2 Containment." *SINTEF Blog*, 16 Dec. 2020.

Mulrooney, Mark Joseph, et al. (2020) "Structural Analysis of the Smeaheia Fault Block, a Potential CO2 Storage Site, Northern Horda Platform, North Sea." *Marine and Petroleum Geology*, vol. 121, Nov. 2020, p. 104598.

National Energy Technology Laboratory, (2022) "Carbon Storage FAQs | netl.doe.gov," 2022. https://netl.doe.gov/carbon-management/carbon-storage/faqs/carbon-storage-faqs (accessed June. 03, 2025).

Nguyen, Ba Nghiep, et al. (2016) "Thermal Impact of CO2 Injection on Geomechanical Response at the FutureGen 2.0 Site: A Three-Dimensional Thermo-Geomechanical Approach." *International Journal of Greenhouse Gas Control*, vol. 54, 7 Sept. 2016, pp. 29–49.

Org, Escholarship, et al. (2008) "Title Large-Scale Impact of CO2 Storage in Deep Saline Aquifers: A Sensitivity Study on Pressure Response in Stratified Systems Publication Date Large-Scale Impact of CO2 Storage in Deep Saline Aquifers: A Sensitivity Study on Pressure Response in Stratified Systems." 2008.

Parisio, Francesco et al. (2020) "Sinking CO_2 in Supercritical Reservoirs." *Geophysical Research Letters*, vol. 47, no. 23, 29 Nov. 2020

Paterson, Lincoln, et al. (2010) "Observations of Thermal and Pressure Transients in Carbon Dioxide Wells." *All Days*, 19 Sept. 2010.

Pekot, Lawrence J, et al. (2011) "Simulation of Two-Phase Flow in Carbon Dioxide Injection Wells." 6 Sept. 2011.

Peng, L, et al. (2022) "Dynamically Coupled Reservoir and Wellbore Simulation Research in Two-Phase Flow Systems: A Critical Review." *Processes*, vol. 10, no. 9, 5 Sept. 2022, pp. 1778–1778.

Peters, E, et al. (2013) "Consequences of Thermal Fracture Developments due to Injection Cold CO2 into Depleted Gas Fields.", 2013.

Pham, V.T.H., et al. (2013) "Assessment of CO2 Injection into the South Utsira-Skade Aquifer, the North Sea, Norway." *Energy*, vol. 55, June 2013, pp. 529–540.

Pogge von Strandmann, Philip A. E., et al. (2019) "Rapid CO2 Mineralisation into Calcite at the CarbFix Storage Site Quantified Using Calcium Isotopes." *Nature Communications*, vol. 10, no. 1, 30 Apr. 2019.

Qu, Hongyan, et al. (2012) "Complex Evolution of Coal Permeability during CO2 Injection under Variable Temperatures." *International Journal of Greenhouse Gas Control*, vol. 9, July 2012, pp. 281–293.

Rajandran, K. V., et al. (2024) "Unlocking Oil Reserves Sustainably: CO2 Injection for Enhanced Oil Recovery (EOR) in the Sarir C-Field." *SPE Symposium and Exhibition - Production Enhancement and Cost Optimisation*, 2 Sept. 2024.

Ramey, H.J. (1962) "Wellbore Heat Transmission." *Journal of Petroleum Technology*, 14, pp. 427-435.

Rezvani, H, et al. (2023) "A Novel Analytical Technique for Determining Inflow Control Devices Flow Area in CO2-EOR and CCUS Projects." *Journal of Petroleum Exploration and Production Technology*, vol. 13, no. 9, 3 June 2023, pp. 1951–1962.

Ringrose, P., Thorsen, R, et al., P. Z. (2017). "Ranking and risking alternative CO2 storage sites offshore Norway." *Presentation made by Equinor*, Fall 2017. Equinor RT.

Romdhane, A., et al. (2022) "Screening, Monitoring, and Remediation of Legacy Wells to Improve Reservoir Integrity for Large-Scale CO2 Storage—an Example from the Smeaheia Structure in the Northern North Sea." *Frontiers in Energy Research*, vol. 10, 16 Mar. 2022.

Roy, Pratanu, et al. (2018) "Effect of Thermal Stress on Wellbore Integrity during CO2 Injection." *International Journal of Greenhouse Gas Control*, vol. 77, 1 Oct. 2018, pp. 14–26.

Saevareid, O, et al. (2021) "PVT and flow behavior of impure CO2 in aquifers." *TCCS-11 - Trondheim Conference on CO2 Capture, Transport and Storage Trondheim*, Norway - June 21-23, 2021.

Salimzadeh, Saeed, et al. (2018) "Effect of Cold CO2 Injection on Fracture Apertures and Growth." *International Journal of Greenhouse Gas Control*, vol. 74, July 2018, pp. 130–141.

Samaroo, Mahendra, et al. (2024) "Injection Temperature Impacts on Reservoir Response during CO2 Storage." *SPE Journal*, vol. 29, no. 05, 15 Feb. 2024, pp. 2638–2661.

Shchipanov, Anton, et al. (2022) "Periodic CO2 Injection for Improved Storage Capacity and Pressure Management under Intermittent CO2 Supply." *Energies*, vol. 15, no. 2, 13 Jan. 2022, p. 566

SINTEF (2015) "Modeling Basics.", *Modeling Basics*, 2015, www.sintef.no/projectweb/mrst/modules/co2lab/modeling-basics/. Accessed 15 May 2025.

SINTEF (2025) "Ledaflow - SINTEF.", 2025, www.sintef.no/en/software/ledaflow/. Accessed 6 May 2025.

Shi, J, and S Durucan. (2005) "CO 2 Storage in Deep Unminable Coal Seams." *Oil & Gas Science and Technology -Rev. IFP*, vol. 60, no. 3, 2005, pp. 547–558.

Solomon, Mithran Daniel, et al. (2024) "Pipeline Infrastructure for CO2 Transport: Cost Analysis and Design Optimization." *Energies*, vol. 17, no. 12, 13 June 2024, pp. 2911–2911.

Span, Roland, and Wolfgang Wagner. (1996) "A New Equation of State for Carbon Dioxide Covering the Fluid Region from the Triple-Point Temperature to 1100 K at Pressures up to 800 MPa." *Journal of Physical and Chemical Reference Data*, vol. 25, no. 6, Nov. 1996, pp. 1509–1596.

Stian Juvet Sørensen, et al. (2022) "Enhanced Oil Recovery Using CO2 Injection and Inflow Control Devices." *Linköping Electronic Conference Proceedings*, vol. 192, 28 Oct. 2022, pp. 378–385.

Strpić, Kristina. (2021) "Modeling of Transient Multiphase Flow in a CO2 Injection Well with the Wellbore-Reservoir Coupled Simulator T2Well-ECO2M." *1st Geoscience & Engineering in Energy Transition Conference*, Jan. 2021.

Szulczewski, M. L., et al. (2013) "Carbon Dioxide Dissolution in Structural and Stratigraphic Traps." *Journal of Fluid Mechanics*, vol. 736, 6 Nov. 2013, pp. 287–315.

Taghavi, S. (2023) "Performance Analysis of Autonomous Inflow Control Valve in a Heterogenous Reservoir Using CO2 Enhanced Oil Recovery." *Dntb.gov.ua*, 2023.

Tavagh Mohammadi, Behnam, et al. (2025) "A Review of Modeling Approaches for CO2 Injection into Depleted Gas Reservoirs: Coupling Transient Wellbore and Reservoir Dynamics." *International Journal of Greenhouse Gas Control*, vol. 145, 17 May 2025.

Terhaar, Jens, et al. (2023) "Ocean Acidification in Emission-Driven Temperature Stabilization Scenarios: The Role of TCRE and Non-CO2 Greenhouse Gases." *Environmental Research Letters*, vol. 18, no. 2, 1 Feb. 2023.

Thu, Eirik Soland. (2019) "Modeling of Transient CO2 Flow in Pipelines and Wells." *Ntnu.no*, vol. 13, 2019.

Trenberth, Kevin E. (2011) "Changes in Precipitation with Climate Change." *Climate Research*, vol. 47, no. 1, 31 Mar. 2011, pp. 123–138.

Tweed, Lucy E.L., et al. (2024) "Transient Joule–Thomson Cooling during CO_2 Injection in Depleted Reservoirs." *Journal of Fluid Mechanics*, vol. 997, 10 Oct. 2024

UNFCCC (2015). "Paris Agreement." *United Nations*, 12 Dec. 2015.

Vilarrasa, Víctor, et al. (2013) "Liquid CO2 Injection for Geological Storage in Deep Saline Aquifers." *International Journal of Greenhouse Gas Control*, vol. 14, May 2013, pp. 84–96

Wang, Y., et al. (2024) "Numerical Analysis of the Effect of Heterogeneity on CO2 Dissolution Enhanced by Gravity Driven Convection." *Authorea (Authorea)*, 4 Feb. 2024.

Wen, Gege, and Sally M. Benson. (2019) "CO2 Plume Migration and Dissolution in Layered Reservoirs." *International Journal of Greenhouse Gas Control*, vol. 87, Aug. 2019, pp. 66–79.

Xing, Tiange, et al. (2022) "Creep of CarbFix Basalt: Influence of Rock–Fluid Interaction." *Solid Earth*, vol. 13, no. 1, 14 Jan. 2022, pp. 137–160.

Younessi. A. (2024) "Impact of CO2 Injection on Stability of Perforation Tunnels." *European Association of Geoscientists & Engineers*, Jan. 2024, pp. 1–3

Zhang, Nan, et al. (2022) "The Optimal Model of Water Control Completion Based on Source Function and Network Model." *Journal of Petroleum Science and Engineering*, vol. 213, 17 Mar. 2022.

Zhao, F., et al. (2024) "Impact of Water Content on Minimum Miscibility Pressure during CO_2 Flooding in High Water-Cut Reservoirs." *E3S Web of Conferences*, vol. 554, 1 Jan. 2024.

Ziabakhsh-Ganji, Zaman, and Henk Kooi. (2014) "Sensitivity of Joule–Thomson Cooling to Impure CO2 Injection in Depleted Gas Reservoirs." *Applied Energy*, vol. 113, Jan. 2014, pp. 434–451.

"CCUS Projects Explorer – Data Tools." IEA, 15 Mar. 2024, www.iea.org/data-and-statistics/data-tools/ccus-projects-explorer.